

Autoregressive Networks with Dependent Edges

Jinyuan Chang^{1,2}, Qin Fang³, Eric D. Kolaczyk⁴, Peter W. MacDonald⁵, and Qiwei Yao⁶

¹*Joint Laboratory of Data Science and Business Intelligence, Southwestern University of Finance and Economics, Chengdu, Sichuan 611130, China*

²*State Key Laboratory of Mathematical Sciences, Academy of Mathematics and Systems Science, Chinese Academy of Sciences, Beijing 100190, China*

³*Business School, University of Sydney, Sydney, 2008, Australia*

⁴*Department of Mathematics and Statistics, McGill University, Montreal, Quebec H3A 0B9, Canada*

⁵*Department of Statistics and Actuarial Science, University of Waterloo, Waterloo, Ontario N2L 3G1, Canada*

⁶*Department of Statistics, London School of Economics and Political Science, London, WC2A 2AE, U.K.*

Abstract

We propose an autoregressive framework for modelling dynamic networks with dependent edges. It encompasses models that accommodate, for example, transitivity, degree heterogeneity, and other stylized features often observed in real network data. By assuming the edges of networks at each time are independent conditionally on their lagged values, the models, which exhibit a close connection with temporal ERGMs, facilitate both simulation and the maximum likelihood estimation in a straightforward manner. Due to the possibly large number of parameters in the models, the natural MLEs may suffer from slow convergence rates. An improved estimator for each component parameter is proposed based on an iteration employing projection, which mitigates the impact of the other parameters (Chang et al., 2021; Chang et al., 2023). Leveraging a martingale difference structure, the asymptotic distribution of the improved estimator is derived without the assumption of stationarity. The limiting distribution is not normal in general, although it reduces to normal when the underlying process satisfies some mixing conditions. Illustration with a transitivity model was carried out in both simulation and a real network data set.

Key words: conditional independence, dynamic networks, maximum likelihood estimation, stylized features of network data, transitivity.

1 Introduction

Dynamic network modelling with dependent edges is practically important and relevant but technically challenging. It is natural that the sequence of edges observed over time between two nodes will depend on the behavior of other edges in the network. This dependence represents known social phenomena such as reciprocity, transitivity, degree heterogeneity (popularity), which are thought to govern the evolution of real-world networks in diverse applications. On the other hand, dependent edges make the dynamic structures of network processes complex, and statistical inference challenging – not only the computation but also the accompanying theory.

In the growing research area of dynamic network modelling, work continues in three interrelated directions: model specification, computation, and theory. Our work contributes model specification, computation, and substantial and highly non-trivial supporting theory. Specifically, we develop a class of dependent-edge autoregressive (AR) models for network data observed in discrete time. This class is amenable to theoretical analysis, with formal asymptotic analysis for the maximum likelihood estimators. Our theoretical results in turn motivate a statistically and computationally efficient approach to parameter estimation, which we implement in an open-source software package.

In more detail, we specify the transition probabilities of forming a new edge or dissolving an existing edge between each pair of nodes explicitly depending on its history, and on the histories of other edge processes. This enlarged form of the transition probabilities makes the model flexible enough to accommodate stylized features such as transitivity and degree heterogeneity. The resulting network processes have dependent edges, which is radically different from previous AR network models. Nevertheless, based on the conditional independence, we can build up a martingale difference structure which facilitates asymptotic

analysis for the maximum likelihood estimators (see Section 5). Additionally, we allow the number of parameters in the model to diverge together with the network size to accommodate, for example, heterogeneity in forming and dissolving edges modelled with node-specific parameters. To the best of our knowledge, high-dimensional asymptotic analysis of this kind has not been done for a discrete-time dynamic network model class as flexible as the one we specify in this work. We visualize the relative scope of this advancement in Table 1, which we will explain in more detail in Section 2.

	<i>Full dep.</i>	dep. edge AR, LNR		(S)TERGM, SAOM	
Between	<i>Local dep.</i>				
snapshot	<i>Edgewise dep.</i>				
	<i>Static/Full ind.</i>			<i>LD-ERGM</i>	<i>ERGM</i>
		<i>Full ind.</i>	<i>Local dep.</i>	<i>Full dep.</i>	
			Within snapshot		

Table 1: Classification of marginal edge dependence structures in some existing static and dynamic network models (see Section 2). Between snapshot dependence structures are contained in one another from low to high. Within snapshot dependence structures are contained in one another from left to right. Our model class, “**dep. edge AR**”, can accommodate dependence structures in the entire shaded region.

The rest of the paper is organized as follows. Section 2 provides a detailed (albeit necessarily still incomplete) review of the literature. Section 3 presents the general AR network framework with dependent edges. We also discuss the relationship between the proposed AR models, and TERGMs in Section 3. Section 4 contains three concrete AR models which are designed to model, respectively, degree heterogeneity, persistence, and transitivity – those are among the stylized features often observed in real network data. Section 5 presents the estimation procedures based on the maximum likelihood principle for the parameters in the AR models and the associated asymptotic theory. In so doing, we introduce the concepts of local parameters and global parameters, which need to be identified and estimated separately and may also entertain different convergence rates. An improved estimator for each component parameter is obtained by projecting the score function onto the corresponding direction, which mitigates the impact of the other parameters (Chang et al., 2021; Chang et al., 2023). The limiting distribution of the improved estimator is

derived without the assumption of stationarity. It is not normal in general, but it reduces to normal when the underlying process satisfies some mixing conditions which hold for many stationary processes. Numerical illustration with a real dynamic network data set is reported in Section 6. An online supplement contains simulation studies for the proposed transitivity model, additional real data results and all the technical proofs.

Notation. For any positive integer r , write $[r] = \{1, \dots, r\}$ and $\mathbb{R}_+^r = \{(x_1, \dots, x_r)^\top : x_i > 0 \text{ for any } i \in [r]\}$. For any $x, y \in \mathbb{R}$, we write $x \vee y = \max(x, y)$. For two positive sequences $\{a_n\}$ and $\{b_n\}$, we write $a_n \ll b_n$ if $\limsup_{n \rightarrow \infty} a_n/b_n = 0$, and $a_n \lesssim b_n$ if $\limsup_{n \rightarrow \infty} a_n/b_n < \infty$. For any vector $\mathbf{b} = (b_1, \dots, b_r)^\top \in \mathbb{R}^r$, we let \mathbf{b}_{-l} denote the sub-vector of \mathbf{b} by removing the l -th component b_l . Given an index set $\mathcal{M} \subset [r]$, we let $\mathbf{b}_{\mathcal{M}}$ denote the sub-vector of \mathbf{b} that consists of the components of \mathbf{b} with the indices in \mathcal{M} . For any $r_1 \times r_2$ real matrix \mathbf{B} , denote by \mathbf{B}^\top its transpose. We use $\lambda_{\min}(\mathbf{B})$ to denote the smallest eigenvalue of a square matrix \mathbf{B} . For any countable set \mathcal{U} , $|\mathcal{U}|$ denotes its cardinality.

2 Literature review

To place our contribution in the literature properly, and to clarify the novelty of our new theoretical results, we give a non-exhaustive overview of this growing research area. We roughly taxonomize some competing classes of dynamic network models in terms of the patterns of dependence which they can capture among the edge variables.

In this work, we study a class of network models which explicitly model marginal edge dependence. This contrasts with many well-studied network models which implicitly model edge dependence through latent variables, including the stochastic block model (SBM, [Karrer and Newman, 2011](#)), and many classes of latent space model (LSM, [Matias and Robin, 2014](#)). While latent variable models do induce marginal edge dependence, this dependence is implicit and cannot be configured easily to accommodate stylized features of real network data (e.g. transitivity).

Our modelling framework is designed for dynamic network data collected as undirected

binary edges on a common node set, with the status of edges changing over time. We adopt a discrete-time view, and assume that we observe time-indexed network *snapshots* at regular intervals, or can coerce relational event data into network snapshots sampled at a constant time resolution. When relational event data with continuous time stamps are available, dynamic network models can be specified which describe the instantaneous effects of network statistics on the rates, or relative rates of events between different node pairs. Extensive work has been done in this setting, including well-developed and computationally robust modelling classes like SAOM ([Snijders, 2017](#); [Koskinen and Snijders, 2023](#)), relational event models ([Perry and Wolfe, 2013](#); [Butts et al., 2023](#); [Bianchi et al., 2024](#)) and network-structured multivariate point processes ([Matias et al., 2018](#)). From our discrete-time viewpoint, with the exception of SAOMs, which have been implemented in a discrete-time setting, we do not compare further to these approaches here. When both discrete and continuous-time modelling is possible, continuous-time model classes may be preferred, depending on the nature of the data and the goals of the analysis. We show in Section 6 that relational event data coerced to discrete-time snapshots at a suitable resolution can be analyzed effectively within our modelling framework. In this case, accumulation of the data over regular intervals can be used to smooth out very non-stationary or periodic behaviour at higher frequencies which may be present in the underlying continuous-time process (see Appendix E of the supplementary material).

In the discrete-time setting, existing classes of models can be loosely characterized in terms of two types of edge dependence: *within-snapshot* and *between-snapshot*. Within-snapshot edge dependence describes the dependence patterns possible among the edge variables in a fixed snapshot, thus we refer to previous work on static networks. The simplest pattern is *full independence*, for instance in the classical Erdos-Renyi (ER) model. Exponential random graph models (ERGM, [Robins et al., 2007](#)) in principle allow for arbitrary *full dependence* patterns among the edge variables; in practice these patterns must be specified through a parametric model. Note that ERGMs can also specify conditional models for edge variables, which depend on exogenous node or edge attributes; we do not pursue this direction

in our modelling framework. In recent years, advances have been made to overcome some practical issues with ERGM inference (Blackburn and Handcock, 2023). However, asymptotic analysis of ERGM parameter estimates remains limited. In recent work, Schweinberger et al. (2020) have considered a restriction of ERGMs to an intermediate *local dependence* regime (LD-ERGM): under a known partition of the network nodes into communities, they model within-community edges and allow for arbitrary dependence among edge variables in the same community, facilitating theoretical advances for parameter estimation and inference (Stewart, 2024).

Between-snapshot edge dependence describes the dependence patterns possible between the edge variables in different snapshots. As in the within-snapshot case, the simplest pattern is *full independence*, which holds if edges in different snapshots are all mutually independent. Previous works on AR network models (Jiang et al., 2023; Jiang et al., 2025) have extended this to *edgewise dependence*: in this case, the only dependence between snapshots is between edge variables with the same (unordered) indices $\{i, j\}$. To our knowledge, more general forms of local dependence based on communities like in Schweinberger et al. (2020) have not yet been studied in the discrete dynamic setting. Seminal work on (S)TERGM (Hanneke et al., 2010; Krivitsky and Handcock, 2014; Krivitsky et al., 2025), a related class of *logistic network regression* models (LNR, Almquist and Butts, 2014), as well as our new class of dependent-edge AR models allow for the specification of *full dependence* patterns among the edge variables between different snapshots. All three frameworks can capture arbitrary patterns of between-snapshot dependence through parametric models which specify the transition distributions of network snapshots.

Between-snapshot dependence can also be induced through latent variable modelling. Both the SBM (Matias and Miele, 2017; Pensky and Zhang, 2019) and LSM (Sewell and Chen, 2015; Durante and Dunson, 2016; Gallagher et al., 2021; Zhang et al., 2024) have been extended to the the dynamic regime, typically by assuming full independence of edge variables (both within and between snapshots), conditional on an evolving sequence of latent variables, as in a hidden Markov model. We note that latent variable modelling does not

preclude additional explicit modelling of edge dependence, see for instance the *co-evolving* network model of [Zhu et al. \(2023\)](#) which specifies both edgewise persistence effects and evolving latent variables which depend on previous network snapshots; or the *block logistic autoregressive* model of [Süveges and Olhede \(2023\)](#), which specifies edgewise autoregressive terms, as well as evolving sequences of latent community memberships for each node.

We summarize this discussion in Table 1, which organizes existing marginal dependence models in terms of patterns of within and between snapshot edge dependence. Our new dependent-edge AR models, (S)TERGMs, and SAOMs are all able to specify arbitrary between-snapshot edge dependence. General (S)TERGMs and SAOMs are more flexible, and can also specify arbitrary within-snapshot dependence. In the case of SAOMs, edge dependence occurs as a consequence of temporal dependence among the edge events which are intermediate to the discrete observation times. Our framework assumes independence of the within-snapshot edges conditional on past snapshots. The same conditional independence assumption is made for LNRs by [Almquist and Butts \(2014\)](#) and TERGMs by [Hanneke et al. \(2010\)](#). Table 1 also clearly identifies avenues for future work. Expanding the allowable patterns of within-snapshot edge dependence would be valuable from a modelling perspective, allowing us to capture behavior currently only possible with (S)TERGMs or SAOMs, while *local within-snapshot* dependence as in [Schweinberger et al. \(2020\)](#) may provide a path to tractable theoretical analysis.

3 AR(m) network framework

3.1 Model

Consider a dynamic network process defined on p nodes denoted by $1, \dots, p$. Let $\mathbf{X}_t \equiv (X_{i,j}^t)_{p \times p}$ be the adjacency matrix at time t , where $X_{i,j}^t = 1$ denotes the existence of an edge between nodes i and j at time t , and $X_{i,j}^t = 0$ otherwise. For simplicity, we only consider undirected networks without self-loops, i.e., $X_{i,i}^t \equiv 0$ and $X_{i,j}^t = X_{j,i}^t$. The main idea can be applied to directed networks.

Definition 1 (AR(m) networks) Conditionally on $\{\mathbf{X}_s\}_{s \leq t-1}$, the edges $\{X_{i,j}^t\}_{1 \leq i < j \leq p}$ are mutually independent with

$$\begin{aligned}\alpha_{i,j}^{t-1} &\equiv \mathbb{P}(X_{i,j}^t = 1 \mid X_{i,j}^{t-1} = 0, \mathbf{X}_{t-1} \setminus X_{i,j}^{t-1}, \mathbf{X}_{t-k} \text{ for } k \geq 2) \\ &= \mathbb{P}(X_{i,j}^t = 1 \mid X_{i,j}^{t-1} = 0, \mathbf{X}_{t-1} \setminus X_{i,j}^{t-1}, \mathbf{X}_{t-2}, \dots, \mathbf{X}_{t-m}),\end{aligned}\quad (1)$$

$$\begin{aligned}\beta_{i,j}^{t-1} &\equiv \mathbb{P}(X_{i,j}^t = 0 \mid X_{i,j}^{t-1} = 1, \mathbf{X}_{t-1} \setminus X_{i,j}^{t-1}, \mathbf{X}_{t-k} \text{ for } k \geq 2) \\ &= \mathbb{P}(X_{i,j}^t = 0 \mid X_{i,j}^{t-1} = 1, \mathbf{X}_{t-1} \setminus X_{i,j}^{t-1}, \mathbf{X}_{t-2}, \dots, \mathbf{X}_{t-m}),\end{aligned}\quad (2)$$

where $m \geq 1$ is an integer.

An AR(m) network process defined above is a Markov chain with order m . Based on (1) and (2), it holds that for $x \in \{0, 1\}$,

$$\mathbb{P}(X_{i,j}^t = x \mid \mathbf{X}_{t-1}, \dots, \mathbf{X}_{t-m}) = (1 - \gamma_{i,j}^{t-1})^{1-x} (\gamma_{i,j}^{t-1})^x,$$

where

$$\gamma_{i,j}^{t-1} = \alpha_{i,j}^{t-1} + X_{i,j}^{t-1} (1 - \alpha_{i,j}^{t-1} - \beta_{i,j}^{t-1}) = \mathbb{P}(X_{i,j}^t = 1 \mid \mathbf{X}_{t-1}, \dots, \mathbf{X}_{t-m}), \quad (3)$$

i.e., $X_{i,j}^t \mid \mathbf{X}_{t-1}, \dots, \mathbf{X}_{t-m} \sim \text{Bernoulli}(\gamma_{i,j}^{t-1})$, $1 \leq i < j \leq p$. Clearly edges $X_{i,j}^t$, for different (i, j) , are not necessarily independent of each other in practice. We may impose various forms for the conditional probabilities $\alpha_{i,j}^{t-1}$ and $\beta_{i,j}^{t-1}$ to reflect different stylized features of network data that capture such dependency. Put

$$\begin{aligned}\alpha_{i,j}^{t-1} &= f_{i,j}(\mathbf{X}_{t-1} \setminus X_{i,j}^{t-1}, \mathbf{X}_{t-2}, \dots, \mathbf{X}_{t-m}; \boldsymbol{\theta}_0), \\ \beta_{i,j}^{t-1} &= g_{i,j}(\mathbf{X}_{t-1} \setminus X_{i,j}^{t-1}, \mathbf{X}_{t-2}, \dots, \mathbf{X}_{t-m}; \boldsymbol{\theta}_0),\end{aligned}\quad (4)$$

where $f_{i,j}$'s and $g_{i,j}$'s are known functions, and $\boldsymbol{\theta}_0 \in \boldsymbol{\Theta} \subset \mathbb{R}^q$ is a q -dimensional unknown true parameter vector. For any $\boldsymbol{\theta} \in \boldsymbol{\Theta}$, write

$$\begin{aligned}\alpha_{i,j}^{t-1}(\boldsymbol{\theta}) &= f_{i,j}(\mathbf{X}_{t-1} \setminus X_{i,j}^{t-1}, \mathbf{X}_{t-2}, \dots, \mathbf{X}_{t-m}; \boldsymbol{\theta}), \\ \beta_{i,j}^{t-1}(\boldsymbol{\theta}) &= g_{i,j}(\mathbf{X}_{t-1} \setminus X_{i,j}^{t-1}, \mathbf{X}_{t-2}, \dots, \mathbf{X}_{t-m}; \boldsymbol{\theta}).\end{aligned}$$

Then $\alpha_{i,j}^{t-1} = \alpha_{i,j}^{t-1}(\boldsymbol{\theta}_0)$ and $\beta_{i,j}^{t-1} = \beta_{i,j}^{t-1}(\boldsymbol{\theta}_0)$.

Modelling dynamic networks by Markov or/and AR models is not new. See, for example, Snijders (2005), Ludkin et al. (2018), Yang et al. (2011), Yudovina et al. (2015), and Jiang et al. (2023). However, most available Markov models are designed for Erdős-Renyi networks with independent edges. Our setting provides a general framework to accommodate various dependency structures across different edges. Some practical network models satisfying this general framework are introduced in Section 4.

For the special AR(1) processes (i.e., $m = 1$), if both $f_{i,j}$ and $g_{i,j}$ in (4) are always positive and smaller than 1 for all $1 \leq i < j \leq p$, $\{\mathbf{X}_t\}_{t \geq 1}$ is an irreducible homogeneous Markov chain with $2^{p(p-1)/2}$ states. Therefore when p is fixed, (i) there exists a unique stationary distribution, and (ii) if \mathbf{X}_0 is activated according to this stationary distribution, the process $\{\mathbf{X}_t\}_{t \geq 1}$ is strictly stationary and ergodic. See Theorems 3.1, 3.3 and 4.1 in Chapter 3 of Brémaud (1998). Hence the degree heterogeneity model introduced below in Section 4.1 and the transitivity model introduced in Section 4.3 are strictly stationary for any fixed constant p if all the transition probability functions $\alpha_{i,j}^{t-1}$ and $\beta_{i,j}^{t-1}$ are strictly between 0 and 1. It is worth pointing out that the ergodicity only holds for any fixed constant p . Hence we cannot take for granted that the sample means of \mathbf{X}_t and/or its summary statistics converge when p diverges together with the sample size, even when \mathbf{X}_t is stationary. This causes the major theoretical challenges. Note that stationarity is not an asymptotic property while ergodicity is.

3.2 Relationship to TERGMs

Our model assumes that the edges are conditionally independent given their lagged values. While general TERGMs can specify models with full within-snapshot dependence, a similar conditional independence assumption is made by Hanneke et al. (2010), to ensure non-degeneracy of the network transition distribution. Compared to this restricted class of TERGMs studied by Hanneke et al. (2010), instead of requiring the transitions to follow an exponential family distribution, we may flexibly define the probability for forming a new

edge in (1), and dissolving an existing edge in (2). Those two probability functions can be in any desired forms as presented in (4), provided that their values lie between 0 and 1. See Section 4 for examples. The numerical analyses in Section 6 and Section B of the supplementary material indicate that the proposed AR models are capable of simulating and reflecting some observed interesting dynamic network phenomena.

A TERGM (Hanneke et al., 2010; Krivitsky and Handcock, 2014) is specified by

$$\mathbb{P}(\mathbf{X}_t | \mathbf{X}_{t-1}, \dots, \mathbf{X}_{t-m}; \boldsymbol{\theta}) \propto \exp\{\boldsymbol{\varsigma}(\boldsymbol{\theta})^\top \boldsymbol{\varrho}(\mathbf{X}_t, \mathbf{X}_{t-1}, \dots, \mathbf{X}_{t-m})\},$$

where $\boldsymbol{\varsigma}$ maps the underlying unknown parameters to a natural parameter, and $\boldsymbol{\varrho}$ maps the present and past network configurations to a low-dimensional vector of sufficient statistics. Under the additional assumption of conditional edge independence, $\boldsymbol{\varrho}$ will decompose into a sum over the edges, and any TERGM can be expressed in our AR(m) framework as

$$\begin{aligned} \alpha_{i,j}^{t-1}(\boldsymbol{\theta}) &= \frac{\exp\{\boldsymbol{\phi}(\boldsymbol{\theta})^\top \mathbf{u}_{i,j}(\mathbf{X}_{t-1} \setminus X_{i,j}^{t-1}, \mathbf{X}_{t-2}, \dots, \mathbf{X}_{t-m})\}}{1 + \exp\{\boldsymbol{\phi}(\boldsymbol{\theta})^\top \mathbf{u}_{i,j}(\mathbf{X}_{t-1} \setminus X_{i,j}^{t-1}, \mathbf{X}_{t-2}, \dots, \mathbf{X}_{t-m})\}}, \\ \beta_{i,j}^{t-1}(\boldsymbol{\theta}) &= \frac{\exp\{\boldsymbol{\psi}(\boldsymbol{\theta})^\top \mathbf{v}_{i,j}(\mathbf{X}_{t-1} \setminus X_{i,j}^{t-1}, \mathbf{X}_{t-2}, \dots, \mathbf{X}_{t-m})\}}{1 + \exp\{\boldsymbol{\psi}(\boldsymbol{\theta})^\top \mathbf{v}_{i,j}(\mathbf{X}_{t-1} \setminus X_{i,j}^{t-1}, \mathbf{X}_{t-2}, \dots, \mathbf{X}_{t-m})\}}, \end{aligned} \quad (5)$$

where $\mathbf{u}_{i,j}(\cdot)$ and $\mathbf{v}_{i,j}(\cdot)$ have closed-form expressions depending on the sufficient statistics of the original TERGM. Notice that the possible forms of the transition probabilities in (5) are restricted: one must take a linear combination of the natural parameter and sufficient statistics, and pass through an inverse logistic link function.

If $\boldsymbol{\phi}(\boldsymbol{\theta})$ and $\boldsymbol{\psi}(\boldsymbol{\theta})$ in (5) are replaced by, respectively, $\boldsymbol{\phi}(\boldsymbol{\theta}_\alpha)$ and $\boldsymbol{\psi}(\boldsymbol{\theta}_\beta)$, where $\boldsymbol{\theta}_\alpha$ and $\boldsymbol{\theta}_\beta$ are two sets of different parameters, \mathbf{X}_t follows a STERGM with conditional independent edges given the past networks (Krivitsky and Handcock, 2014). See Section A of the supplementary material for detailed discussion and derivations regarding the relationship of the proposed dependent-edge AR models and TERGMs.

4 Some interesting AR network models

To illustrate the usefulness of the AR(m) framework proposed above, we state three AR(m) network models which reflect various stylized features in real network data. In all three models, the parameters $\{\xi_i\}_{i=1}^p$ and $\{\eta_i\}_{i=1}^p$ reflect node heterogeneity in, respectively, forming a new edge and dissolving an existing edge. Specifically, the larger ξ_i is, the more likely node i will form new edges with other nodes, and the larger η_i is, the more likely the existing edges between node i and the others will be dissolved. Instances of these three models can be simulated using our development R package `arnetworks`. Our package provides an implementation of our maximum-likelihood-based parameter estimation and inference procedure for the transitivity model (Section 4.3), as described in Section 5 and Section B of the supplementary material, and a general method-of-moments-based estimation approach introduced in Section D of the supplementary material, which can be applied to a broad class of dynamic network models, including but not limited to the three models discussed below. More details are available at <https://github.com/peterwmacd/arnetworks>.

4.1 Degree heterogeneity model

For any $i \neq j$, let

$$\vartheta_{i,j}^{t-1} = \exp\{a_0 D_{-i,-j}^{t-1} + a_1(D_i^{t-1} + D_j^{t-1})\},$$

$$\varpi_{i,j}^{t-1} = \exp\{b_0(1 - D_{-i,-j}^{t-1}) + b_1(2 - D_i^{t-1} - D_j^{t-1})\},$$

with

$$D_{-i,-j}^{t-1} = \frac{1}{(p-2)(p-3)} \sum_{k,\ell: k,\ell \neq i,j, k \neq \ell} X_{k,\ell}^{t-1}, \quad D_i^{t-1} = \frac{1}{p-1} \sum_{\ell: \ell \neq i} X_{i,\ell}^{t-1},$$

where D_i^{t-1} and D_j^{t-1} are, respectively, the (normalized) degrees of node i and node j at time $t-1$, and $D_{-i,-j}^{t-1}$ is the (normalized) average degree excluding nodes i and j at time

$t - 1$. We specify the transition probabilities as follows:

$$\alpha_{i,j}^{t-1}(\boldsymbol{\theta}) = \frac{\xi_i \xi_j \vartheta_{i,j}^{t-1}}{1 + \vartheta_{i,j}^{t-1} + \varpi_{i,j}^{t-1}}, \quad \beta_{i,j}^{t-1}(\boldsymbol{\theta}) = \frac{\eta_i \eta_j \varpi_{i,j}^{t-1}}{1 + \vartheta_{i,j}^{t-1} + \varpi_{i,j}^{t-1}}. \quad (1)$$

This is an AR(1) model with parameter vector $\boldsymbol{\theta} = (a_0, a_1, b_0, b_1, \xi_1, \dots, \xi_p, \eta_1, \dots, \eta_p)^\top \in \boldsymbol{\Theta} \subset \mathbb{R}_+^{2p+4}$. This model is able to capture a “rich get richer” effect in network evolution, whereby nodes with higher degree at time $t - 1$ are more likely to form new connections at time t , and vice versa. In particular, the propensity to form a new edge between nodes i and j at time t is positively impacted by $D_{-i,-j}^{t-1}$, D_i^{t-1} and D_j^{t-1} , and the propensity to dissolve an existing edge between nodes i and j at time t is negatively impacted by these three quantities.

[Hanneke et al. \(2010\)](#) proposed a TERGM including a density statistic (equivalent to network average degree). In (1), we explicitly specify the impact from the previous snapshot’s average degree on forming a new edge and dissolving an existing edge, while the model defined in Section 2.1 of [Hanneke et al. \(2010\)](#) depends on the current snapshot’s average degree, and does not differentiate the representations for these two types of impact. Within the STERGM framework, the edge counts model of [Krivitsky and Handcock \(2014\)](#) assumes that the collection of all newly formed edges is conditionally independent of the collection of all newly dissolved edges given their history, and the two conditional distributions are controlled by different parameters.

4.2 Persistence model

We define the transition probabilities

$$\begin{aligned} \alpha_{i,j}^{t-1}(\boldsymbol{\theta}) &= \xi_i \xi_j \exp[-1 - a\{(1 - X_{i,j}^{t-2}) + (1 - X_{i,j}^{t-2})(1 - X_{i,j}^{t-3})\}], \\ \beta_{i,j}^{t-1}(\boldsymbol{\theta}) &= \eta_i \eta_j \exp\{-1 - b(X_{i,j}^{t-2} + X_{i,j}^{t-2} X_{i,j}^{t-3})\}. \end{aligned} \quad (2)$$

This is an AR(3) model with parameter vector $\boldsymbol{\theta} = (a, b, \xi_1, \dots, \xi_p, \eta_1, \dots, \eta_p)^\top \in \boldsymbol{\Theta} \subset \mathbb{R}_+^{2p+2}$. The probability to form a new edge between nodes i and j at time t is reduced if $X_{i,j}^{t-2} = 0$,

and it is reduced further if, in addition, $X_{i,j}^{t-3} = 0$. The probability to dissolve an existing edge is reduced if $X_{i,j}^{t-2} = 1$, and it is reduced further if, in addition, $X_{i,j}^{t-3} = 1$. Hence if the edge status between two nodes is unchanged for 2 or 3 time periods, the probability for it remaining unchanged next time is larger than that otherwise.

Model (2) defines an AR(3) network process $\mathbf{X}_t = (X_{i,j}^t)_{p \times p}$ with $p(p-1)/2$ independent edge processes. Although the conclusion on the AR(1) stationarity in the last paragraph of Section 3.1 does not apply directly, this AR(3) network process is also strictly stationary, which is implied by the fact that $\{X_{i,j}^t\}_{t \geq 1}$ is strictly stationary for each $1 \leq i < j \leq p$. Formally, for given (i, j) such that $1 \leq i < j \leq p$, let $\mathbf{Y}_t = (X_{i,j}^t, X_{i,j}^{t-1}, X_{i,j}^{t-2})^\top$. Then $\{\mathbf{Y}_t\}_{t \geq 1}$ is a homogeneous Markov chain with $2^3 = 8$ states. Let \mathbf{P} denote the transition probability matrix of $\{\mathbf{Y}_t\}_{t \geq 1}$. Then \mathbf{P} is a 8×8 matrix with only 2 positive elements in each row and each column, provided that $\xi_i \xi_j, \eta_i \eta_j \in (0, e)$. It is straightforward to check that each row or column of \mathbf{P}^2 has only 4 positive elements, and, more importantly, all the elements of \mathbf{P}^3 is positive. Hence, the Markov chain $\{\mathbf{Y}_t\}_{t \geq 1}$ is irreducible. By Theorems 3.1 and 3.3 in Chapter 3 of [Brémaud \(1998\)](#), the process $\{\mathbf{Y}_t\}_{t \geq 1}$ is strictly stationary, and so is $\{X_{i,j}^t\}_{t \geq 1}$.

Persistent connectivity or non-connectivity is widely observed in, for example, brain networks, gene connections and social networks. A related TERGM including a stability statistic defined in [Hanneke et al. \(2010\)](#), does not consider lags of order 2 and 3, and does not differentiate between the propensity for retaining an existing edge and that for retaining a no-edge status.

4.3 Transitivity model

We propose an AR(1) model to reflect the feature of transitivity which refers to the phenomenon that nodes are more likely to link if they share links in common (i.e., “the friend of

my friend is also my friend”). To this end, we specify the transition probabilities as follows:

$$\begin{aligned}\alpha_{i,j}^{t-1}(\boldsymbol{\theta}) &= \frac{\xi_i \xi_j \exp(a U_{i,j}^{t-1})}{1 + \exp(a U_{i,j}^{t-1}) + \exp(b V_{i,j}^{t-1})}, \\ \beta_{i,j}^{t-1}(\boldsymbol{\theta}) &= \frac{\eta_i \eta_j \exp(b V_{i,j}^{t-1})}{1 + \exp(a U_{i,j}^{t-1}) + \exp(b V_{i,j}^{t-1})},\end{aligned}\tag{3}$$

where $\boldsymbol{\theta} = (a, b, \xi_1, \dots, \xi_p, \eta_1, \dots, \eta_p)^\top \in \mathbb{R}_+^{2p+2}$, and

$$\begin{aligned}U_{i,j}^{t-1} &= \frac{1}{p-2} \sum_{k: k \neq i,j} X_{i,k}^{t-1} X_{j,k}^{t-1}, \\ V_{i,j}^{t-1} &= \frac{1}{p-2} \sum_{k: k \neq i,j} \{X_{i,k}^{t-1} (1 - X_{j,k}^{t-1}) + (1 - X_{i,k}^{t-1}) X_{j,k}^{t-1}\}.\end{aligned}\tag{4}$$

The pair $(U_{i,j}^{t-1}, V_{i,j}^{t-1})$ characterizes the number of nodes with which both nodes i and j are connected, and the number of nodes with which only one of i and j is connected at time $t-1$. The larger $U_{i,j}^{t-1}$ is (i.e., the more common friends i and j share at time $t-1$), the more likely $X_{i,j}^t = 1$. The larger $V_{i,j}^{t-1}$ is, the more likely $X_{i,j}^t = 0$. This reflects the transitivity of the networks. High levels of transitivity are found in various networks including friendship networks, industrial supply-chains, international trade flows, and alliances across firms and nations. Note that the quantity $U_{i,j}^{t-1}$, used in [Graham \(2016\)](#) to define the edge status of $X_{i,j}^t$, reflects the information based on which companies such as Facebook and LinkedIn have recommended new links to their customers. Also see the TERGM including a transitivity statistic defined in [Hanneke et al. \(2010\)](#).

We may use different parameters a and b in defining $\alpha_{i,j}^{t-1}(\boldsymbol{\theta})$ and $\beta_{i,j}^{t-1}(\boldsymbol{\theta})$ in (3). We do not pursue this more general form as (i) using different ξ_i and η_i reflects already the differences in the propensity between forming a new edge and dissolving an existing edge, and, perhaps more importantly, (ii) since most practical networks are sparse, the effective sample size for estimating the transition probability from the state of an existing edge is small. Therefore estimating the parameters only occurring in $\beta_{i,j}^{t-1}(\boldsymbol{\theta})$ will be harder than those in $\alpha_{i,j}^{t-1}(\boldsymbol{\theta})$. Using the same a and b in both $\alpha_{i,j}^{t-1}(\boldsymbol{\theta})$ and $\beta_{i,j}^{t-1}(\boldsymbol{\theta})$ improves the estimation by pulling the information together. See also the relevant simulation results in Section C.3

of the supplementary material.

5 Estimation

In this section, we present estimation procedures based on the maximum likelihood principle, and show they are valid if the number of nodes p and the sample size n satisfy the restriction $p \ll n^\delta$ for some constant $\delta > 0$, which allows the number of nodes p to either be fixed or diverge together with n . When p diverges with n , both the ergodicity and the central limit theorem for stationary Markov chains no longer apply even when \mathbf{X}_t is stationary (see the last paragraph in Section 3.1). This causes the major theoretical challenges faced here. Based on the conditional independence in our setting, we can construct an appropriate martingale difference sequence, which facilitates the required asymptotic analysis without the stationarity assumption, regardless of whether p is fixed or diverges together with n .

5.1 General approach

The natural units of observation in our model are the $X_{i,j}^t$, indicating presence or absence of an edge between nodes i and j at time t . Intuitively, the extent to which these observations can contribute useful information to the estimation of a given element of $\boldsymbol{\theta}_0$ depends in turn on the extent to which that element plays a consistent role over time t in the corresponding probabilities

$$\gamma_{i,j}^{t-1}(\boldsymbol{\theta}) = \alpha_{i,j}^{t-1}(\boldsymbol{\theta}) + X_{i,j}^{t-1}\{1 - \alpha_{i,j}^{t-1}(\boldsymbol{\theta}) - \beta_{i,j}^{t-1}(\boldsymbol{\theta})\}.$$

By (3), we have $\gamma_{i,j}^{t-1} = \gamma_{i,j}^{t-1}(\boldsymbol{\theta}_0)$. We formalize the above intuition as follows.

Definition 2 (Global/local parameters) *Write $\boldsymbol{\theta} = (\theta_1, \dots, \theta_q)^\top$, where $q \geq 1$ is the total number of parameters. Let*

$$\mathcal{G} = \{l \in [q] : \gamma_{i,j}^{t-1}(\boldsymbol{\theta}) \text{ involves } \theta_l \text{ for all } 1 \leq i < j \leq p \text{ and } t \in [n] \setminus [m]\}.$$

We call $\boldsymbol{\theta}_{\mathcal{G}}$ and $\boldsymbol{\theta}_{\mathcal{G}^c}$, respectively, the global parameter vector and the local parameter vector.

In the degree heterogeneity model described in Section 4.1, the global parameter vector takes the form $\boldsymbol{\theta}_{\mathcal{G}} = (a_0, a_1, b_0, b_1)^\top$. For the persistence and transitivity models introduced in Sections 4.2 and 4.3, we have $\boldsymbol{\theta}_{\mathcal{G}} = (a, b)^\top$. In these three models, the local parameters are represented by $\boldsymbol{\theta}_{\mathcal{G}^c} = (\xi_1, \dots, \xi_p, \eta_1, \dots, \eta_p)^\top$. Recall that m denotes the order of the AR network process. We have $m = 1$ for both the degree heterogeneity model and transitivity model, and $m = 3$ for the persistence model. As we will discuss in Section 5.2, the global parameter vector $\boldsymbol{\theta}_{0,\mathcal{G}}$ and the local parameter vector $\boldsymbol{\theta}_{0,\mathcal{G}^c}$ need to be treated differently, which we accomplish via partial likelihoods. The resulting estimators may also entertain different convergence rates.

We develop the estimation theory for our models in three stages below. Sufficient conditions for identification of $\boldsymbol{\theta}_0$ are established with respect to an expected partial log-likelihood $\ell_{n,p}^{(l)}(\boldsymbol{\theta})$, defined in (1) below. An initial estimator $\tilde{\boldsymbol{\theta}}$ results from maximizing the corresponding partial log-likelihoods $\hat{\ell}_{n,p}^{(l)}(\boldsymbol{\theta})$ defined in (5) below, for each $l \in [q]$. Finally, because of the potential high-dimensionality of our models (number of local parameters increasing with number of nodes), these estimators suffer from slow rates of convergence. We offer estimators with improved rate of convergence, derived as a refinement of the initial estimator via the notion of projected score functions. To study the convergence properties of the proposed estimation procedures, a key step is to investigate the convergence rate of $\sup_{\boldsymbol{\theta} \in \Theta} |\hat{\ell}_{n,p}^{(l)}(\boldsymbol{\theta}) - \ell_{n,p}^{(l)}(\boldsymbol{\theta})|$. As standard techniques are not applicable due to the temporal dependence inherent in our dependent-edge AR network models, we construct a martingale difference structure for the network models and use such structure to address the theoretical challenge rigorously. See Lemma 2 and its proof in the supplementary material for further details.

5.2 Identification of $\boldsymbol{\theta}_0$

Let \mathcal{F}_t be the σ -field generated by $\{\mathbf{X}_1, \dots, \mathbf{X}_t\}$. For any $l \in [q]$, define

$$\mathcal{S}_l = \{(i, j) : 1 \leq i < j \leq p \text{ and } \gamma_{i,j}^{t-1}(\boldsymbol{\theta}) \text{ involves } \theta_l \text{ for any } t \in [n] \setminus [m]\}.$$

If θ_l is a global parameter, $\mathcal{S}_l = \{(i, j) : 1 \leq i < j \leq p\}$. For estimating θ_l for $l \in [q]$, put

$$\ell_{n,p}^{(l)}(\boldsymbol{\theta}) = \frac{1}{(n-m)|\mathcal{S}_l|} \sum_{t=m+1}^n \sum_{(i,j) \in \mathcal{S}_l} \mathbb{E}_{\mathcal{F}_{t-1}} \left\{ \log \left[\{\gamma_{i,j}^{t-1}(\boldsymbol{\theta})\}^{X_{i,j}^t} \{1 - \gamma_{i,j}^{t-1}(\boldsymbol{\theta})\}^{1-X_{i,j}^t} \right] \right\}, \quad (1)$$

where $\mathbb{E}_{\mathcal{F}_{t-1}}(\cdot)$ denotes the conditional expectation given \mathcal{F}_{t-1} with the unknown true parameter vector $\boldsymbol{\theta}_0$. For any $t \in [n] \setminus [m]$ and $1 \leq i < j \leq p$, due to $\log x \leq x - 1$ for any $x > 0$, we have

$$\begin{aligned} & \mathbb{E}_{\mathcal{F}_{t-1}} \left\{ \log \left[\{\gamma_{i,j}^{t-1}(\boldsymbol{\theta})\}^{X_{i,j}^t} \{1 - \gamma_{i,j}^{t-1}(\boldsymbol{\theta})\}^{1-X_{i,j}^t} \right] \right\} \\ & \quad - \mathbb{E}_{\mathcal{F}_{t-1}} \left\{ \log \left[\{\gamma_{i,j}^{t-1}(\boldsymbol{\theta}_0)\}^{X_{i,j}^t} \{1 - \gamma_{i,j}^{t-1}(\boldsymbol{\theta}_0)\}^{1-X_{i,j}^t} \right] \right\} \\ & \leq \mathbb{E}_{\mathcal{F}_{t-1}} \left[\frac{\{\gamma_{i,j}^{t-1}(\boldsymbol{\theta})\}^{X_{i,j}^t} \{1 - \gamma_{i,j}^{t-1}(\boldsymbol{\theta})\}^{1-X_{i,j}^t}}{\{\gamma_{i,j}^{t-1}(\boldsymbol{\theta}_0)\}^{X_{i,j}^t} \{1 - \gamma_{i,j}^{t-1}(\boldsymbol{\theta}_0)\}^{1-X_{i,j}^t}} \right] - 1 \\ & = \frac{\gamma_{i,j}^{t-1}(\boldsymbol{\theta})}{\gamma_{i,j}^{t-1}(\boldsymbol{\theta}_0)} \cdot \gamma_{i,j}^{t-1}(\boldsymbol{\theta}_0) + \frac{1 - \gamma_{i,j}^{t-1}(\boldsymbol{\theta})}{1 - \gamma_{i,j}^{t-1}(\boldsymbol{\theta}_0)} \cdot \{1 - \gamma_{i,j}^{t-1}(\boldsymbol{\theta}_0)\} - 1 = 0, \end{aligned}$$

which implies $\ell_{n,p}^{(l)}(\boldsymbol{\theta}) \leq \ell_{n,p}^{(l)}(\boldsymbol{\theta}_0)$ for any $\boldsymbol{\theta} \in \boldsymbol{\Theta}$. Notice that

$$\begin{aligned} & \mathbb{E}_{\mathcal{F}_{t-1}} \left\{ \log \left[\{\gamma_{i,j}^{t-1}(\boldsymbol{\theta})\}^{X_{i,j}^t} \{1 - \gamma_{i,j}^{t-1}(\boldsymbol{\theta})\}^{1-X_{i,j}^t} \right] \right\} \\ & \quad - \mathbb{E}_{\mathcal{F}_{t-1}} \left\{ \log \left[\{\gamma_{i,j}^{t-1}(\boldsymbol{\theta}_0)\}^{X_{i,j}^t} \{1 - \gamma_{i,j}^{t-1}(\boldsymbol{\theta}_0)\}^{1-X_{i,j}^t} \right] \right\} = 0 \end{aligned}$$

if and only if

$$\frac{\{\gamma_{i,j}^{t-1}(\boldsymbol{\theta})\}^{X_{i,j}^t} \{1 - \gamma_{i,j}^{t-1}(\boldsymbol{\theta})\}^{1-X_{i,j}^t}}{\{\gamma_{i,j}^{t-1}(\boldsymbol{\theta}_0)\}^{X_{i,j}^t} \{1 - \gamma_{i,j}^{t-1}(\boldsymbol{\theta}_0)\}^{1-X_{i,j}^t}} = 1, \quad (2)$$

where (2) is equivalent to $\gamma_{i,j}^{t-1}(\boldsymbol{\theta}) = \gamma_{i,j}^{t-1}(\boldsymbol{\theta}_0)$. Hence, for any $\boldsymbol{\theta} \in \boldsymbol{\Theta} \setminus \{\boldsymbol{\theta}_0\}$, $\ell_{n,p}^{(l)}(\boldsymbol{\theta}) = \ell_{n,p}^{(l)}(\boldsymbol{\theta}_0)$ if and only if $\gamma_{i,j}^{t-1}(\boldsymbol{\theta}) = \gamma_{i,j}^{t-1}(\boldsymbol{\theta}_0)$ for any $t \in [n] \setminus [m]$ and $(i, j) \in \mathcal{S}_l$. To guarantee the identification of $\boldsymbol{\theta}_0$, we impose the following regularity conditions.

Condition 1 (i) *There exists some universal constant $C_1 > 0$ such that*

$$\min_{t \in [n] \setminus [m]} \min_{i,j: 1 \leq i < j \leq p} \inf_{\boldsymbol{\theta} \in \Theta} \gamma_{i,j}^{t-1}(\boldsymbol{\theta}) \{1 - \gamma_{i,j}^{t-1}(\boldsymbol{\theta})\} \geq C_1.$$

(ii) *For any $1 \leq i < j \leq p$ and $t \in [n] \setminus [m]$, $\gamma_{i,j}^{t-1}(\boldsymbol{\theta})$ is thrice continuously differentiable with respect to $\boldsymbol{\theta} \in \Theta$. Furthermore, there exists some universal constant $C_2 > 0$ such that*

$$\max_{t \in [n] \setminus [m]} \max_{i,j: 1 \leq i < j \leq p} \sup_{\boldsymbol{\theta} \in \Theta} \left| \frac{\partial^k \gamma_{i,j}^{t-1}(\boldsymbol{\theta})}{\partial \boldsymbol{\theta}^k} \right|_{\infty} \leq C_2$$

for any $k \in [3]$.

Condition 1 specifies conditions for the parameter space Θ . We assume C_1 is a universal constant for simplifying the presentation. Our proposed methods also work when C_1 converges slowly to zero as $p \rightarrow \infty$. Recall that $\gamma_{i,j}^{t-1}(\boldsymbol{\theta}) = \alpha_{i,j}^{t-1}(\boldsymbol{\theta}) + X_{i,j}^{t-1} \{1 - \alpha_{i,j}^{t-1}(\boldsymbol{\theta}) - \beta_{i,j}^{t-1}(\boldsymbol{\theta})\}$. Due to $X_{i,j}^{t-1} \in \{0, 1\}$, Condition 1(i) holds if there exist four universal constants $c_1, c_2, c_3, c_4 \in (0, 1)$ with $c_1 < c_2$ and $c_3 < c_4$ such that

$$c_1 \leq \alpha_{i,j}^{t-1}(\boldsymbol{\theta}) \leq c_2 \quad \text{and} \quad 1 - c_4 \leq \beta_{i,j}^{t-1}(\boldsymbol{\theta}) \leq 1 - c_3$$

for any $\boldsymbol{\theta} \in \Theta$, $t \in [n] \setminus [m]$ and $1 \leq i < j \leq p$. Also, Condition 1(ii) holds provided that

$$\left| \frac{\partial^k \alpha_{i,j}^{t-1}(\boldsymbol{\theta})}{\partial \boldsymbol{\theta}^k} \right|_{\infty} \leq C_2 \quad \text{and} \quad \left| \frac{\partial^k \beta_{i,j}^{t-1}(\boldsymbol{\theta})}{\partial \boldsymbol{\theta}^k} \right|_{\infty} \leq C_2$$

for any $\boldsymbol{\theta} \in \Theta$, $t \in [n] \setminus [m]$ and $1 \leq i < j \leq p$. Based on the explicit forms of $\alpha_{i,j}^{t-1}(\boldsymbol{\theta})$ and $\beta_{i,j}^{t-1}(\boldsymbol{\theta})$ in the specific models, we can identify the associated restrictions for the parameter space Θ .

For any $1 \leq i < j \leq p$, we define

$$\mathcal{I}_{i,j} = \{l \in [q] : \gamma_{i,j}^{t-1}(\boldsymbol{\theta}) \text{ involves } \theta_l \text{ for any } t \in [n] \setminus [m]\}.$$

Condition 2 *There exists a universal constant $s \geq 1$ such that $\max_{1 \leq i < j \leq p} |\mathcal{I}_{i,j}| \leq s$.*

Condition 2 requires that the dynamics of each edge process $\{X_{i,j}^t\}_{t \geq 1}$ be driven by a finite number of parameters. Hence, the number of global parameters is finite while the total number of local parameters may diverge together with p . For the degree heterogeneity model introduced in Section 4.1, we have $\boldsymbol{\theta}_{\mathcal{I}_{i,j}} = (a_0, a_1, b_0, b_1, \xi_i, \xi_j, \eta_i, \eta_j)^\top$ with $s = 8$. For both the persistence model and transitivity model introduced in Sections 4.2 and 4.3, we have $\boldsymbol{\theta}_{\mathcal{I}_{i,j}} = (a, b, \xi_i, \xi_j, \eta_i, \eta_j)^\top$ with $s = 6$.

Condition 3 *There exists a universal constant $C_3 > 0$ such that*

$$\min_{i,j: 1 \leq i < j \leq p} \lambda_{\min} \left\{ \frac{1}{n-m} \sum_{t=m+1}^n \frac{\partial \gamma_{i,j}^{t-1}(\boldsymbol{\theta}_0)}{\partial \boldsymbol{\theta}_{\mathcal{I}_{i,j}}} \frac{\partial \gamma_{i,j}^{t-1}(\boldsymbol{\theta}_0)}{\partial \boldsymbol{\theta}_{\mathcal{I}_{i,j}}^\top} \right\} \geq C_3$$

with probability approaching one when $n \rightarrow \infty$.

Proposition 1 *Let Conditions 1–3 hold, and $C_* = 2(2C_1^{-2} + C_1^{-3})C_2^3 + 3(C_1^{-1} + C_1^{-2})C_2^2 + C_1^{-1}C_2$ with (C_1, C_2) specified in Condition 1. Assume $\sup_{\boldsymbol{\theta} \in \Theta} |\boldsymbol{\theta} - \boldsymbol{\theta}_0|_\infty < 2C_3/(C_* s^3)$. As $n \rightarrow \infty$, it holds with probability approaching one that*

$$\ell_{n,p}^{(l)}(\boldsymbol{\theta}_0) - \ell_{n,p}^{(l)}(\boldsymbol{\theta}) \geq \frac{\bar{C}}{|\mathcal{S}_l|} \sum_{(i,j) \in \mathcal{S}_l} |\boldsymbol{\theta}_{\mathcal{I}_{i,j}} - \boldsymbol{\theta}_{0,\mathcal{I}_{i,j}}|_2^2$$

for any $\boldsymbol{\theta} \in \Theta$ and $l \in [q]$, where $\bar{C} > 0$ is a universal constant.

The proof of Proposition 1 is given in Section F.1 of the supplementary material. Notice that $|\mathcal{S}_l \cap \mathcal{S}_{l'}| = |\mathcal{S}_l|$ for any $l' \in \mathcal{G} \cup \{l\}$. By Proposition 1, it holds with probability approaching one that for any $\boldsymbol{\theta} \in \Theta$ and $l \in [q]$,

$$\begin{aligned} \ell_{n,p}^{(l)}(\boldsymbol{\theta}_0) - \ell_{n,p}^{(l)}(\boldsymbol{\theta}) &\geq \frac{\bar{C}}{|\mathcal{S}_l|} \sum_{(i,j) \in \mathcal{S}_l} \sum_{l' \in \mathcal{I}_{i,j}} |\theta_{l'} - \theta_{0,l'}|_2^2 = \frac{\bar{C}}{|\mathcal{S}_l|} \sum_{l'=1}^q \sum_{(i,j) \in \mathcal{S}_l \cap \mathcal{S}_{l'}} |\theta_{l'} - \theta_{0,l'}|_2^2 \\ &= \bar{C} \sum_{l' \in \mathcal{G} \cup \{l\}} |\theta_{l'} - \theta_{0,l'}|_2^2 + \bar{C} \sum_{l' \in \mathcal{G}^c \setminus \{l\}} \frac{|\mathcal{S}_l \cap \mathcal{S}_{l'}| |\theta_{l'} - \theta_{0,l'}|_2^2}{|\mathcal{S}_l|}. \end{aligned} \tag{3}$$

Hence, for any $l \in [q]$, the function $\ell_{n,p}^{(l)}(\cdot)$ defined as (1) is a good candidate for identifying $\theta_{0,l}$ and the global parameter vector $\boldsymbol{\theta}_{0,\mathcal{G}}$ but is powerless in identifying $\theta_{0,l'}$ with $l' \in \mathcal{G}^c \setminus \{l\}$

if $|\mathcal{S}_l \cap \mathcal{S}_{l'}| \ll |\mathcal{S}_l|$. In the degree heterogeneity model, persistence model, and transitivity model introduced in Section 4, given $l \in [q]$ and $l' \in \mathcal{G}^c \setminus \{l\}$, we have (i) $|\mathcal{S}_l \cap \mathcal{S}_{l'}| = 1$ and $|\mathcal{S}_l| = p - 1$ if $l \in \mathcal{G}^c$, and (ii) $|\mathcal{S}_l \cap \mathcal{S}_{l'}| = p - 1$ and $|\mathcal{S}_l| = p(p - 1)/2$ if $l \in \mathcal{G}$, reaffirming that $\ell_{n,p}^{(l)}(\cdot)$ is informative for the identification of $\theta_{0,l}$ and the global parameters, yet ineffective for identifying $\theta_{0,l'}$ with $l' \in \mathcal{G}^c \setminus \{l\}$. Therefore, for the three models introduced in Section 4, we need to employ $\ell_{n,p}^{(l)}(\cdot)$ to identify each $\theta_{0,l}$ for $l \in [q]$.

5.3 Initial estimation for $\boldsymbol{\theta}_0$

With available observations $\mathbf{X}_1, \dots, \mathbf{X}_n$, since $\{\mathbf{X}_t\}_{t \geq 1}$ is a Markov chain with order m , the likelihood function for $\boldsymbol{\theta}$, conditionally on $\mathbf{X}_1, \dots, \mathbf{X}_m$, admits the form

$$\mathcal{L}_{n,p}(\mathbf{X}_n, \dots, \mathbf{X}_{m+1} \mid \mathbf{X}_m, \dots, \mathbf{X}_1; \boldsymbol{\theta}) = \prod_{t=m+1}^n L_{t,p}(\mathbf{X}_t \mid \mathbf{X}_{t-1}, \dots, \mathbf{X}_{t-m}; \boldsymbol{\theta}),$$

where $L_{t,p}(\mathbf{X}_t \mid \mathbf{X}_{t-1}, \dots, \mathbf{X}_{t-m}; \boldsymbol{\theta})$ is the transition probability of \mathbf{X}_t given $\mathbf{X}_{t-1}, \dots, \mathbf{X}_{t-m}$.

By (3), the (normalized) log-likelihood admits the form

$$\begin{aligned} & \frac{2}{(n-m)p(p-1)} \log \mathcal{L}_{n,p}(\mathbf{X}_n, \dots, \mathbf{X}_{m+1} \mid \mathbf{X}_m, \dots, \mathbf{X}_1; \boldsymbol{\theta}) \\ &= \frac{2}{(n-m)p(p-1)} \sum_{t=m+1}^n \sum_{i,j: 1 \leq i < j \leq p} \log [\{\gamma_{i,j}^{t-1}(\boldsymbol{\theta})\}^{X_{i,j}^t} \{1 - \gamma_{i,j}^{t-1}(\boldsymbol{\theta})\}^{1-X_{i,j}^t}], \end{aligned} \quad (4)$$

which is the sample version of $\ell_{n,p}^{(l)}(\boldsymbol{\theta})$ defined as (1) with $l \in \mathcal{G}$. As pointed out below (3), we should not estimate the local parameters based on this full log-likelihood. Therefore, for each $l \in [q]$, we define

$$\hat{\ell}_{n,p}^{(l)}(\boldsymbol{\theta}) = \frac{1}{(n-m)|\mathcal{S}_l|} \sum_{t=m+1}^n \sum_{(i,j) \in \mathcal{S}_l} \log [\{\gamma_{i,j}^{t-1}(\boldsymbol{\theta})\}^{X_{i,j}^t} \{1 - \gamma_{i,j}^{t-1}(\boldsymbol{\theta})\}^{1-X_{i,j}^t}], \quad (5)$$

which contains only the terms depending on θ_l on the right-hand side of (4) (with a rescaled normalized constant).

For any $l \in [q]$, Lemma 2 in the supplementary material shows that $\hat{\ell}_{n,p}^{(l)}(\boldsymbol{\theta})$ converges

in probability to $\ell_{n,p}^{(l)}(\boldsymbol{\theta})$ defined as (1) uniformly over $\boldsymbol{\theta} \in \Theta$. Together with Proposition 1, we can estimate the global parameter vector $\boldsymbol{\theta}_{0,\mathcal{G}}$ by maximizing the full log-likelihood $\hat{\ell}_{n,p}^{(l')}\!(\boldsymbol{\theta})$ with some $l' \in \mathcal{G}$, and estimate the local parameter $\theta_{0,l}$ with $l \in \mathcal{G}^c$ by maximizing the corresponding (partial) log-likelihood $\hat{\ell}_{n,p}^{(l)}(\boldsymbol{\theta})$. More specifically, letting

$$(\hat{\theta}_{*,1}^{(l)}, \dots, \hat{\theta}_{*,q}^{(l)})^\top = \arg \max_{\boldsymbol{\theta} \in \Theta} \hat{\ell}_{n,p}^{(l)}(\boldsymbol{\theta})$$

for each $l \in [q]$, we define the initial estimator $\tilde{\boldsymbol{\theta}} = (\tilde{\boldsymbol{\theta}}_{\mathcal{G}}^\top, \tilde{\boldsymbol{\theta}}_{\mathcal{G}^c}^\top)^\top$ for $\boldsymbol{\theta}_0$ as

$$\tilde{\boldsymbol{\theta}}_{\mathcal{G}} = (\hat{\theta}_{*,l}^{(l')})_{l \in \mathcal{G}} \quad \text{and} \quad \tilde{\boldsymbol{\theta}}_{\mathcal{G}^c} = (\hat{\theta}_{*,l}^{(l)})_{l \in \mathcal{G}^c} \quad (6)$$

for some $l' \in \mathcal{G}$. Due to $\mathcal{S}_l = \{(i, j) : 1 \leq i < j \leq p\}$ for any $l \in \mathcal{G}$, we know $\hat{\ell}_{n,p}^{(l_1)}(\boldsymbol{\theta}) = \hat{\ell}_{n,p}^{(l_2)}(\boldsymbol{\theta})$ for any $l_1, l_2 \in \mathcal{G}$, which implies that the estimator $\tilde{\boldsymbol{\theta}}_{\mathcal{G}}$ given in (6) does not depend on the selection of $l' \in \mathcal{G}$.

To investigate the theoretical properties of the estimator $\tilde{\boldsymbol{\theta}} = (\tilde{\boldsymbol{\theta}}_{\mathcal{G}}^\top, \tilde{\boldsymbol{\theta}}_{\mathcal{G}^c}^\top)^\top$, we define

$$\begin{cases} c_{n,\mathcal{G}}^2 = \frac{q \log(np)}{\sqrt{np}} + \frac{q^{3/2} \log^{3/2}(np)}{\sqrt{np^2}}, \\ c_{n,\mathcal{G}^c}^2 = \frac{q \log(nS_{\mathcal{G}^c,\min})}{\sqrt{nS_{\mathcal{G}^c,\min}}} + \frac{q^{3/2} \log^{3/2}(nS_{\mathcal{G}^c,\min})}{\sqrt{nS_{\mathcal{G}^c,\min}}}, \end{cases} \quad (7)$$

where $S_{\mathcal{G}^c,\min} = \min_{l \in \mathcal{G}^c} |\mathcal{S}_l|$. Theorem 1 shows that the convergence rate of the initial estimator for the local parameters is slower than that of the global parameters if $S_{\mathcal{G}^c,\min} \ll p^2$. The proof of Theorem 1 is given in Section F.2 of the supplementary material.

Theorem 1 *Let the conditions of Proposition 1 hold. Then $|\tilde{\boldsymbol{\theta}}_{\mathcal{G}} - \boldsymbol{\theta}_{0,\mathcal{G}}|_2 = O_p(c_{n,\mathcal{G}})$ and $|\tilde{\boldsymbol{\theta}}_{\mathcal{G}^c} - \boldsymbol{\theta}_{0,\mathcal{G}^c}|_\infty = O_p(c_{n,\mathcal{G}^c})$.*

Remark 1 *By Theorem 1, the initial estimator $\tilde{\boldsymbol{\theta}}_{\mathcal{G}}$ for the global parameters is consistent provided that*

$$q \ll \min \left\{ \frac{\sqrt{np}}{\log(np)}, \frac{n^{1/3}p^{4/3}}{\log(np)} \right\},$$

and the initial estimator $\tilde{\boldsymbol{\theta}}_{\mathcal{G}^c}$ for the local parameters is consistent provided that

$$q \ll \min \left\{ \frac{\sqrt{nS_{\mathcal{G}^c, \min}}}{\log(nS_{\mathcal{G}^c, \min})}, \frac{n^{1/3}S_{\mathcal{G}^c, \min}^{2/3}}{\log(nS_{\mathcal{G}^c, \min})} \right\}.$$

For the degree heterogeneity model introduced in Section 4.1, we have $q = 2p+4$ and $S_{\mathcal{G}^c, \min} = p - 1$. For both the persistence model and transitivity model introduced in Sections 4.2 and 4.3, we have $q = 2p + 2$ and $S_{\mathcal{G}^c, \min} = p - 1$. Hence, for these three models, Theorem 1 gives the convergence rates of $\tilde{\boldsymbol{\theta}}_{\mathcal{G}}$ and $\tilde{\boldsymbol{\theta}}_{\mathcal{G}^c}$ as follows:

$$\begin{aligned} |\tilde{\boldsymbol{\theta}}_{\mathcal{G}} - \boldsymbol{\theta}_{0, \mathcal{G}}|_2 &= O_p \left\{ \frac{\log^{1/2}(np)}{n^{1/4}} \vee \frac{\log^{3/4}(np)}{(np)^{1/4}} \right\}, \\ |\tilde{\boldsymbol{\theta}}_{\mathcal{G}^c} - \boldsymbol{\theta}_{0, \mathcal{G}^c}|_\infty &= O_p \left\{ \frac{p^{1/4} \log^{1/2}(np)}{n^{1/4}} \vee \frac{p^{1/4} \log^{3/4}(np)}{n^{1/4}} \right\}, \end{aligned}$$

which implies the consistency of $\tilde{\boldsymbol{\theta}}_{\mathcal{G}}$ provided that $\log p \ll n^{1/2}$, and the consistency of $\tilde{\boldsymbol{\theta}}_{\mathcal{G}^c}$ provided that $p \ll n(\log n)^{-3}$.

Remark 2 Motivated by (3), we can approximate $\tilde{\boldsymbol{\theta}}_{\mathcal{G}}$ well by solving an alternative optimization problem involving $|\mathcal{G}|$ parameters, and each $\tilde{\theta}_l$ for $l \in \mathcal{G}^c$ through a univariate optimization. See Section B.1 of the supplementary material for a detailed discussion. Since each optimization is of finite dimension, standard numerical methods such as the Newton–Raphson or a Quasi-Newton algorithm can be efficiently applied. For each $l \in [q]$, evaluating $\hat{\ell}_{n,p}^{(l)}(\boldsymbol{\theta})$ in (5), together with its gradient and Hessian, requires $O(n|\mathcal{S}_l|)$ operations per iteration. The subsequent step, i.e., solving a small linear system in Newton–Raphson or updating the inverse-Hessian approximation in Quasi-Newton, does not introduce any higher-order computational cost. Therefore, for the three models introduced in Section 4, the per-iteration complexity is $O(np^2)$ for the global parameters and $O(np)$ for each local parameter.

5.4 Improved estimation for $\boldsymbol{\theta}_0$

Recall $\boldsymbol{\theta} = (\theta_1, \dots, \theta_q)^\top$. The initial estimator $\tilde{\boldsymbol{\theta}}$ specified in (6) suffers from slow convergence rates due to the high dimensionality of $\boldsymbol{\theta}$. In this section, we improve the estimation for

each component $\theta_{0,l}$ by projecting the score function onto certain direction. See (9) below for details. An improved estimator for $\theta_{0,l}$ is then obtained by solving the projected score function while letting $\boldsymbol{\theta}_{-l} = \tilde{\boldsymbol{\theta}}_{-l}$. The projection mitigates the impact of $\tilde{\boldsymbol{\theta}}_{-l}$ in the improved estimation for $\theta_{0,l}$. This strategy was initially proposed by [Chang et al. \(2021\)](#) and [Chang et al. \(2023\)](#) for constructing the valid confidence regions of some low-dimensional subvector of the whole parameters in high-dimensional models with removing the impact of the high-dimensional nuisance parameters.

For $(c_{n,\mathcal{G}}, c_{n,\mathcal{G}^c})$ defined as (7), put

$$\Delta_n = \max \{ |\mathcal{G}| c_{n,\mathcal{G}}^2, |\mathcal{G}^c|^2 c_{n,\mathcal{G}^c}^2 \}. \quad (8)$$

For any $t \in [n] \setminus [m]$, $l \in [q]$ and $\boldsymbol{\theta} \in \Theta$, we define

$$\mathbf{g}_t^{(l)}(\boldsymbol{\theta}) = \frac{1}{|\mathcal{S}_l|} \sum_{(i,j) \in \mathcal{S}_l} \frac{X_{i,j}^t - \gamma_{i,j}^{t-1}(\boldsymbol{\theta})}{\gamma_{i,j}^{t-1}(\boldsymbol{\theta}) \{1 - \gamma_{i,j}^{t-1}(\boldsymbol{\theta})\}} \frac{\partial \gamma_{i,j}^{t-1}(\boldsymbol{\theta})}{\partial \boldsymbol{\theta}}.$$

Then the score function can be written as

$$\frac{\partial \hat{\ell}_{n,p}^{(l)}(\boldsymbol{\theta})}{\partial \boldsymbol{\theta}} = \frac{1}{n-m} \sum_{t=m+1}^n \mathbf{g}_t^{(l)}(\boldsymbol{\theta}).$$

To estimate $\theta_{0,l}$, $\boldsymbol{\theta}_{-l}$ can be treated as a nuisance parameter vector. Following [Chang et al. \(2021\)](#) and [Chang et al. \(2023\)](#), we project $\mathbf{g}_t^{(l)}(\boldsymbol{\theta})$ to form a new estimating function:

$$\hat{f}_t^{(l)}(\boldsymbol{\theta}) = \hat{\boldsymbol{\varphi}}_l^\top \mathbf{g}_t^{(l)}(\boldsymbol{\theta}),$$

where $\hat{\boldsymbol{\varphi}}_l$ is defined as

$$\hat{\boldsymbol{\varphi}}_l = \arg \min_{\mathbf{u} \in \mathbb{R}^q} |\mathbf{u}|_1 \quad \text{s.t.} \quad \left| \left\{ \frac{1}{n-m} \sum_{t=m+1}^n \frac{\partial \mathbf{g}_t^{(l)}(\tilde{\boldsymbol{\theta}})}{\partial \boldsymbol{\theta}} \right\}^\top \mathbf{u} - \mathbf{e}_l \right|_\infty \leq \tau. \quad (9)$$

In the above expression, $\tau > 0$ is a tuning parameter satisfying $\tau \lesssim \Delta_n^{1/2}$ with Δ_n defined as

(8), $\tilde{\boldsymbol{\theta}} = (\tilde{\theta}_1, \dots, \tilde{\theta}_q)^\top$ is the initial estimator defined as (6), and \mathbf{e}_l is a q -dimensional vector with the l -th component being 1 and other components being 0. Then we can re-estimate $\boldsymbol{\theta}_0$ by $\check{\boldsymbol{\theta}} = (\check{\theta}_1, \dots, \check{\theta}_q)^\top$, where

$$\check{\theta}_l = \arg \min_{\theta_l \in B(\tilde{\theta}_l, \tilde{r})} \left| \frac{1}{n-m} \sum_{t=m+1}^n \hat{f}_t^{(l)}(\theta_l, \tilde{\boldsymbol{\theta}}_{-l}) \right|^2 \quad (10)$$

for some $\tilde{r} > 0$ satisfying $\max\{c_{n,\mathcal{G}}, c_{n,\mathcal{G}^c}\} \ll \tilde{r} \ll 1$.

To construct the convergence rate of $|\check{\boldsymbol{\theta}} - \boldsymbol{\theta}_0|_\infty$, we need the following regularity condition, which is analogous to Condition 1 of Chang et al. (2021) and Condition 7 of Chang et al. (2023). See the discussion there for the validity of such condition.

Condition 4 *For each $l \in [q]$, there is a nonrandom vector $\boldsymbol{\varphi}_l \in \mathbb{R}^q$ such that $|\boldsymbol{\varphi}_l|_1 \leq C_4$ for some universal constant $C_4 > 0$, and $\max_{l \in [q]} |\hat{\boldsymbol{\varphi}}_l - \boldsymbol{\varphi}_l|_1 = O_p(\omega_n)$ for some $\omega_n \rightarrow 0$ satisfying $\omega_n(\log q)^{1/2} \log(qn) = o(1)$.*

Proposition 2 shows that $\check{\boldsymbol{\theta}}$ has faster convergence rate than the initial estimator $\tilde{\boldsymbol{\theta}}$ given in (6). The proof of Proposition 2 is given in Section F.3 of the supplementary material.

Proposition 2 *Let the conditions of Proposition 1 and Condition 4 hold. Then $|\check{\boldsymbol{\theta}} - \boldsymbol{\theta}_0|_\infty = O_p(\Delta_n)$, where Δ_n is defined as (8).*

Based on the obtained $\check{\boldsymbol{\theta}}$, we consider the final estimate $\hat{\boldsymbol{\theta}} = (\hat{\theta}_1, \dots, \hat{\theta}_q)^\top$ for $\boldsymbol{\theta}_0$ defined as follows:

$$\hat{\theta}_l = \arg \min_{\theta_l \in B(\check{\theta}_l, \check{r})} \left| \frac{1}{n-m} \sum_{t=m+1}^n \hat{f}_t^{(l)}(\theta_l, \check{\boldsymbol{\theta}}_{-l}) \right|^2 \quad (11)$$

for some $\check{r} > 0$ satisfying $q\Delta_n \ll \check{r} \ll 1$ with Δ_n defined as (8).

Remark 3 *Given the initial estimate $\tilde{\boldsymbol{\theta}}$, there are three tuning parameters $(\tau, \tilde{r}, \check{r})$ for deriving our final estimate $\hat{\boldsymbol{\theta}}$. For the degree heterogeneity model introduced in Section 4.1, we have $|\mathcal{G}| = 4$ and $|\mathcal{G}^c| = 2p$. For both the persistence model and transitivity model introduced in Sections 4.2 and 4.3, we have $|\mathcal{G}| = 2$ and $|\mathcal{G}^c| = 2p$. Together with Remark 1, we have*

$\Delta_n = n^{-1/2} p^{5/2} \log^{3/2}(np)$ for these three models. The improved estimation procedure thus requires $\tau \lesssim n^{-1/4} p^{5/4} \log^{3/4}(np)$, $n^{-1/4} p^{1/4} \log^{3/4}(np) \ll \tilde{r} \ll 1$ and $n^{-1/2} p^{7/2} \log^{3/2}(np) \ll \check{r} \ll 1$, which suggests $p \ll n^{1/7} (\log n)^{-3/7}$. In practice, for the three models introduced in Section 4, we compute the final estimate $\hat{\boldsymbol{\theta}}$ with τ proportional to $n^{-1/4} p^{5/4} \log^{3/4}(np)$ and adopting reasonably large \tilde{r} and \check{r} . Numerical experiments in Section 6 and Section B of the supplementary material validate the robustness of our proposed estimation procedure regarding the selections of \tilde{r} and \check{r} as long as $\boldsymbol{\theta}_0$ falls within the defined search range.

Remark 4 In terms of computational complexity, for each $l \in [q]$, $\hat{\boldsymbol{\varphi}}_l$ in (9) is obtained by solving a well-studied and efficiently solvable linear programming (LP) problem that involves computing a Hessian matrix. Recall that Condition 2 implies that the dynamics of each edge process $\{X_{i,j}^t\}_{t \geq 1}$ depend on a finite number of parameters. Evaluating each Hessian matrix within the LP thus requires $O(n|\mathcal{S}_l|)$ operations. Similar to Remark 2, we use the Newton-Raphson or a Quasi-Newton algorithm to obtain $\check{\theta}_l$ in (10) and $\hat{\theta}_l$ in (11) with $O(nq|\mathcal{S}_l|)$ computations incurred per iteration for $l \in [q]$. Hence, for the three models introduced in Section 4, each iteration has a computational cost of $O(np^3)$ for each global parameter and $O(np^2)$ for each local parameter. Compared with the detailed computational cost of the initial estimation for these three models as reported in Remark 2, the additional factor of p for both the global and local parameters arises from the extra projection operation required for $\hat{f}_t^{(l)}(\boldsymbol{\theta})$, which eventually leads to faster convergence rates of $\hat{\boldsymbol{\theta}}$ and substantially improved empirical performance. See Theorem 2, Remark 6, and Section B.2 of the supplementary material for further details. Importantly, the sequence of computations in (9), (10), and (11) can be performed in parallel across l within each step to improve computational efficiency.

For any $\boldsymbol{\theta} \in \Theta$ and $l \in [q]$, define

$$\zeta_{n,l}(\boldsymbol{\theta}) = \frac{1}{(n-m)|\mathcal{S}_l|} \sum_{t=m+1}^n \sum_{(i,j) \in \mathcal{S}_l} \frac{1}{\gamma_{i,j}^{t-1}(\boldsymbol{\theta}) \{1 - \gamma_{i,j}^{t-1}(\boldsymbol{\theta})\}} \left\{ \boldsymbol{\varphi}_l^\top \frac{\partial \gamma_{i,j}^{t-1}(\boldsymbol{\theta})}{\partial \boldsymbol{\theta}} \right\}^2,$$

where $\boldsymbol{\varphi}_l$ is given in Condition 4. Under Conditions 1 and 4, we have $|\zeta_{n,l}(\boldsymbol{\theta})| \leq C_1^{-1} C_2^2 C_4^2$, which implies that, for any $\boldsymbol{\theta} \in \Theta$, $\zeta_{n,l}(\boldsymbol{\theta})$ is a bounded random variable. To construct the

asymptotic distribution of each $\hat{\theta}_l$, we require the following condition.

Condition 5 For each $l \in [q]$, there exists some random variable $\kappa_l \geq 0$ such that $\zeta_{n,l}(\boldsymbol{\theta}_0) \rightarrow \kappa_l$ in probability as $n \rightarrow \infty$.

Remark 5 For each $l \in [q]$ and $t \geq m+1$, let

$$v_l^{t-1} = \frac{1}{|\mathcal{S}_l|} \sum_{(i,j) \in \mathcal{S}_l} \frac{1}{\gamma_{i,j}^{t-1}(\boldsymbol{\theta}_0) \{1 - \gamma_{i,j}^{t-1}(\boldsymbol{\theta}_0)\}} \left\{ \boldsymbol{\varphi}_l^\top \frac{\partial \gamma_{i,j}^{t-1}(\boldsymbol{\theta}_0)}{\partial \boldsymbol{\theta}} \right\}^2.$$

As $\{\zeta_{n,l}(\boldsymbol{\theta}_0)\}_{n \geq m+1}$ is a bounded sequence of random variables for each $l \in [q]$, Condition 5 is mild and κ_l is a random variable in general. Generally speaking, the asymptotic distribution of $\hat{\theta}_l$ is a mixture of normal distributions. See Theorem 2 below for details. However, if the long-run variance of $\{v_l^{t-1}\}_{t=m+1}^n$ satisfies the condition

$$\text{Var} \left(\frac{1}{\sqrt{n-m}} \sum_{t=m+1}^n v_l^{t-1} \right) = o(\sqrt{n}), \quad (12)$$

κ_l is reduced to a constant

$$\kappa_l = \lim_{n \rightarrow \infty} \mathbb{E} \left(\frac{1}{n-m} \sum_{t=m+1}^n v_l^{t-1} \right).$$

Then Theorem 2 implies that $\hat{\theta}_l$ is asymptotically normal distributed. When the sequence $\{v_l^t\}_{t \geq m}$ is α -mixing with the mixing coefficients attaining certain convergence rates, (12) holds automatically.

Theorem 2 Let the conditions of Proposition 1 and Conditions 4 and 5 hold. For each $l \in [q]$, if $\sqrt{n|\mathcal{S}_l|} \max\{q\Delta_n^{3/2}, q^2\Delta_n^2\} = o(1)$ with Δ_n defined as (8), it then holds that

$$\sqrt{n|\mathcal{S}_l|}(\hat{\theta}_l - \theta_{0,l}) \rightarrow \sqrt{\kappa_l} \cdot Z$$

in distribution as $n \rightarrow \infty$, where Z is a standard normally distributed random variable independent of κ_l specified in Condition 5.

The proof of Theorem 2 is given in Section F.4 of the supplementary material.

Remark 6 (i) *Theorem 2 shows that, for the global parameter θ_l with $l \in \mathcal{G}$,*

$$|\hat{\theta}_l - \theta_{0,l}| = O_p\left(\frac{1}{\sqrt{np}}\right),$$

provided that

$$q \ll \min \left\{ \frac{n^{1/10}p^{1/5}}{|\mathcal{G}|^{3/5} \log^{3/5}(np)}, \frac{n^{1/13}p^{8/13}}{|\mathcal{G}|^{6/13} \log^{9/13}(np)}, \right. \\ \left. \frac{n^{1/10}S_{\mathcal{G}^c, \min}^{3/10}}{|\mathcal{G}^c|^{6/5}p^{2/5} \log^{3/5}(nS_{\mathcal{G}^c, \min})}, \frac{n^{1/13}S_{\mathcal{G}^c, \min}^{6/13}}{|\mathcal{G}^c|^{12/13}p^{4/13} \log^{9/13}(nS_{\mathcal{G}^c, \min})} \right\},$$

and for the local parameter θ_l with $l \in \mathcal{G}^c$,

$$|\hat{\theta}_l - \theta_{0,l}| = O_p\left(\frac{1}{\sqrt{n|\mathcal{S}_l|}}\right),$$

provided that

$$q \ll \min \left\{ \frac{n^{1/10}p^{3/5}}{|\mathcal{G}|^{3/5}|\mathcal{S}_l|^{1/5} \log^{3/5}(np)}, \frac{n^{1/13}p^{12/13}}{|\mathcal{G}|^{6/13}|\mathcal{S}_l|^{2/13} \log^{9/13}(np)}, \frac{n^{1/8}p^{1/2}}{|\mathcal{G}|^{1/2}|\mathcal{S}_l|^{1/8} \log^{1/2}(np)}, \right. \\ \left. \frac{n^{1/10}S_{\mathcal{G}^c, \min}^{3/10}}{|\mathcal{G}^c|^{6/5}|\mathcal{S}_l|^{1/5} \log^{3/5}(nS_{\mathcal{G}^c, \min})}, \frac{n^{1/13}S_{\mathcal{G}^c, \min}^{6/13}}{|\mathcal{G}^c|^{12/13}|\mathcal{S}_l|^{2/13} \log^{9/13}(nS_{\mathcal{G}^c, \min})} \right\}.$$

In particular, for the three models introduced in Section 4, the estimators satisfy $|\hat{\theta}_l - \theta_{0,l}| = O_p(n^{-1/2}p^{-1})$ for $l \in \mathcal{G}$ if $p \ll n^{1/23}(\log n)^{-9/23}$, and $|\hat{\theta}_l - \theta_{0,l}| = O_p\{(np)^{-1/2}\}$ for $l \in \mathcal{G}^c$ if $p \ll n^{1/21}(\log n)^{-3/7}$. Compared with the results in Theorem 1, the improved estimator $\hat{\theta}$ achieves a faster convergence rate than the initial estimator $\tilde{\theta}$.

(ii) *For each $l \in [q]$, write*

$$\hat{\zeta}_{n,l}(\hat{\theta}) = \frac{1}{(n-m)|\mathcal{S}_l|} \sum_{t=m+1}^n \sum_{(i,j) \in \mathcal{S}_l} \frac{1}{\gamma_{i,j}^{t-1}(\hat{\theta})\{1 - \gamma_{i,j}^{t-1}(\hat{\theta})\}} \left\{ \hat{\varphi}_l^\top \frac{\partial \gamma_{i,j}^{t-1}(\hat{\theta})}{\partial \theta} \right\}^2$$

with $\hat{\varphi}_l$ defined as (9). Since $\hat{\zeta}_{n,l}(\hat{\theta}) - \zeta_{n,l}(\theta_0) \rightarrow 0$ in probability as $n \rightarrow \infty$, by Corollary

3.2 of Hall and Heyde (1980), it holds that

$$\sqrt{\frac{n|\mathcal{S}_l|}{\hat{\zeta}_{n,l}(\hat{\boldsymbol{\theta}})}}(\hat{\theta}_l - \theta_{0,l}) \rightarrow \mathcal{N}(0, 1) \quad (13)$$

in distribution as $n \rightarrow \infty$, provided that $\mathbb{P}(\kappa_l > 0) = 1$. We can use (13) to construct the confidence interval for each θ_l .

6 Real data analysis: Email interactions

We studied estimation and coverage properties in the transitivity model (3) and an extended version of that model. See Sections B and C of the supplementary material for a summary of results. In this section, we apply the transitivity model (3) to a dynamic network dataset of email interactions in a medium-sized Polish manufacturing company, from January to September 2010 (Michalski et al., 2014). We analyze a subset of the data among $p = 106$ of the most active participants out of an original 167 employees. The organizational tree of direct reports in the company is also available for these employees. Each of the $n = 39$ network snapshots corresponds to a non-overlapping time window, with $X_{i,j}^t = 1$ if participants i and j exchanged at least one email in week t . Binarizing the communications at a weekly scale removes periodic effects and irregular behaviours which are present at higher frequencies.

In Section E.1 of the supplementary material, we inspect the stationarity of the network and the effective sample size. Our preliminary plots of edge density and dynamic activity suggest a change point in the network sequence, hence we fit our model separately to the first 13 and last 26 snapshots, referred to as “period 1” and “period 2”. Overall, the proportion of non-edges that form in the next snapshot is about 5%, while the proportion of existing edges which persist in the next snapshot is about 55%, clear evidence of temporal edge dependence. Basic summaries also identify empirical evidence for transitivity effects (See Figure S3 in Section E.1 of the supplementary material).

The presence of transitivity effects is confirmed by the fit of our model parameters,

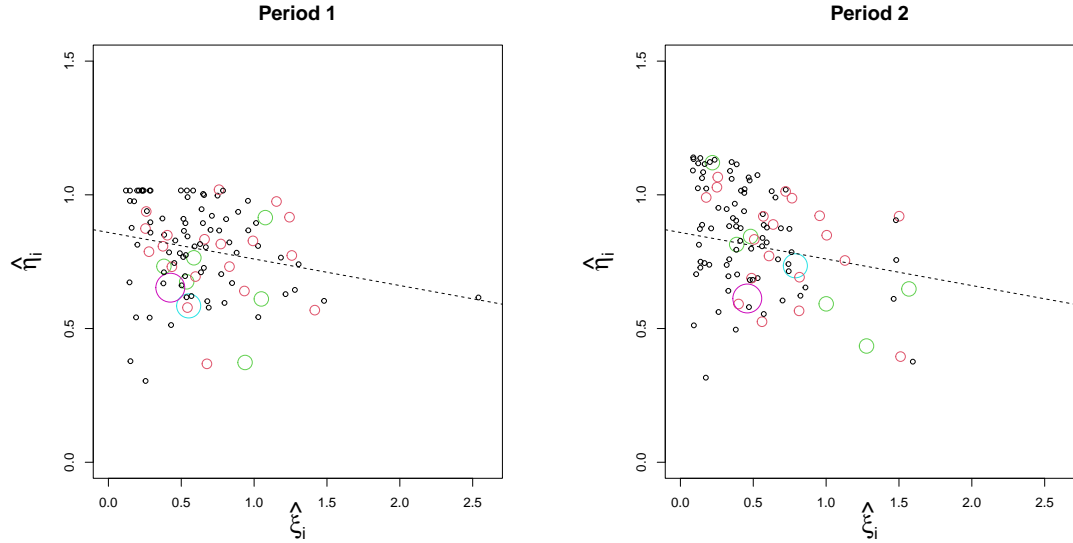


Figure 1: Scatter plots of estimates $\{\hat{\xi}_i\}_{i=1}^{106}$ and $\{\hat{\eta}_i\}_{i=1}^{106}$ for periods 1 and 2, email interaction data. Circles are sized and coloured according to their level in the company organizational tree from 1 (no direct reports) to 5 (CEO). Level 1: black, smallest; level 2: red; level 3: green; level 4: cyan; level 5: purple, largest.

using the estimation algorithm described in Section B of the supplementary material. This algorithm applies the estimation procedure introduced in Section 5 and is implemented in our development R package `arnetworks`. For period 1, we estimate the global parameters $\hat{a} = 13.64$ and $\hat{b} = 9.51$, suggesting a tendency towards edge growth given more common neighbours, and edge dissolution given more distinct neighbours. We interpret the estimates of the local parameters $\{\xi_i\}_{i=1}^{106}$ and $\{\eta_i\}_{i=1}^{106}$ in the left panel of Figure 1. The estimates $\{\hat{\xi}_i\}_{i=1}^{106}$ have mean 0.62 and skew towards the right, implying node heterogeneity in the edge growth. Conversely, the estimates $\{\hat{\eta}_i\}_{i=1}^{106}$ have mean 0.80 and skew towards the left. There is a decreasing relationship between the paired parameters: employees who tend to grow new edges also tend to maintain existing edges. Finally, there is an observed relationship between email behavior and company hierarchy: managers (non-leaf nodes in the organizational tree) tend to have larger estimates $\{\hat{\xi}_i\}_{i=1}^{106}$ compared to non-managers (means 0.72 and 0.59 respectively), implying that managers are more likely to grow edges. However, this increasing pattern does not continue at higher levels of the organizational tree.

The model fit to period 2 shows many of the same patterns. We estimate $\hat{a} = 22.01$ and $\hat{b} = 11.31$ and summarize the estimates $\{\hat{\xi}_i\}_{i=1}^{106}$ and $\{\hat{\eta}_i\}_{i=1}^{106}$ in the right panel of Figure 1.

Model	Period 1		Period 2	
	AIC	BIC	AIC	BIC
Transitivity AR model	33462	35412	53221	55327
Global AR model	36309	36327	58267	58287
Edgewise AR model	42717	144102	55840	165394
Edgewise mean model	33248	83941	47133	101910
Degree parameter mean model	41730	42695	68969	70013

Table 2: AIC and BIC performance for email interaction data, periods 1 and 2.

Relative to period 1, the larger estimate of a implies a stronger transitivity effect in this time period. The estimates $\{\hat{\xi}_i\}_{i=1}^{106}$ now have mean 0.52 and the estimates $\{\hat{\eta}_i\}_{i=1}^{106}$ have mean 0.84, to model overall lower edge density than in period 1. The decreasing relationship between the paired parameters is stronger, and the means of $\hat{\xi}_i$ for managers and non-managers are, respectively, 0.74 and 0.45. Along with the stronger transitivity effect, we interpret that the decreased edge density in period 2 has led to a concentration of email activity among a smaller group of employees, many of whom are managers.

We compare our model to some competing models from the literature in terms of Akaike and Bayesian information criteria (AIC, BIC). To briefly describe these competitors: the “global AR model” and “edgewise AR model” fit the model of [Jiang et al. \(2023\)](#), with two global switching parameters or two parameters for each edge, respectively. The “edgewise mean model” assumes $X_{i,j}^t \stackrel{\text{i.i.d.}}{\sim} \text{Bernoulli}(P_{i,j})$ with no temporal dependence, and estimates the edge probability $\{P_{i,j}\}_{i,j: i < j}$ for each node pair by its relative frequency of having an edge in the observed network snapshots; and the “degree parameter mean model” assumes $X_{i,j}^t \stackrel{\text{i.i.d.}}{\sim} \text{Bernoulli}(\nu_i \nu_j)$ and estimates the degree parameters $\{\nu_i\}_{i=1}^{106}$ by fitting 1-dimensional adjacency spectral embedding ([Athreya et al., 2017](#)) to the mean adjacency matrix over the observed network snapshots. The edgewise mean model has $O(p^2)$ parameters, while the degree parameter model has $O(p)$ parameters, like our AR network model with transitivity. All of these models can be directly compared using the likelihoods under their respective AR network formulations, although only our AR network model with transitivity incorporates edge dependence, and the final two models do not incorporate any temporal dependence. Results for both periods are reported in Table 2.

In both periods, our AR network model with transitivity is outperformed only by the

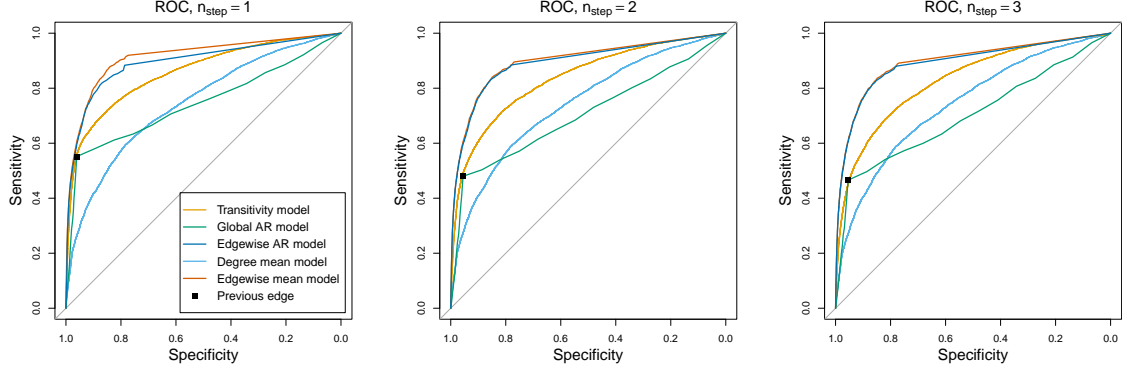


Figure 2: ROC curves for link prediction performance, email interaction data.

edgewise mean model in terms of AIC, and achieves the lowest BIC, as it uses fewer parameters. This reduction of the parameter space is important for modelling sparse dynamic network data: although there is clear temporal edge dependence in this data, the edgewise mean model outperforms the edgewise AR model, as there is low effective sample size to estimate the local edge dissolution parameters.

Finally, we compare the performances of those models in an edge forecasting task on the final 26 network snapshots (period 2). For $n_{\text{train}} = 10, \dots, 23$, we train these models on the first n_{train} snapshots of period 2, then forecast the state of each edge n_{step} steps forward, for $n_{\text{step}} = 1, 2, 3$. The combined results are presented in Figure 2 as receiver operating characteristic (ROC) curves. We also include a single point summarizing the performance of naively forecasting the state of each edge by its state in the n_{train} -th (last available observed) network snapshot (“previous edge”).

For all choices of n_{step} , the ROC curve for our AR network model with transitivity dominates or is competitive with the global AR model, degree mean model, and the naive previous edge prediction. However, the two highly parameterized edgewise models achieve better performance in terms of area under the ROC, which suggests the presence of higher order structure in this network that cannot be modeled with only two parameters per node. The edgewise mean and edgewise AR models give very similar, but not identical edge predictions; due to network sparsity the edgewise AR model has a low effective sample size to estimate the dissolution parameters, leading to slightly worse forecasting performance.

Last but not least, the analysis above is based on the combined information for each

pair (i, j) in each week into a simple binary $X_{i,j}^t$, though the original data set contains more information including the precise time stamp on each email exchange. While we did not make the full use of the available data, the information accumulation over one week makes data more stationary. See Figure S4 in comparison with Figure S2 in Section E.1 of the supplementary material. Filtering out some irregular behaviours at higher frequencies also reveals more clearly the transitivity patterns in this data set. See Figure S5 in comparison with Figure S3.

Funding

Jinyuan Chang was supported in part by the National Natural Science Foundation of China (Grant nos. 72125008 and 72495122). Eric D. Kolaczyk was supported in part by U.S. National Science Foundation grant SES-2120115, Canadian NSERC RGPIN-2023-03566 and NSERC DGDND-2023-03566. Peter W. MacDonald was partially supported by a Postdoctoral Fellowship from the Natural Sciences and Engineering Research Council of Canada. Qiwei Yao was partially supported by the U.K. Engineering and Physical Sciences Research Council (Grants nos. EP/V007556/1 and EP/X002195/1).

Data availability

The R package `arnetworks`, which implements the proposed estimation and inference procedure, along with the data used in this paper, is publicly available at: <https://github.com/peterwmacd/arnetworks>.

Supplementary material

Supplementary material contains a detailed analysis on the relationship between the proposed AR models and TERGMs, simulation studies with transitivity model, the method-of-moments-based estimation, additional real data results and all technical proofs.

References

Almquist, Z. W. and Butts, C. T. (2014). Logistic network regression for scalable analysis of networks with joint edge/vertex dynamics, *Sociological Methodology* **44**: 273–321.

Athreya, A., Fishkind, D. E., Tang, M., Priebe, C. E., Park, Y., Vogelstein, J. T., Levin, K., Lyzinski, V., Qin, Y. and Sussman, D. L. (2017). Statistical inference on random dot product graphs: a survey, *Journal of Machine Learning Research* **18**: Paper No. 226, 92.

Bianchi, F., Filippi-Mazzola, E., Lomi, A. and Wit, E. C. (2024). Relational event modeling, *Annual Review of Statistics and its Application* **11**: 297–319.

Blackburn, B. and Handcock, M. S. (2023). Practical network modeling via tapered exponential-family random graph models, *Journal of Computational and Graphical Statistics* **32**: 388–401.

Brémaud, P. (1998). *Markov Chains: Gibbs Fields, Monte Carlo Simulation, and Queues*, Springer.

Butts, C. T., Lomi, A., Snijders, T. A. and Stadtfeld, C. (2023). Relational event models in network science, *Network Science* **11**: 175–183.

Chang, J., Chen, S. X., Tang, C. Y. and Wu, T. (2021). High-dimensional empirical likelihood inference, *Biometrika* **108**: 127–147.

Chang, J., Shi, Z. and Zhang, J. (2023). Culling the herd of moments with penalized empirical likelihood, *Journal of Business & Economic Statistics* **41**: 791–805.

Durante, D. and Dunson, D. B. (2016). Locally adaptive dynamic networks, *The Annals of Applied Statistics* **10**: 2203–2232.

Gallagher, I., Jones, A. and Rubin-Delanchy, P. (2021). Spectral embedding for dynamic networks with stability guarantees, *Advances in Neural Information Processing Systems* **34**: 10158–10170.

Graham, B. S. (2016). Homophily and transitivity in dynamic network formation, *NBER Working Paper 22186*, National Bureau of Economic Research.

Hall, P. and Heyde, C. C. (1980). *Martingale Limit Theory and its Application*, Academic Press.

Hanneke, S., Fu, W. and Xing, E. (2010). Discrete temporal models of social networks, *Electronic Journal of Statistics* **4**: 585–605.

Jiang, B., Leng, C., Yan, T., Yao, Q. and Yu, X. (2025). A two-way heterogeneity model for dynamic networks, *The Annals of Statistics, in press*.

Jiang, B., Li, J. and Yao, Q. (2023). Autoregressive networks, *Journal of Machine Learning Research* **24**: Paper No. 227, 69.

Karrer, B. and Newman, M. E. (2011). Stochastic blockmodels and community structure in networks, *Physical Review E* **83**: 016107.

Koskinen, J. and Snijders, T. A. (2023). Multilevel longitudinal analysis of social networks, *Journal of the Royal Statistical Society Series A: Statistics in Society* **186**: 376–400.

Krivitsky, N. and Handcock, M. (2014). A separable model for dynamic networks, *Journal of the Royal Statistical Society, Series B* **76**: 29–48.

Krivitsky, P. N., Handcock, M. S., Hunter, D. R., Butts, C. T., Bojanowski, M., Klumb, C., Goodreau, S. M. and Morris, M. (2025). Statnet: Tools for the statistical modeling of network data.

URL: <https://statnet.org>

Ludkin, M., Eckley, I. and Neal, P. (2018). Dynamic stochastic block models: parameter estimation and detection of changes in community structure, *Statistics and Computing* **28**: 1201–1213.

Matias, C. and Miele, V. (2017). Statistical clustering of temporal networks through a dynamic stochastic block model, *Journal of the Royal Statistical Society, Series B* **79**: 1119–1141.

Matias, C., Rebafka, T. and Villers, F. (2018). A semiparametric extension of the stochastic block model for longitudinal networks, *Biometrika* **105**: 665–680.

Matias, C. and Robin, S. (2014). Modeling heterogeneity in random graphs through latent space models: a selective review, *ESAIM: Proceedings and Surveys* **47**: 55–74.

Michalski, R., Kajdanowicz, T., Bródka, P. and Kazienko, P. (2014). Seed selection for spread of influence in social networks: Temporal vs. static approach, *New Generation Computing* **32**: 213–235.

Pensky, M. and Zhang, T. (2019). Spectral clustering in the dynamic stochastic block model, *Electronic Journal of Statistics* **13**: 678–709.

Perry, P. O. and Wolfe, P. J. (2013). Point process modelling for directed interaction networks, *Journal of the Royal Statistical Society, Series B* **75**: 821–849.

Robins, G., Pattison, P., Kalish, Y. and Lusher, D. (2007). An introduction to exponential random graph (p^*) models for social networks, *Social networks* **29**: 173–191.

Schweinberger, M., Krivitsky, P., Butts, C. and Stewart, J. (2020). Exponential-family models of random graphs: Inference in finite, super and infinite population scenarios, *Statistical Science* **35**: 627–662.

Sewell, D. K. and Chen, Y. (2015). Latent space models for dynamic networks, *Journal of the American Statistical Association* **110**: 1646–1657.

Snijders, T. A. (2017). Stochastic actor-oriented models for network dynamics, *Annual Review of Statistics and its Application* **4**: 343–363.

Snijders, T. A. B. (2005). Models for longitudinal network data, *Models and Methods in Social Network Analysis*, Cambridge University Press, New York, chapter 11.

Stewart, J. R. (2024). Rates of convergence and normal approximations for estimators of local dependence random graph models, *arXiv preprint arXiv:2404.11464*.

Süveges, M. and Olhede, S. C. (2023). Networks with correlated edge processes, *Journal of the Royal Statistical Society, Series A* **186**: 441–462.

Yang, T., Chi, Y., Zhu, S., Gong, Y. and Jin, R. (2011). Detecting communities and their evolutions in dynamic social networks—a Bayesian approach, *Machine Learning* **82**: 157–189.

Yudovina, E., Banerjee, M. and Michailidis, G. (2015). Changepoint inference for erdős-rényi random graphs, *Stochastic Models, Statistics and Their Applications*, Springer, pp. 197–205.

Zhang, Y., Zhang, J., Sun, Y. and Wang, J. (2024). Change point detection in dynamic networks via regularized tensor decomposition, *Journal of Computational and Graphical Statistics* **33**: 515–524.

Zhu, X., Caliskan, C., Christenson, D. P., Spiliopoulos, K., Walker, D. and Kolaczyk, E. D. (2023). Disentangling positive and negative partisanship in social media interactions using a coevolving latent space network with attractors model, *Journal of the Royal Statistical Society Series A: Statistics in Society* **186**: 463–480.

Supplementary material to “Autoregressive Networks with Dependent Edges”

Jinyuan Chang, Qin Fang, Eric D. Kolaczyk, Peter W. MacDonald, and Qiwei Yao

This supplementary material contains a detailed analysis on the relationship between the proposed AR models and TERGMs (Section A), simulation studies with transitivity model (Section B), additional simulation results (Section C), the method-of-moments-based estimation (Section D), the analysis of an additional dynamic network dataset (Section E), and all the technical proofs (Section F).

A Relationship to TERGMs

A dynamic network sequence follows a TERGM of order m if it satisfies

$$\mathbb{P}(\mathbf{X}_t | \mathbf{X}_{t-1}, \dots, \mathbf{X}_{t-m}; \boldsymbol{\theta}) \propto \exp\{\boldsymbol{\varsigma}(\boldsymbol{\theta})^\top \boldsymbol{\varrho}(\mathbf{X}_t, \mathbf{X}_{t-1}, \dots, \mathbf{X}_{t-m})\}, \quad (\text{A.1})$$

where $\boldsymbol{\varsigma} : \mathbb{R}^q \rightarrow \mathbb{R}^p$ maps the parameter vector $\boldsymbol{\theta}$ to the vector of natural parameters, and $\boldsymbol{\varrho}$ maps the data, including the past network snapshots, to the corresponding sufficient statistics.

As in Equation (2) of [Hanneke et al. \(2010\)](#), suppose $\boldsymbol{\varrho}$ factors over the edges of the present snapshot,

$$\boldsymbol{\varrho}(\mathbf{X}_t, \mathbf{X}_{t-1}, \dots, \mathbf{X}_{t-m}) = \sum_{i,j: i < j} \boldsymbol{\varrho}_{i,j}(X_{i,j}^t; \mathbf{X}_{t-1}, \dots, \mathbf{X}_{t-m}).$$

Then

$$\begin{aligned} \mathbb{P}(\mathbf{X}_t | \mathbf{X}_{t-1}, \dots, \mathbf{X}_{t-m}; \boldsymbol{\theta}) \\ \propto \prod_{i,j: i < j} \exp \{ \boldsymbol{\varsigma}(\boldsymbol{\theta})^\top \boldsymbol{\varrho}_{i,j}(X_{i,j}^t; X_{i,j}^{t-1}, \mathbf{X}_{t-1} \setminus X_{i,j}^{t-1}, \mathbf{X}_{t-2}, \dots, \mathbf{X}_{t-m}) \}, \end{aligned} \quad (\text{A.2})$$

which implies \mathbf{X}_t will have mutually independent edges conditional on the past snapshots. We refer to this as the edge conditional independence assumption, which is a property of

AR network models defined in Definition 1 of the main document. We will show that any edge conditionally independent TERGM can be rewritten as an AR network model.

Denote the logit function by $\sigma(x) = \log\{x/(1-x)\}$, and specify an AR network model defined in Definition 1 by setting

$$\begin{aligned} \alpha_{i,j}^{t-1} &= \sigma^{-1} [\boldsymbol{\varsigma}(\boldsymbol{\theta})^\top \{ \boldsymbol{\varrho}_{i,j}(1; 0, \mathbf{X}_{t-1} \setminus X_{i,j}^{t-1}, \mathbf{X}_{t-2}, \dots, \mathbf{X}_{t-m}) \\ &\quad - \boldsymbol{\varrho}_{i,j}(0; 0, \mathbf{X}_{t-1} \setminus X_{i,j}^{t-1}, \mathbf{X}_{t-2}, \dots, \mathbf{X}_{t-m}) \}] \\ &:= \sigma^{-1} [\boldsymbol{\varsigma}(\boldsymbol{\theta})^\top (\boldsymbol{\varrho}_{i,j,10}^{t-1} - \boldsymbol{\varrho}_{i,j,00}^{t-1})], \end{aligned} \quad (\text{A.3})$$

$$\begin{aligned} \beta_{i,j}^{t-1} &= \sigma^{-1} [\boldsymbol{\varsigma}(\boldsymbol{\theta})^\top \{ \boldsymbol{\varrho}_{i,j}(0; 1, \mathbf{X}_{t-1} \setminus X_{i,j}^{t-1}, \mathbf{X}_{t-2}, \dots, \mathbf{X}_{t-m}) \\ &\quad - \boldsymbol{\varrho}_{i,j}(1; 1, \mathbf{X}_{t-1} \setminus X_{i,j}^{t-1}, \mathbf{X}_{t-2}, \dots, \mathbf{X}_{t-m}) \}] \\ &:= \sigma^{-1} [\boldsymbol{\varsigma}(\boldsymbol{\theta})^\top (\boldsymbol{\varrho}_{i,j,01}^{t-1} - \boldsymbol{\varrho}_{i,j,11}^{t-1})]. \end{aligned} \quad (\text{A.4})$$

With renormalization, we have

$$\begin{aligned} \alpha_{i,j}^{t-1} &= \frac{\exp\{\boldsymbol{\varsigma}(\boldsymbol{\theta})^\top \boldsymbol{\varrho}_{i,j,10}^{t-1}\}}{\exp\{\boldsymbol{\varsigma}(\boldsymbol{\theta})^\top \boldsymbol{\varrho}_{i,j,10}^{t-1}\} + \exp\{\boldsymbol{\varsigma}(\boldsymbol{\theta})^\top \boldsymbol{\varrho}_{i,j,00}^{t-1}\}}, \\ 1 - \alpha_{i,j}^{t-1} &= \frac{\exp\{\boldsymbol{\varsigma}(\boldsymbol{\theta})^\top \boldsymbol{\varrho}_{i,j,00}^{t-1}\}}{\exp\{\boldsymbol{\varsigma}(\boldsymbol{\theta})^\top \boldsymbol{\varrho}_{i,j,10}^{t-1}\} + \exp\{\boldsymbol{\varsigma}(\boldsymbol{\theta})^\top \boldsymbol{\varrho}_{i,j,00}^{t-1}\}}, \\ \beta_{i,j}^{t-1} &= \frac{\exp\{\boldsymbol{\varsigma}(\boldsymbol{\theta})^\top \boldsymbol{\varrho}_{i,j,01}^{t-1}\}}{\exp\{\boldsymbol{\varsigma}(\boldsymbol{\theta})^\top \boldsymbol{\varrho}_{i,j,01}^{t-1}\} + \exp\{\boldsymbol{\varsigma}(\boldsymbol{\theta})^\top \boldsymbol{\varrho}_{i,j,11}^{t-1}\}}, \\ 1 - \beta_{i,j}^{t-1} &= \frac{\exp\{\boldsymbol{\varsigma}(\boldsymbol{\theta})^\top \boldsymbol{\varrho}_{i,j,11}^{t-1}\}}{\exp\{\boldsymbol{\varsigma}(\boldsymbol{\theta})^\top \boldsymbol{\varrho}_{i,j,01}^{t-1}\} + \exp\{\boldsymbol{\varsigma}(\boldsymbol{\theta})^\top \boldsymbol{\varrho}_{i,j,11}^{t-1}\}}. \end{aligned}$$

For the AR network model with $(\alpha_{i,j}^{t-1}, \beta_{i,j}^{t-1})$ specified in (A.3) and (A.4), it holds that

$$\begin{aligned} \mathbb{P}(\mathbf{X}_t \mid \mathbf{X}_{t-1}, \dots, \mathbf{X}_{t-m}; \boldsymbol{\theta}) &= \prod_{i,j: i < j} \mathbb{P}(X_{i,j}^t \mid \mathbf{X}_{t-1}, \dots, \mathbf{X}_{t-m}; \boldsymbol{\theta}) \\ &= \prod_{i,j: i < j, X_{i,j}^t = 0, X_{i,j}^{t-1} = 0} (1 - \alpha_{i,j}^{t-1}) \cdot \prod_{i,j: i < j, X_{i,j}^t = 1, X_{i,j}^{t-1} = 0} \alpha_{i,j}^{t-1} \\ &\quad \cdot \prod_{i,j: i < j, X_{i,j}^t = 0, X_{i,j}^{t-1} = 1} \beta_{i,j}^{t-1} \cdot \prod_{i,j: i < j, X_{i,j}^t = 1, X_{i,j}^{t-1} = 1} (1 - \beta_{i,j}^{t-1}) \\ &\propto \prod_{i,j: i < j, X_{i,j}^t = 0, X_{i,j}^{t-1} = 0} \exp\{\boldsymbol{\varsigma}(\boldsymbol{\theta})^\top \boldsymbol{\varrho}_{i,j,00}^{t-1}\} \cdot \prod_{i,j: i < j, X_{i,j}^t = 1, X_{i,j}^{t-1} = 0} \exp\{\boldsymbol{\varsigma}(\boldsymbol{\theta})^\top \boldsymbol{\varrho}_{i,j,10}^{t-1}\} \end{aligned}$$

$$\begin{aligned}
& \cdot \prod_{i,j: i < j, X_{i,j}^t = 0, X_{i,j}^{t-1} = 1} \exp\{\boldsymbol{\varsigma}(\boldsymbol{\theta})^\top \boldsymbol{\varrho}_{i,j,01}^{t-1}\} \cdot \prod_{i,j: i < j, X_{i,j}^t = 1, X_{i,j}^{t-1} = 1} \exp\{\boldsymbol{\varsigma}(\boldsymbol{\theta})^\top \boldsymbol{\varrho}_{i,j,11}^{t-1}\} \\
& = \prod_{i,j: i < j} \exp\{\boldsymbol{\varsigma}(\boldsymbol{\theta})^\top \boldsymbol{\varrho}_{i,j}(X_{i,j}^t; X_{i,j}^{t-1}, \mathbf{X}_{t-1} \setminus X_{i,j}^{t-1}, \mathbf{X}_{t-2}, \dots, \mathbf{X}_{t-m})\},
\end{aligned}$$

which shares the same form as (A.2). Thus, for any edge conditionally independent TERGM, we can specify an AR network model with the same distribution.

Conversely, suppose we have specified an AR network model such that

$$\begin{aligned}
\sigma(\alpha_{i,j}^{t-1}) &= \boldsymbol{\phi}(\boldsymbol{\theta})^\top \mathbf{u}_{i,j}(\mathbf{X}_{t-1} \setminus X_{i,j}^{t-1}, \mathbf{X}_{t-2}, \dots, \mathbf{X}_{t-m}), \\
\sigma(\beta_{i,j}^{t-1}) &= \boldsymbol{\psi}(\boldsymbol{\theta})^\top \mathbf{v}_{i,j}(\mathbf{X}_{t-1} \setminus X_{i,j}^{t-1}, \mathbf{X}_{t-2}, \dots, \mathbf{X}_{t-m}),
\end{aligned}$$

for some functions of the parameter vector $\boldsymbol{\theta}$, and the past network behavior. We claim that this AR network model can be written as an edge conditionally independent TERGM (A.1) with $\boldsymbol{\varsigma}(\boldsymbol{\theta}) = (\boldsymbol{\phi}(\boldsymbol{\theta})^\top, \boldsymbol{\psi}(\boldsymbol{\theta})^\top)^\top$ and $\boldsymbol{\varrho}(\mathbf{X}_t, \mathbf{X}_{t-1}, \dots, \mathbf{X}_{t-m}) = (\boldsymbol{\varrho}_\alpha^\top, \boldsymbol{\varrho}_\beta^\top)^\top$, where $\boldsymbol{\varrho}_\alpha = \sum_{i,j: i < j} \boldsymbol{\varrho}_{\alpha,i,j}$ and $\boldsymbol{\varrho}_\beta = \sum_{i,j: i < j} \boldsymbol{\varrho}_{\beta,i,j}$ with

$$\begin{aligned}
& \boldsymbol{\varrho}_{\alpha,i,j}(X_{i,j}^t; X_{i,j}^{t-1}, \mathbf{X}_{t-1} \setminus X_{i,j}^{t-1}, \mathbf{X}_{t-2}, \dots, \mathbf{X}_{t-m}) \\
& = \mathbf{u}_{i,j}(\mathbf{X}_{t-1} \setminus X_{i,j}^{t-1}, \mathbf{X}_{t-2}, \dots, \mathbf{X}_{t-m}) I(X_{i,j}^t = 1, X_{i,j}^{t-1} = 0), \\
& \boldsymbol{\varrho}_{\beta,i,j}(X_{i,j}^t; X_{i,j}^{t-1}, \mathbf{X}_{t-1} \setminus X_{i,j}^{t-1}, \mathbf{X}_{t-2}, \dots, \mathbf{X}_{t-m}) \\
& = \mathbf{v}_{i,j}(\mathbf{X}_{t-1} \setminus X_{i,j}^{t-1}, \mathbf{X}_{t-2}, \dots, \mathbf{X}_{t-m}) I(X_{i,j}^t = 0, X_{i,j}^{t-1} = 1).
\end{aligned}$$

Krivitsky and Handcock (2014) define the concept of separability of a dynamic model for binary networks. Define two subnetworks \mathbf{X}_t^+ and \mathbf{X}_t^- , where

$$X_{i,j}^{t,+} = 1 - I(X_{i,j}^t = 0, X_{i,j}^{t-1} = 0) \quad \text{and} \quad X_{i,j}^{t,-} = I(X_{i,j}^t = 1, X_{i,j}^{t-1} = 1), \quad (\text{A.5})$$

for all i, j . A dynamic network model is said to be separable if \mathbf{X}_t^+ and \mathbf{X}_t^- are independent conditional on the past, and do not share any parameters. In particular, a separable TERGM (STERGM) can be specified by a product of a formation model and a dissolution model:

$$\begin{aligned}
& \mathbb{P}(\mathbf{X}_t \mid \mathbf{X}_{t-1}, \dots, \mathbf{X}_{t-m}; \boldsymbol{\theta}) \\
& \propto \exp\{\boldsymbol{\varsigma}^+(\boldsymbol{\theta}^+)^{\top} \boldsymbol{\varrho}^+(\mathbf{X}_t^+, \mathbf{X}_{t-1}, \dots, \mathbf{X}_{t-m}) + \boldsymbol{\varsigma}^-(\boldsymbol{\theta}^-)^{\top} \boldsymbol{\varrho}^-(\mathbf{X}_t^-, \mathbf{X}_{t-1}, \dots, \mathbf{X}_{t-m})\}, \quad (\text{A.6})
\end{aligned}$$

where ς^+ and ς^- map parameter vectors $\boldsymbol{\theta}^+$ and $\boldsymbol{\theta}^-$ to the vectors of natural parameters, and $\boldsymbol{\varrho}^+$ and $\boldsymbol{\varrho}^-$ map the data, including the past network snapshots, to the corresponding sufficient statistics.

Under the edge conditional independence assumption, we can write

$$\boldsymbol{\varrho}^+(\mathbf{X}_t^+, \mathbf{X}_{t-1}, \dots, \mathbf{X}_{t-m}) = \sum_{i < j} \boldsymbol{\varrho}_{i,j}^+(X_{i,j}^{t,+}; X_{i,j}^{t-1}, \mathbf{X}_{t-1} \setminus X_{i,j}^{t-1}, \dots, \mathbf{X}_{t-m}),$$

or equivalently

$$\boldsymbol{\varrho}^+(\mathbf{X}_t^+, \mathbf{X}_{t-1}, \dots, \mathbf{X}_{t-m}) = \sum_{i < j} \tilde{\boldsymbol{\varrho}}_{i,j}^+(X_{i,j}^t; X_{i,j}^{t-1}, \mathbf{X}_{t-1} \setminus X_{i,j}^{t-1}, \dots, \mathbf{X}_{t-m}),$$

since for all $i < j$, $X_{i,j}^{t,+}$ can be recovered from $X_{i,j}^t$ and $X_{i,j}^{t-1}$. Define $\tilde{\boldsymbol{\varrho}}_{i,j}^-$ analogously for the dissolution model.

In this way X_t is an edge conditionally independent TERGM with parameter vector $(\boldsymbol{\theta}^+, \boldsymbol{\theta}^-)$, natural parameter

$$(\varsigma^+(\boldsymbol{\theta}^+), \varsigma^-(\boldsymbol{\theta}^-)),$$

and sufficient statistic

$$\left(\sum_{i < j} \tilde{\boldsymbol{\varrho}}_{i,j}^+, \sum_{i < j} \tilde{\boldsymbol{\varrho}}_{i,j}^- \right).$$

Following the above construction to rewrite this as an AR network model, we can write

$$\begin{aligned} \alpha_{i,j}^{t-1} = \sigma^{-1} & \left[\varsigma^+(\boldsymbol{\theta}^+)^{\top} \left\{ \tilde{\boldsymbol{\varrho}}_{i,j}^+(1; 0, \mathbf{X}_{t-1} \setminus X_{i,j}^{t-1}, \mathbf{X}_{t-2}, \dots, \mathbf{X}_{t-m}) \right. \right. \\ & - \tilde{\boldsymbol{\varrho}}_{i,j}^+(0; 0, \mathbf{X}_{t-1} \setminus X_{i,j}^{t-1}, \mathbf{X}_{t-2}, \dots, \mathbf{X}_{t-m}) \left. \right\} \\ & + \varsigma^-(\boldsymbol{\theta}^-)^{\top} \left\{ \tilde{\boldsymbol{\varrho}}_{i,j}^-(1; 0, \mathbf{X}_{t-1} \setminus X_{i,j}^{t-1}, \mathbf{X}_{t-2}, \dots, \mathbf{X}_{t-m}) \right. \\ & \left. \left. - \tilde{\boldsymbol{\varrho}}_{i,j}^-(0; 0, \mathbf{X}_{t-1} \setminus X_{i,j}^{t-1}, \mathbf{X}_{t-2}, \dots, \mathbf{X}_{t-m}) \right\} \right], \end{aligned}$$

and note that

$$\begin{aligned} \tilde{\boldsymbol{\varrho}}_{i,j}^-(1; 0, \mathbf{X}_{t-1} \setminus X_{i,j}^{t-1}, \mathbf{X}_{t-2}, \dots, \mathbf{X}_{t-m}) &= \tilde{\boldsymbol{\varrho}}_{i,j}^-(0; 0, \mathbf{X}_{t-1} \setminus X_{i,j}^{t-1}, \mathbf{X}_{t-2}, \dots, \mathbf{X}_{t-m}) \\ &= \boldsymbol{\varrho}_{i,j}^-(0; 0, \mathbf{X}_{t-1} \setminus X_{i,j}^{t-1}, \mathbf{X}_{t-2}, \dots, \mathbf{X}_{t-m}) \end{aligned}$$

for all $i < j$ and t , since $X_{i,j}^{t,-} = 0$ whenever $X_{i,j}^{t-1} = 0$. Thus $\alpha_{i,j}^{t-1}$ is free of $\boldsymbol{\theta}^-$. Similarly, we

can write

$$\begin{aligned}
\beta_{i,j}^{t-1} = \sigma^{-1} & \left[\boldsymbol{\varsigma}^+(\boldsymbol{\theta}^+)^{\top} \left\{ \tilde{\boldsymbol{\varrho}}_{i,j}^+(0; 1, \mathbf{X}_{t-1} \setminus X_{i,j}^{t-1}, \mathbf{X}_{t-2}, \dots, \mathbf{X}_{t-m}) \right. \right. \\
& - \tilde{\boldsymbol{\varrho}}_{i,j}^+(1; 1, \mathbf{X}_{t-1} \setminus X_{i,j}^{t-1}, \mathbf{X}_{t-2}, \dots, \mathbf{X}_{t-m}) \left. \right\} \\
& + \boldsymbol{\varsigma}^-(\boldsymbol{\theta}^-)^{\top} \left\{ \tilde{\boldsymbol{\varrho}}_{i,j}^-(0; 1, \mathbf{X}_{t-1} \setminus X_{i,j}^{t-1}, \mathbf{X}_{t-2}, \dots, \mathbf{X}_{t-m}) \right. \\
& \left. \left. - \tilde{\boldsymbol{\varrho}}_{i,j}^-(1; 1, \mathbf{X}_{t-1} \setminus X_{i,j}^{t-1}, \mathbf{X}_{t-2}, \dots, \mathbf{X}_{t-m}) \right\} \right],
\end{aligned}$$

and

$$\begin{aligned}
\tilde{\boldsymbol{\varrho}}_{i,j}^+(0; 1, \mathbf{X}_{t-1} \setminus X_{i,j}^{t-1}, \mathbf{X}_{t-2}, \dots, \mathbf{X}_{t-m}) &= \tilde{\boldsymbol{\varrho}}_{i,j}^+(1; 1, \mathbf{X}_{t-1} \setminus X_{i,j}^{t-1}, \mathbf{X}_{t-2}, \dots, \mathbf{X}_{t-m}) \\
&= \boldsymbol{\varrho}_{i,j}^+(1; 1, \mathbf{X}_{t-1} \setminus X_{i,j}^{t-1}, \mathbf{X}_{t-2}, \dots, \mathbf{X}_{t-m})
\end{aligned}$$

for all $i < j$ and t , since $X_{i,j}^{t,+} = 1$ whenever $X_{i,j}^{t-1} = 1$. Then $\beta_{i,j}^{t-1}$ is free of $\boldsymbol{\theta}^+$. Hence, any edge conditionally independent TERGM can be written as an AR network model with separable parameters.

Conversely, suppose we have specified an AR network model such that

$$\begin{aligned}
\sigma(\alpha_{i,j}^{t-1}) &= \boldsymbol{\phi}(\boldsymbol{\theta}_\alpha)^{\top} \mathbf{u}_{i,j}(\mathbf{X}_{t-1} \setminus X_{i,j}^{t-1}, \mathbf{X}_{t-2}, \dots, \mathbf{X}_{t-m}) \\
\sigma(\beta_{i,j}^{t-1}) &= \boldsymbol{\psi}(\boldsymbol{\theta}_\beta)^{\top} \mathbf{v}_{i,j}(\mathbf{X}_{t-1} \setminus X_{i,j}^{t-1}, \mathbf{X}_{t-2}, \dots, \mathbf{X}_{t-m})
\end{aligned}$$

with separable parameters $\boldsymbol{\theta}_\alpha$ and $\boldsymbol{\theta}_\beta$.

We follow the same construction as above to rewrite this model as an edge conditionally independent TERGM, with parameter vector $\boldsymbol{\varsigma}(\boldsymbol{\theta}) = (\boldsymbol{\phi}(\boldsymbol{\theta}_\alpha)^{\top}, \boldsymbol{\psi}(\boldsymbol{\theta}_\beta)^{\top})^{\top}$ and sufficient statistics $\boldsymbol{\varrho}(\mathbf{X}_t, \mathbf{X}_{t-1}, \dots, \mathbf{X}_{t-m}) = (\boldsymbol{\varrho}_\alpha^{\top}, \boldsymbol{\varrho}_\beta^{\top})^{\top}$, where $\boldsymbol{\varrho}_\alpha = \sum_{i,j: i < j} \boldsymbol{\varrho}_{\alpha,i,j}$ and $\boldsymbol{\varrho}_\beta = \sum_{i,j: i < j} \boldsymbol{\varrho}_{\beta,i,j}$ with

$$\begin{aligned}
\boldsymbol{\varrho}_{\alpha,i,j}(X_{i,j}^t; X_{i,j}^{t-1}, \mathbf{X}_{t-1} \setminus X_{i,j}^{t-1}, \mathbf{X}_{t-2}, \dots, \mathbf{X}_{t-m}) \\
&= \mathbf{u}_{i,j}(\mathbf{X}_{t-1} \setminus X_{i,j}^{t-1}, \mathbf{X}_{t-2}, \dots, \mathbf{X}_{t-m}) I(X_{i,j}^t = 1, X_{i,j}^{t-1} = 0) \\
&= \mathbf{u}_{i,j}(\mathbf{X}_{t-1} \setminus X_{i,j}^{t-1}, \mathbf{X}_{t-2}, \dots, \mathbf{X}_{t-m}) I(X_{i,j}^{t,+} = 1, X_{i,j}^{t-1} = 0), \tag{A.7}
\end{aligned}$$

$$\begin{aligned}
\boldsymbol{\varrho}_{\beta,i,j}(X_{i,j}^t; X_{i,j}^{t-1}, \mathbf{X}_{t-1} \setminus X_{i,j}^{t-1}, \mathbf{X}_{t-2}, \dots, \mathbf{X}_{t-m}) \\
&= \mathbf{v}_{i,j}(\mathbf{X}_{t-1} \setminus X_{i,j}^{t-1}, \mathbf{X}_{t-2}, \dots, \mathbf{X}_{t-m}) I(X_{i,j}^t = 0, X_{i,j}^{t-1} = 1) \\
&= \mathbf{v}_{i,j}(\mathbf{X}_{t-1} \setminus X_{i,j}^{t-1}, \mathbf{X}_{t-2}, \dots, \mathbf{X}_{t-m}) I(X_{i,j}^{t,-} = 0, X_{i,j}^{t-1} = 1). \tag{A.8}
\end{aligned}$$

Note that in (A.7) and (A.8), the sufficient statistics depend on $X_{i,j}^t$ only through $X_{i,j}^{t,+}$ and $X_{i,j}^{t,-}$ respectively. It follows that when written as a conditionally independent TERGM, the distribution factors into a product of a formation model and dissolution model, as in (A.6). Thus, this AR network model is an edge conditionally independent STERGM.

B Simulations with transitivity model

In this section, we use the transitivity model introduced in Section 4.3 as an example to illustrate numerical behaviour of the initial estimation proposed in Section 5.3 and the improved estimation suggested in Section 5.4.

B.1 Implementation details

Network data $\{\mathbf{X}_1, \dots, \mathbf{X}_n\}$ used in the experiments described below are generated according to (1), (2) and (3). For each sample, we generate a sequence of length $n + 200$, and discard the first 200 observations.

Regarding the implementation of our estimation procedures in Sections 5.3 and 5.4, recall that \mathcal{G} and \mathcal{G}^c are, respectively, the index sets of the global parameters and the local parameters. For the transitivity model (3), we have the parameter vector $\boldsymbol{\theta} = (a, b, \xi_1, \dots, \xi_p, \eta_1, \dots, \eta_p)^\top$, where a and b are the global parameters and $\{\xi_i\}_{i=1}^p$ and $\{\eta_i\}_{i=1}^p$ are the local parameters. Hence, for this model we have $|\mathcal{S}_l| = p(p-1)/2$ and $|\mathcal{S}_l \cap \mathcal{S}_{l'}| = p-1$ when $l \in \mathcal{G}$ and $l' \in \mathcal{G}^c$. By (3), for each given $l \in \mathcal{G}$ and $\boldsymbol{\theta} \in \Theta$, it holds with probability approaching one that $\ell_{n,p}^{(l)}(\boldsymbol{\theta}_0) - \ell_{n,p}^{(l)}(\boldsymbol{\theta}) \geq \bar{C}|\boldsymbol{\theta}_{\mathcal{G}} - \boldsymbol{\theta}_{0,\mathcal{G}}|_2^2 + 2\bar{C}p^{-1}|\boldsymbol{\theta}_{\mathcal{G}^c} - \boldsymbol{\theta}_{0,\mathcal{G}^c}|_2^2$ for some universal constant $\bar{C} > 0$ independent of $\boldsymbol{\theta}$, which means that the function $\ell_{n,p}^{(l)}(\cdot)$ defined as (1) exhibits robustness against fluctuations in the values of local parameters when $l \in \mathcal{G}$ and p is large.

Motivated by this fact, when we compute the initial estimator $\tilde{\boldsymbol{\theta}}_{\mathcal{G}}$ for the global parameter vector $\boldsymbol{\theta}_{0,\mathcal{G}}$, we can just approximate $\tilde{\boldsymbol{\theta}}_{\mathcal{G}}$ by $\tilde{\boldsymbol{\theta}}_{\mathcal{G}}^{(\text{app})} = \arg \max_{\boldsymbol{\theta}_{\mathcal{G}}} \hat{\ell}_{n,p}^{(l)}(\boldsymbol{\theta}_{\mathcal{G}}, \bar{\boldsymbol{\theta}}_{\mathcal{G}^c})$, for some given $\bar{\boldsymbol{\theta}}_{\mathcal{G}^c}$ and $\hat{\ell}_{n,p}^{(l)}(\boldsymbol{\theta})$ defined as (5) for some $l \in \mathcal{G}$. This simple idea can significantly improve the computational efficiency. Specifically, note that computing the original $\tilde{\boldsymbol{\theta}}_{\mathcal{G}}$ requires solving an optimization problem with $2p + 2$ variables while this alternative approach only requires solving an optimization problem with two variables. Our above discussion guarantees $\tilde{\boldsymbol{\theta}}_{\mathcal{G}}^{(\text{app})}$ can approximate $\tilde{\boldsymbol{\theta}}_{\mathcal{G}}$ well. Similarly, when we compute the initial estimator $\tilde{\boldsymbol{\theta}}_l$ for the local parameter $\theta_{0,l}$ with $l \in \mathcal{G}^c$, we can approximate it by $\tilde{\boldsymbol{\theta}}_l^{(\text{app})} = \arg \max_{\boldsymbol{\theta}_l} \hat{\ell}_{n,p}^{(l)}(\tilde{\boldsymbol{\theta}}_{\mathcal{G}}^{(\text{app})}, \boldsymbol{\theta}_l, \bar{\boldsymbol{\theta}}_{\mathcal{G}^c \setminus \{l\}})$.

with some given $\bar{\boldsymbol{\theta}}_{\mathcal{G}^c \setminus \{l\}}$.

In practice, we first estimate the global parameters a and b via the Quasi-Newton method, given certain initial values for the local parameters $\{\xi_i\}_{i=1}^p$ and $\{\eta_i\}_{i=1}^p$. To be specific, we consider 9 different sets of the initial values between 0.5 and 0.9 for $\{\xi_i\}_{i=1}^p$ and $\{\eta_i\}_{i=1}^p$, and compute $\tilde{a}^{(\nu)}$ and $\tilde{b}^{(\nu)}$ for the ν -th initial setting. With $a = \tilde{a}^{(\nu)}$ and $b = \tilde{b}^{(\nu)}$, we then compute $\tilde{\xi}_1^{(\nu)}, \dots, \tilde{\xi}_p^{(\nu)}, \tilde{\eta}_1^{(\nu)}, \dots, \tilde{\eta}_p^{(\nu)}$ through maximizing each of the associated $\hat{\ell}_{n,p}^{(l)}(\boldsymbol{\theta})$ with $l \in \mathcal{G}^c$. To reduce sensitivity to initial values and enhance numerical stability, we subsequently apply a computationally efficient method-of-moments-based estimation, which leverages the separable structure between the global and local components of the transition probabilities (3) in the transitivity model. See Section D below for implementation details. The improved estimates $\hat{a}^{(\nu)}, \hat{b}^{(\nu)}, \hat{\xi}_1^{(\nu)}, \dots, \hat{\xi}_p^{(\nu)}, \hat{\eta}_1^{(\nu)}, \dots, \hat{\eta}_p^{(\nu)}$ are then obtained according to (11) with $(\tilde{r}, \check{r}) = (0.2, 0.05)$ for the local parameters and $(\tilde{r}, \check{r}) = (10, 2)$ for the global parameters. The tuning parameter τ required in (9) is selected individually for each parameter θ_l based on the principle of minimizing $\text{Var}(\check{\theta}_l)$, where $\check{\theta}_l$ is defined in (10). Specifically, for each $l \in [2 + 2p]$, we consider a sequence of $\tilde{\tau}_l$ values. For each candidate value, we compute the corresponding projection vector $\hat{\boldsymbol{\varphi}}_l$ via (9) with $\tau = \tilde{\tau}_l \Delta_n^{1/2}$ and subsequently obtain the updated estimator $\check{\theta}_l$ via (10). The optimal τ is then chosen to minimize the empirical variance approximation, i.e.,

$$\frac{\hat{\boldsymbol{\varphi}}_l^\top \sum_{t=2}^n [\mathbf{g}_t^{(l)}(\check{\theta}_l, \tilde{\boldsymbol{\theta}}_{-l}) \mathbf{g}_t^{(l)}(\check{\theta}_l, \tilde{\boldsymbol{\theta}}_{-l})^\top] \hat{\boldsymbol{\varphi}}_l}{[\hat{\boldsymbol{\varphi}}_l^\top \sum_{t=2}^n \nabla_{\theta_l} \mathbf{g}_t^{(l)}(\check{\theta}_l, \tilde{\boldsymbol{\theta}}_{-l})]^2}.$$

Finally, we apply (13) to construct the 95% confidence interval for each θ_l .

B.2 Estimation errors and coverage probabilities

Here we report results on experiments exploring the behavior of the initial estimator $\tilde{\boldsymbol{\theta}}$ given in (6), the improved estimator $\hat{\boldsymbol{\theta}}$ given in (11) and the coverage probabilities of the associated confidence intervals constructed using (13). For simplicity, we set all the true values for $\{\xi_i\}_{i=1}^p$ to be the same, and those for $\{\eta_i\}_{i=1}^p$ also to be the same. The same three sets of parameter values were used as in Section C.1. We set $n \in \{100, 200\}$ and $p \in \{50, 100\}$. For each setting, we replicate the estimation 100 times. The simulations in this section utilise our development R package `arnetworks`, which provides a user-friendly implementation of the estimation and inference procedure described above.

Table S1: The means and STDs (in parenthesis) of rMAEs for estimating parameters in the transitivity model (3) over 100 replications, and the corresponding coverage probabilities of the 95% confidence intervals.

(ξ_i, η_i, a, b)	p	$n = 100$				$n = 200$				
		ξ_i	η_i	a	b	ξ_i	η_i	a	b	
$(0.8, 0.9, 10, 10)$	50	Initial	0.131 (0.001)	0.133 (0.010)	0.743 (0.045)	0.157 (0.002)	0.128 (0.001)	0.134 (0.008)	0.737 (0.031)	0.157 (0.001)
		Improved	0.083 (0.006)	0.033 (0.003)	0.063 (0.044)	0.020 (0.012)	0.068 (0.005)	0.023 (0.002)	0.042 (0.033)	0.019 (0.011)
		Coverage	0.951	0.969	0.933	0.948	0.927	0.958	0.958	0.949
	100	Initial	0.140 (0.001)	0.122 (0.005)	1.248 (0.034)	0.154 (0.001)	0.139 (0.001)	0.123 (0.004)	1.246 (0.025)	0.154 (0.001)
		Improved	0.088 (0.011)	0.049 (0.011)	0.049 (0.027)	0.058 (0.035)	0.055 (0.006)	0.024 (0.002)	0.058 (0.019)	0.026 (0.003)
		Coverage	0.953	0.922	0.955	0.931	0.953	0.934	0.941	0.950
$(0.8, 0.9, 25, 15)$	50	Initial	0.129 (0.002)	0.144 (0.012)	0.305 (0.015)	0.140 (0.001)	0.126 (0.001)	0.145 (0.008)	0.304 (0.011)	0.140 (0.001)
		Improved	0.077 (0.008)	0.031 (0.003)	0.031 (0.022)	0.017 (0.011)	0.058 (0.006)	0.022 (0.002)	0.022 (0.017)	0.015 (0.008)
		Coverage	0.956	0.942	0.950	0.954	0.940	0.952	0.963	0.944
	100	Initial	0.142 (0.001)	0.133 (0.008)	0.455 (0.020)	0.141 (0.001)	0.140 (0.001)	0.133 (0.005)	0.457 (0.015)	0.141 (0.001)
		Improved	0.064 (0.003)	0.026 (0.002)	0.025 (0.015)	0.014 (0.005)	0.055 (0.002)	0.018 (0.001)	0.018 (0.011)	0.012 (0.005)
		Coverage	0.937	0.946	0.944	0.952	0.950	0.940	0.947	0.959
$(0.7, 0.9, 15, 10)$	50	Initial	0.159 (0.002)	0.122 (0.010)	0.433 (0.015)	0.196 (0.004)	0.155 (0.001)	0.122 (0.007)	0.432 (0.011)	0.196 (0.003)
		Improved	0.082 (0.007)	0.039 (0.003)	0.046 (0.035)	0.019 (0.011)	0.066 (0.005)	0.026 (0.002)	0.031 (0.024)	0.019 (0.012)
		Coverage	0.938	0.954	0.946	0.946	0.943	0.955	0.967	0.943
	100	Initial	0.170 (0.001)	0.111 (0.004)	0.653 (0.013)	0.196 (0.002)	0.168 (0.001)	0.110 (0.003)	0.651 (0.009)	0.196 (0.001)
		Improved	0.131 (0.011)	0.086 (0.007)	0.121 (0.026)	0.146 (0.020)	0.048 (0.003)	0.029 (0.003)	0.027 (0.015)	0.025 (0.006)
		Coverage	0.964	0.931	0.958	0.953	0.959	0.932	0.934	0.947

Table S1 presents the means and the standard errors, over the 100 replications, of the relative mean absolute errors (rMAE):

$$\text{rMAE}(\hat{\xi}_i) = \frac{1}{9} \sum_{\nu=1}^9 \frac{1}{p} \sum_{i=1}^p \left| \frac{\hat{\xi}_i^{(\nu)} - \xi_i}{\xi_i} \right| \quad \text{and} \quad \text{rMAE}(\hat{a}) = \frac{1}{9} \sum_{\nu=1}^9 \left| \frac{\hat{a}^{(\nu)} - a}{a} \right|,$$

where the sum over ν corresponds to taking the average over the 9 initial values discussed in Section B.1. Also reported are the coverage probabilities of the 95% confidence intervals constructed based on the limiting distribution in (13), for local parameters ξ_i and η_i with $i = p$, and global parameters a and b . Since each replication includes results from 9 different initializations, the coverage probabilities are based on a total of 900 experiments per setting. Several conclusions can be drawn here. First, the improved estimator $\hat{\theta}$ significantly outperforms the initial estimator $\tilde{\theta}$ in terms of estimation accuracy across all settings. For example, under the setting $(0.8, 0.9, 10, 10)$, the rMAE for estimating a decreases from 1.248 to 0.049 when $n = 100$ and $p = 100$, reflecting an approximate 95% improvement. This demonstrates the effectiveness of the projection strategy in (9) for computing $\hat{\theta}$, as it successfully reduces the impact of nuisance parameter vector θ_{-l} and substantially improves the estimation of the target parameter $\theta_{0,l}$. Second, the improved estimator $\hat{\theta}$ achieves higher accuracy as n increases. Notably, when $n = 200$, we observe comparable or even better estimation performance as the network size p increases, which highlights the robustness and scalability of our method in high-dimensional settings. Lastly, the coverage probabilities remain consistently close to the nominal level 95%, indicating the validity of the proposed asymptotic normal approximation in (13).

C Additional simulation results

Further to Section B, we report more simulation results on the transitivity model.

C.1 Stationarity and ergodicity

As stated in the last paragraph of Section 3.1, for each fixed constant p , $\{\mathbf{X}_t\}_{t \geq 1}$ defined by the transitivity model (3) is stationary and ergodic as long as $\alpha_{i,j}^{t-1}$ and $\beta_{i,j}^{t-1}$ are strictly between 0 and 1. Nevertheless, it is a Markov chain with $2^{p(p-1)/2}$ states. When p is a fixed constant, the ergodicity of \mathbf{X}_t (i.e., the average in time converges to the average over the state space) may take a long time to be observed; see Theorem 4.1 in Chapter 3 of [Bremaud \(1998\)](#). However, the ergodicity of some scalar summary statistics of \mathbf{X}_t can be observed in much short time spans, as indicated in the simulation reported below.

We consider the following three network statistics measures at each time t :

$$D_t = \frac{\sum_{i,j: i < j} X_{i,j}^t}{p(p-1)/2}, \quad D_{1,t} = \frac{\sum_{i,j: i < j} (1 - X_{i,j}^{t-1}) X_{i,j}^t}{p(p-1)/2}, \quad D_{0,t} = \frac{\sum_{i,j: i < j} X_{i,j}^{t-1} (1 - X_{i,j}^t)}{p(p-1)/2}, \quad (\text{C.1})$$

where D_t is the edge density at time t , and $D_{1,t}$ and $D_{0,t}$ are, respectively, the (normalized) number of newly formed edges and newly dissolved edges at time t . If $\{\mathbf{X}_t\}_{t \geq 1}$ is stationary, all three density sequences $\{D_t\}_{t \geq 1}$, $\{D_{1,t}\}_{t \geq 2}$ and $\{D_{0,t}\}_{t \geq 2}$ are also stationary. We also plot

$$\bar{D}_t = \frac{1}{t} \sum_{u=1}^t D_u, \quad \bar{D}_{1,t} = \frac{1}{t} \sum_{u=1}^t D_{1,u}, \quad \bar{D}_{0,t} = \frac{1}{t} \sum_{u=1}^t D_{0,u},$$

against t , for $t \geq 2$, to see how quickly the ergodicity can be observed. These are sample means of one-dimensional network summaries. We expect that their convergences are much faster than that for the sample mean of $p \times p$ network \mathbf{X}_t itself.

Setting $\xi_1 = \dots = \xi_p$ and $\eta_1 = \dots = \eta_p$, we let (ξ_i, η_i, a, b) take three different sets of values: $(0.8, 0.9, 10, 10)$, $(0.8, 0.9, 25, 15)$ and $(0.7, 0.9, 15, 10)$. Figure S1 displays the time series plots of simulated $\{D_t\}_{t=2}^{200}$, $\{D_{1,t}\}_{t=2}^{200}$, $\{D_{0,t}\}_{t=2}^{200}$, $\{\bar{D}_t\}_{t=2}^{200}$, $\{\bar{D}_{1,t}\}_{t=2}^{200}$ and $\{\bar{D}_{0,t}\}_{t=2}^{200}$ when $p = 50$. As expected, all simulated series $\{D_t\}_{t \geq 2}$, $\{D_{1,t}\}_{t \geq 2}$ and $\{D_{0,t}\}_{t \geq 2}$ exhibit patterns in line with stationarity. The convergence of their sample means is observed with the sample sizes greater than 50.

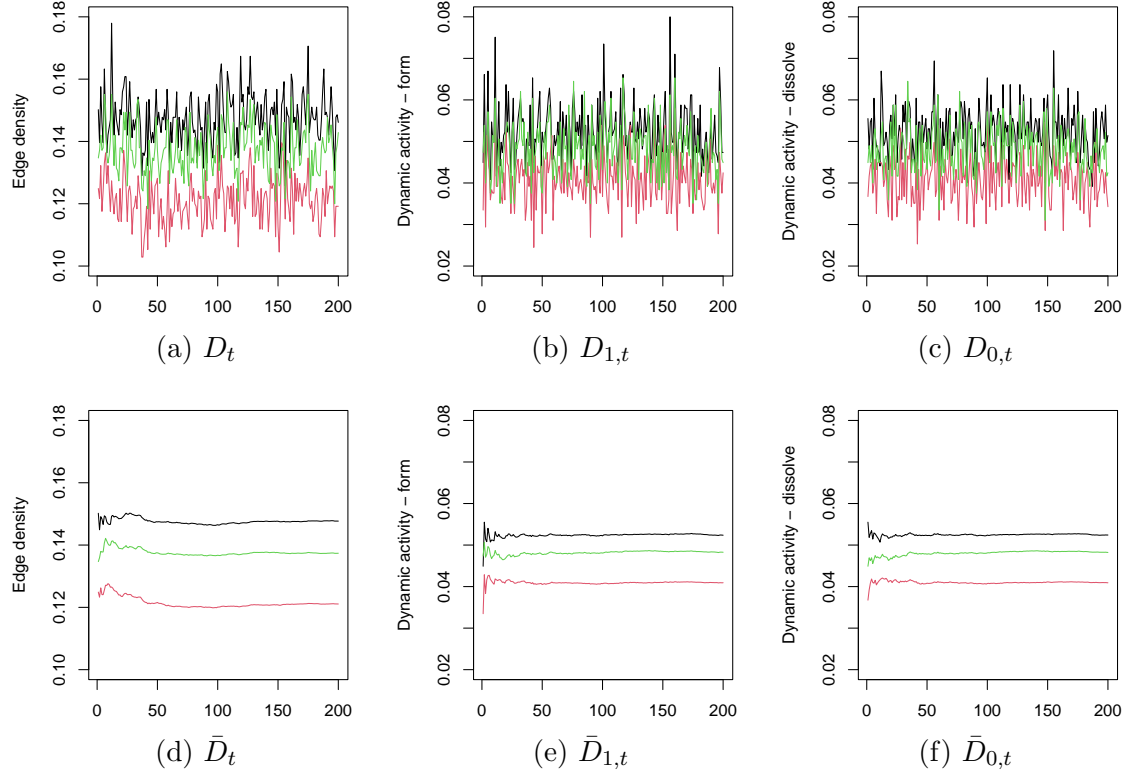


Figure S1: Time series plots of $\{D_t\}_{t=2}^{200}$, $\{D_{1,t}\}_{t=2}^{200}$, $\{D_{0,t}\}_{t=2}^{200}$, $\{\bar{D}_t\}_{t=2}^{200}$, $\{\bar{D}_{1,t}\}_{t=2}^{200}$ and $\{\bar{D}_{0,t}\}_{t=2}^{200}$ for the three simulated settings with $p = 50$. The black, red and green curves correspond to the settings $(\xi_i, \eta_i, a, b) = (0.8, 0.9, 10, 10)$, $(0.8, 0.9, 25, 15)$ and $(0.7, 0.9, 15, 10)$, respectively.

C.2 The transitivity model with $p = 500$

We further examine larger networks with $p = 500$ and $n = 100$ under the transitivity model, and report in Table S2 the means and the standard errors of rMAEs over the 100 replications. The initial values of $\{\xi_i\}_{i=1}^p$ and $\{\eta_i\}_{i=1}^p$ are sampled independently from Uniform[0.5, 0.9]. It can be seen that the proposed estimation procedure remains effective when $p = 500$, with the improved estimator $\hat{\theta}$ significantly outperforming the initial estimator $\tilde{\theta}$.

Table S2: The means and STDs (in parenthesis) of rMAEs for estimating parameters in the transitivity model (3) with $n = 100$ and $p = 500$ over 100 replications.

(ξ_i, η_i, a, b)	Estimation	ξ_i	η_i	a	b
$(0.8, 0.9, 10, 10)$	Initial	0.105 (0.049)	0.048 (0.001)	3.506 (0.077)	0.187 (0.006)
	Improved	0.069 (0.037)	0.035 (0.012)	0.678 (0.138)	0.126 (0.027)
$(0.8, 0.9, 25, 15)$	Initial	0.112 (0.051)	0.047 (0.001)	1.330 (0.034)	0.097 (0.007)
	Improved	0.082 (0.050)	0.036 (0.009)	0.234 (0.069)	0.094 (0.016)
$(0.7, 0.9, 15, 10)$	Initial	0.138 (0.056)	0.047 (0.001)	1.890 (0.055)	0.285 (0.007)
	Improved	0.113 (0.027)	0.014 (0.004)	0.685 (0.133)	0.032 (0.026)

Table S3: The means and STDs (in parenthesis) of rMAEs for estimating parameters in transitivity model (C.2) with 100 replications.

$(\xi_i, a_1, b_1, \eta_i, a_2, b_2)$	n	Estimation	$\alpha_{i,j}^{t-1}(\boldsymbol{\theta})$			$\beta_{i,j}^{t-1}(\boldsymbol{\theta})$		
			ξ_i	a_1	b_1	η_i	a_2	b_2
$(0.8, 10, 10, 0.9, 10, 10)$	100	Initial	0.183 (0.001)	0.611 (0.042)	0.285 (0.005)	0.131 (0.021)	11.953 (21.723)	52.369 (26.797)
		Improved	0.059 (0.006)	0.069 (0.052)	0.020 (0.015)	0.103 (0.015)	11.843 (22.698)	52.629 (29.730)
	200	Initial	0.182 (0.001)	0.609 (0.026)	0.285 (0.003)	0.128 (0.022)	10.082 (18.822)	53.861 (29.054)
		Improved	0.045 (0.005)	0.043 (0.032)	0.013 (0.010)	0.104 (0.032)	9.900 (19.676)	54.005 (32.168)
$(0.8, 25, 15, 0.9, 25, 15)$	100	Initial	0.173 (0.001)	0.331 (0.015)	0.216 (0.002)	0.117 (0.021)	6.265 (10.585)	34.119 (23.249)
		Improved	0.062 (0.007)	0.025 (0.021)	0.015 (0.010)	0.060 (0.020)	6.238 (11.305)	33.400 (25.999)
	200	Initial	0.172 (0.001)	0.333 (0.013)	0.216 (0.002)	0.113 (0.022)	4.389 (7.712)	32.834 (25.108)
		Improved	0.048 (0.005)	0.018 (0.014)	0.081 (0.009)	0.065 (0.033)	4.031 (8.166)	31.552 (28.022)
$(0.7, 15, 10, 0.9, 15, 10)$	100	Initial	0.177 (0.002)	0.379 (0.012)	0.248 (0.004)	0.142 (0.025)	12.506 (18.162)	54.621 (29.036)
		Improved	0.060 (0.006)	0.051 (0.036)	0.022 (0.017)	0.112 (0.014)	12.747 (18.630)	55.040 (31.396)
	200	Initial	0.172 (0.001)	0.375 (0.010)	0.247 (0.002)	0.135 (0.029)	2.748 (5.513)	49.116 (30.803)
		Improved	0.046 (0.004)	0.035 (0.025)	0.075 (0.005)	0.112 (0.041)	2.415 (5.850)	48.528 (34.177)

C.3 A more general model

As stated towards the end of Section 4.3, a more general transitivity model admits the form:

$$\alpha_{i,j}^{t-1}(\boldsymbol{\theta}) = \frac{\xi_i \xi_j e^{a_1 U_{i,j}^{t-1}}}{1 + e^{a_1 U_{i,j}^{t-1}} + e^{b_1 V_{i,j}^{t-1}}}, \quad \beta_{i,j}^{t-1}(\boldsymbol{\theta}) = \frac{\eta_i \eta_j e^{b_2 V_{i,j}^{t-1}}}{1 + e^{a_2 U_{i,j}^{t-1}} + e^{b_2 V_{i,j}^{t-1}}}, \quad (\text{C.2})$$

with $\boldsymbol{\theta} = (a_1, b_1, a_2, b_2, \xi_1, \dots, \xi_p, \eta_1, \dots, \eta_p)^\top \in \mathbb{R}_+^{2p+4}$. Different from the transitivity model (3) introduced in Section 4.3, we allow $a_1 \neq a_2$ and $b_1 \neq b_2$ in (C.2). We adopt the same simulation settings as above, i.e., $(\xi_i, a_1, b_1, \eta_i, a_2, b_2) \in \{(0.8, 10, 10, 0.9, 10, 10), (0.8, 25, 15, 0.9, 25, 15), (0.7, 15, 10, 0.9, 15, 10)\}$.

We implement the estimation procedure in the same manner as in Section B.2. Table S3 reports the resulting rMAEs over 100 replications with $p = 50$ and $n \in \{100, 200\}$. The estimation for the parameters in $\alpha_{i,j}^{t-1}(\boldsymbol{\theta})$, namely ξ_i, a_1 and b_1 , exhibits the similar patterns as in Table S1. In contrast, the estimation for parameters in $\beta_{i,j}^{t-1}(\boldsymbol{\theta})$ deteriorates significantly, and especially for a_2 and b_2 . Note that only some components of \mathbf{X}_{t-1} with $X_{i,j}^{t-1} = 1$, $t \in [n] \setminus [m]$ and $j \neq i$, were used in estimating parameters a_2 and b_2 . For sparse networks, the total number of those data points is small. This is the intrinsic difficulty in estimating the parameters in $\beta_{i,j}^{t-1}(\boldsymbol{\theta})$. See also the relevant discussion at the end of Section 4.3.

D Method of moments estimation

In this section, we leverage the structural similarities across the three AR network models introduced in Section 4 and propose a computationally efficient estimation procedure, termed Iterative Method of Moments (IMoM).

D.1 IMoM algorithm

Consider a simplified formulation of the transition probabilities, given by

$$\begin{aligned}\alpha_{i,j}^{t-1}(\boldsymbol{\theta}) &= \xi_i \xi_j \tilde{f}_{i,j}(\mathbf{X}_{t-1} \setminus X_{i,j}^{t-1}, \mathbf{X}_{t-2}, \dots, \mathbf{X}_{t-m}; \boldsymbol{\theta}_{\mathcal{G}}), \\ \beta_{i,j}^{t-1}(\boldsymbol{\theta}) &= \eta_i \eta_j \tilde{g}_{i,j}(\mathbf{X}_{t-1} \setminus X_{i,j}^{t-1}, \mathbf{X}_{t-2}, \dots, \mathbf{X}_{t-m}; \boldsymbol{\theta}_{\mathcal{G}}),\end{aligned}\tag{D.1}$$

where $\{\xi_i\}_{i=1}^p$ and $\{\eta_i\}_{i=1}^p$ are local parameters capturing node-specific heterogeneity in edge formation and dissolution, respectively, and $\tilde{f}_{i,j}$'s and $\tilde{g}_{i,j}$'s are known functions that depend only on the global parameters $\boldsymbol{\theta}_{\mathcal{G}}$. This separable structure between the local and global components allows us to develop the IMoM estimation procedure as follows.

For illustrative purposes, we focus on the AR(m) network with $m = 1$. We start with some initial values for the local parameters $\{\xi_i\}_{i=1}^p$ and $\{\eta_i\}_{i=1}^p$, denoted as $\{\xi_i^{(0)}\}_{i=1}^p$ and $\{\eta_i^{(0)}\}_{i=1}^p$, respectively. At the $(\iota+1)$ -th iteration, we first update the global parameter vector by solving an optimization problem similar to the computation of $\tilde{\boldsymbol{\theta}}_{\mathcal{G}}^{(\text{app})}$ in Section B.1. Specifically, we write $\mathring{\boldsymbol{\theta}}_{\mathcal{G}^c}^{(\iota)} = (\xi_1^{(\iota)}, \dots, \xi_p^{(\iota)}, \eta_1^{(\iota)}, \dots, \eta_p^{(\iota)})^\top$ with $\xi_1^{(\iota)}, \dots, \xi_p^{(\iota)}, \eta_1^{(\iota)}, \dots, \eta_p^{(\iota)}$ denoting the ι -th iterate of local parameters, and obtain $\mathring{\boldsymbol{\theta}}_{\mathcal{G}}^{(\iota+1)} = \arg \max_{\boldsymbol{\theta}_{\mathcal{G}}} \hat{\ell}_{n,p}^{(l)}(\boldsymbol{\theta}_{\mathcal{G}}, \mathring{\boldsymbol{\theta}}_{\mathcal{G}^c}^{(\iota)})$, for $\hat{\ell}_{n,p}^{(l)}(\boldsymbol{\theta})$ defined in (5) for some $l \in \mathcal{G}$. As discussed in Section B.1, this low-dimensional optimization step is computationally more efficient and offers a reliable approximation of the global parameters.

Let $\Xi_{i,j} = \xi_i \xi_j$ and $\Gamma_{i,j} = \eta_i \eta_j$ denote the edgewise local parameters for $1 \leq i \neq j \leq p$. We next turn to updating these parameters via a method-of-moments approach. Denote by $I(\cdot)$ the indicator function. Inspired by the fact that

$$\begin{aligned}\mathbb{P}(X_{i,j}^t = 1 \mid X_{i,j}^{t-1} = 0) &= \mathbb{E}\{\mathbb{P}(X_{i,j}^t = 1 \mid X_{i,j}^{t-1} = 0, \mathbf{X}_{t-1} \setminus X_{i,j}^{t-1}) \mid X_{i,j}^{t-1} = 0\} \\ &= \mathbb{E}(\alpha_{i,j}^{t-1} \mid X_{i,j}^{t-1} = 0) = \frac{\mathbb{E}\{\alpha_{i,j}^{t-1} I(X_{i,j}^{t-1} = 0)\}}{\mathbb{P}(X_{i,j}^{t-1} = 0)},\end{aligned}$$

we compute the $(\iota+1)$ -th iterate for $\Xi_{i,j}$ by

$$\mathring{\Xi}_{i,j}^{(\iota+1)} = \frac{\sum_{t=2}^n X_{i,j}^t (1 - X_{i,j}^{t-1})}{\sum_{t=2}^n \tilde{f}_{i,j}\{\mathbf{X}_{t-1} \setminus X_{i,j}^{t-1}; \boldsymbol{\theta}_{\mathcal{G}}^{(\iota+1)}\} (1 - X_{i,j}^{t-1})} \equiv \mathring{\xi}_i^{(\iota+1)} \mathring{\xi}_j^{(\iota+1)}. \tag{D.2}$$

Similarly, we update

$$\mathring{\Gamma}_{i,j}^{(\iota+1)} = \frac{\sum_{t=2}^n (1 - X_{i,j}^t) X_{i,j}^{t-1}}{\sum_{t=2}^n \tilde{g}_{i,j} \{ \mathbf{X}_{t-1} \setminus X_{i,j}^{t-1}; \mathring{\theta}_{\mathcal{G}}^{(\iota+1)} \} X_{i,j}^{t-1}} \equiv \mathring{\eta}_i^{(\iota+1)} \mathring{\eta}_j^{(\iota+1)}. \quad (\text{D.3})$$

Finally, we recover the individual local parameters $\{\xi_i\}_{i=1}^p$ and $\{\eta_i\}_{i=1}^p$ by solving a strongly convex optimization problem. Set $\mathring{\Xi}_{i,i}^{(\iota+1)} = \mathring{\Gamma}_{i,i}^{(\iota+1)} = 0$ for all $i \in [p]$ and define $\mathbf{\Xi}^{(\iota+1)} = \{\mathring{\Xi}_{i,j}^{(\iota+1)}\}_{i,j \in [p]}$ and $\mathbf{\Gamma}^{(\iota+1)} = \{\mathring{\Gamma}_{i,j}^{(\iota+1)}\}_{i,j \in [p]}$. Let $\mathbf{1}_p$ denote the p -dimensional column vector of ones. We then compute the log-transformed local parameters $\{\log(\xi_i)\}_{i \in [p]}$ and $\{\log(\eta_i)\}_{i \in [p]}$, respectively, as $\hat{\mathbf{x}}_{\iota+1} = \arg \min_{\mathbf{x} \in \mathbb{R}^p} \mathring{\ell}(\mathbf{x}; \mathbf{\Xi}^{(\iota+1)} \mathbf{1}_p)$ and $\hat{\mathbf{y}}_{\iota+1} = \arg \min_{\mathbf{y} \in \mathbb{R}^p} \mathring{\ell}(\mathbf{y}; \mathbf{\Gamma}^{(\iota+1)} \mathbf{1}_p)$, where the function $\mathring{\ell}(\cdot; \cdot)$ is specified in Lemma 1 below. The strong convexity of $\mathring{\ell}(\cdot; \cdot)$ ensures that these minimizers are unique and can be computed efficiently. See Section D.2 below for further technical details. Write $\hat{\mathbf{x}}_{\iota+1} = (\hat{x}_{1,\iota+1}, \dots, \hat{x}_{p,\iota+1})^\top$ and $\hat{\mathbf{y}}_{\iota+1} = (\hat{y}_{1,\iota+1}, \dots, \hat{y}_{p,\iota+1})^\top$. The updated local parameters are obtained via $\mathring{\xi}_i^{(\iota+1)} = \exp(\hat{x}_{i,\iota+1})$ and $\mathring{\eta}_i^{(\iota+1)} = \exp(\hat{y}_{i,\iota+1})$ for all $i \in [p]$.

We iterate the above three steps until convergence to obtain the final IMoM estimator $\mathring{\theta}$. The complete estimation procedure is summarized in Algorithm 1. One possible alternative is to iterate only between Steps (i) and (ii), deferring the recovery of the individual local parameters, i.e., Step (iii), to the final iteration. While such an approach introduces a slight reduction in computational effort per iteration, our numerical experiments indicate that it leads to lower estimation accuracy and slower convergence in practice. We therefore incorporate Step (iii) into each iteration, as described in Algorithm 1.

D.2 Technical support

We present Lemma 1 to establish the strong convexity of $\mathring{\ell}(\mathbf{x}; \mathbf{v})$ and provide relevant discussion to justify Step (iii) in Algorithm 1.

Lemma 1 *For any $\mathbf{x} = (x_1, \dots, x_p)^\top \in \mathbb{R}^p$ and $\mathbf{v} = (v_1, \dots, v_p)^\top \in \mathbb{R}^p$, define*

$$\mathring{\ell}(\mathbf{x}; \mathbf{v}) = \sum_{i,j: 1 \leq i < j \leq p} \exp(x_i + x_j) - \sum_{i=1}^p x_i v_i.$$

Then $\mathring{\ell}(\mathbf{x}; \mathbf{v})$ is strongly convex in $\mathbf{x} \in \mathbb{R}^p$.

Algorithm 1 IMoM for AR networks with transition probabilities in (D.1).

1. Input: Initial values for local parameters, i.e., $\{\xi_i^{(0)}\}_{i=1}^p$ and $\{\eta_i^{(0)}\}_{i=1}^p$.

2. For $\iota = 0, 1, \dots$ until convergence:

(i) Update the global parameter vector via

$$\mathring{\boldsymbol{\theta}}_{\mathcal{G}}^{(\iota+1)} = \arg \max_{\boldsymbol{\theta}_{\mathcal{G}}} \hat{\ell}_{n,p}^{(l)}(\boldsymbol{\theta}_{\mathcal{G}}, \mathring{\boldsymbol{\theta}}_{\mathcal{G}^c}^{(\iota)}),$$

where $\mathring{\boldsymbol{\theta}}_{\mathcal{G}^c}^{(\iota)} = (\xi_1^{(\iota)}, \dots, \xi_p^{(\iota)}, \eta_1^{(\iota)}, \dots, \eta_p^{(\iota)})^\top$ and $\hat{\ell}_{n,p}^{(l)}(\boldsymbol{\theta})$ is defined in (5) for some $l \in \mathcal{G}$.

(ii) Compute the edgewise local parameters $\mathring{\Xi}_{i,j}^{(\iota+1)}$ and $\mathring{\Gamma}_{i,j}^{(\iota+1)}$ using method-of-moments-based approach in (D.2) and (D.3), respectively.

(iii) Recover the log-transformed local parameters by solving

$$\hat{\mathbf{x}}_{\iota+1} = \arg \min_{\mathbf{x} \in \mathbb{R}^p} \mathring{\ell}(\mathbf{x}; \boldsymbol{\Xi}^{(\iota+1)} \mathbf{1}_p), \quad \hat{\mathbf{y}}_{\iota+1} = \arg \min_{\mathbf{y} \in \mathbb{R}^p} \mathring{\ell}(\mathbf{y}; \boldsymbol{\Gamma}^{(\iota+1)} \mathbf{1}_p),$$

where $\hat{\mathbf{x}}_{\iota+1} = (\hat{x}_{1,\iota+1}, \dots, \hat{x}_{p,\iota+1})^\top$, $\hat{\mathbf{y}}_{\iota+1} = (\hat{y}_{1,\iota+1}, \dots, \hat{y}_{p,\iota+1})^\top$ and $\mathring{\ell}(\cdot; \cdot)$ is specified in Lemma 1. Then obtain $\mathring{\xi}_i^{(\iota+1)} = \exp(\hat{x}_{i,\iota+1})$, $\mathring{\eta}_i^{(\iota+1)} = \exp(\hat{y}_{i,\iota+1})$ for $i \in [p]$.

3. Output: Final estimator

$$\mathring{\boldsymbol{\theta}} = (\{\mathring{\boldsymbol{\theta}}_{\mathcal{G}}^{(\iota+1)}\}^\top, \{\mathring{\boldsymbol{\theta}}_{\mathcal{G}^c}^{(\iota+1)}\}^\top)^\top,$$

where $\mathring{\boldsymbol{\theta}}_{\mathcal{G}^c}^{(\iota+1)} = (\mathring{\xi}_1^{(\iota+1)}, \dots, \mathring{\xi}_p^{(\iota+1)}, \mathring{\eta}_1^{(\iota+1)}, \dots, \mathring{\eta}_p^{(\iota+1)})^\top$.

Proof. Let $\mathbf{H}(\mathbf{x}) = \{H_{i,j}(\mathbf{x})\}_{i,j \in [p]}$ denote the Hessian matrix of $\mathring{\ell}(\mathbf{x}; \mathbf{v})$. By basic calculations, we obtain that

$$H_{i,i}(\mathbf{x}) = \sum_{j: j \neq i} \exp(x_i + x_j), \quad \text{for } i \in [p],$$

$$H_{i,j}(\mathbf{x}) = \exp(x_i + x_j), \quad \text{for } 1 \leq i \neq j \leq p.$$

For any $\mathbf{x} \in \mathbb{R}^p$ and $\mathbf{z} = (z_1, \dots, z_p)^\top \in \mathbb{R}^p$, it follows that

$$\mathbf{z}^\top \mathbf{H}(\mathbf{x}) \mathbf{z} = \sum_{i,j: 1 \leq i < j \leq p} (z_i + z_j)^2 \exp(x_i + x_j) \geq 0,$$

with equality if and only if $z_1 = \dots = z_p = 0$. We thus complete the proof of Lemma 1. \square

Lemma 1 indicates that $\hat{\ell}(\mathbf{x}; \mathbf{v})$ admits a unique minimizer. Observe that

$$\frac{\partial \hat{\ell}(\mathbf{x}; \mathbf{v})}{\partial x_i} = \sum_{j: j \neq i} \exp(x_i + x_j) - v_i. \quad (\text{D.4})$$

Recall $\Xi^{(\iota+1)} = \{\hat{\Xi}_{i,j}^{(\iota+1)}\}_{i,j \in [p]}$ and note that

$$\sum_{j: j \neq i} \exp \{ \log(\hat{\xi}_i^{(\iota+1)}) + \log(\hat{\xi}_j^{(\iota+1)}) \} = \sum_{j=1}^p \hat{\Xi}_{i,j}^{(\iota+1)}. \quad (\text{D.5})$$

Comparing (D.4) and (D.5), the log-transformed local parameters $\{\log(\xi_i)\}_{i \in [p]}$ can be identified by solving

$$\hat{\mathbf{x}}_{\iota+1} = (\hat{x}_{1,\iota+1}, \dots, \hat{x}_{p,\iota+1})^\top = \arg \min_{\mathbf{x} \in \mathbb{R}^p} \hat{\ell}(\mathbf{x}; \Xi^{(\iota+1)} \mathbf{1}_p),$$

and then we update $\{\xi_i\}_{i \in [p]}$ via $\hat{\xi}_i^{(\iota+1)} = \exp(\hat{x}_{i,\iota+1})$ for all $i \in [p]$. Analogously, we compute

$$\hat{\mathbf{y}}_{\iota+1} = (\hat{y}_{1,\iota+1}, \dots, \hat{y}_{p,\iota+1})^\top = \arg \min_{\mathbf{y} \in \mathbb{R}^p} \hat{\ell}(\mathbf{y}; \Gamma^{(\iota+1)} \mathbf{1}_p),$$

leading to the update $\hat{\eta}_i^{(\iota+1)} = \exp(\hat{y}_{i,\iota+1})$ for all $i \in [p]$.

E Additional real data analysis

E.1 Preliminary summaries of email interaction

In this section, we present some preliminary summaries of the dynamic email network dataset analyzed in Section 6. The behavior shown in Figure S2 suggests a change point in the network behavior, in terms of both edge density D_t and two dynamic (normalized) formation and dissolution measures $D_{1,t}$ and $D_{0,t}$ defined by

$$D_t = \frac{\sum_{i,j: i < j} X_{i,j}^t}{p(p-1)/2}, \quad D_{1,t} = \frac{\sum_{i,j: i < j} (1 - X_{i,j}^{t-1}) X_{i,j}^t}{p(p-1)/2}, \quad D_{0,t} = \frac{\sum_{i,j: i < j} X_{i,j}^{t-1} (1 - X_{i,j}^t)}{p(p-1)/2}.$$

See also (C.1). Based on this analysis, we split the dataset into the first 13 and last 26 snapshots, referred to as ‘‘period 1’’ and ‘‘period 2’’. In the right panel, about 4% of node pairs see a grown edge or a dissolved edge between consecutive snapshots. However, dissolution

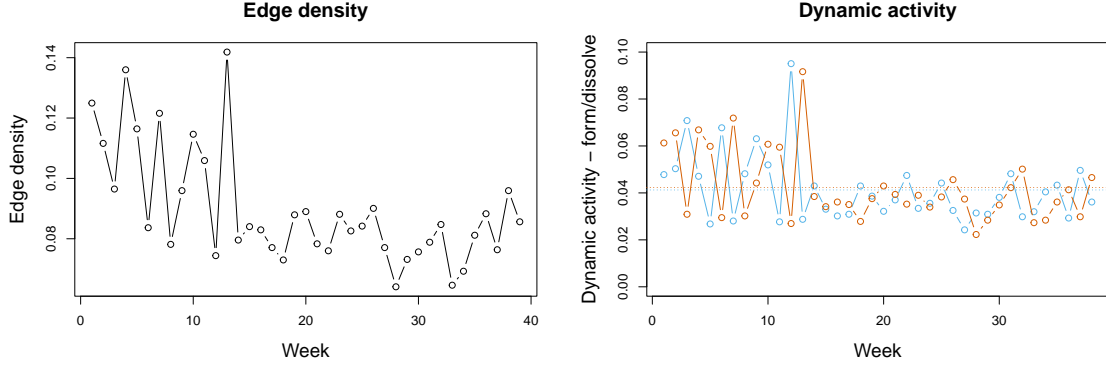


Figure S2: Evolution of edge density D_t (left panel), percentage of grown $D_{1,t}$ (blue) and dissolved $D_{0,t}$ (orange) edges (right panel), email interaction networks.

can only occur for an active edge, and as we see in the left panel of Figure S2, this network has relatively low edge density. On average (over time), the proportion of non-edge that form in the next snapshot is about 5%, while the proportion of existing edges which persist in the next snapshot is about 55%.

We also inspect the data for empirical evidence of transitivity effects. This is demonstrated in Figure S3. To construct these plots, we partition the edge variables as follows: for each integer $\ell \geq 0$, define

$$\begin{aligned}\mathcal{U}_\ell &= \{(i, j, t) : 1 \leq i < j \leq p, t \in [n] \setminus \{1\}, X_{i,j}^{t-1} = 0, U_{i,j}^{t-1} = \ell/(p-2)\}, \\ \mathcal{V}_\ell &= \{(i, j, t) : 1 \leq i < j \leq p, t \in [n] \setminus \{1\}, X_{i,j}^{t-1} = 1, V_{i,j}^{t-1} = \ell/(p-2)\}, \\ \mathcal{U}_\ell^1 &= \{(i, j, t) \in \mathcal{U}_\ell, X_{i,j}^t = 1\}, \quad \mathcal{V}_\ell^0 = \{(i, j, t) \in \mathcal{V}_\ell, X_{i,j}^t = 0\},\end{aligned}$$

where $U_{i,j}^{t-1}$ and $V_{i,j}^{t-1}$ are given in (4).

The left panel plots the relative frequency $|\mathcal{U}_\ell^1|/|\mathcal{U}_\ell|$ against ℓ for $\ell = 0, 1, \dots$, showing that this frequency of grown edges tends to be higher for node pairs with more common neighbours in the previous snapshot. The right panel analogously plots the relative frequency $|\mathcal{V}_\ell^0|/|\mathcal{V}_\ell|$ against ℓ , and shows a similar increasing relationship between disjoint neighbours and frequency of dissolved edges.

The analysis above is based on the weekly email network data. As the original data contain the time stamp of each email exchange, we can also construct daily networks based on if there is any email exchange or not between two individuals on each day. Figure S4 plots the daily edge density, the daily density of forming new edges and that of dissolving existing edges. By comparing it with Figure S2, the daily data exhibit more nonstationary features

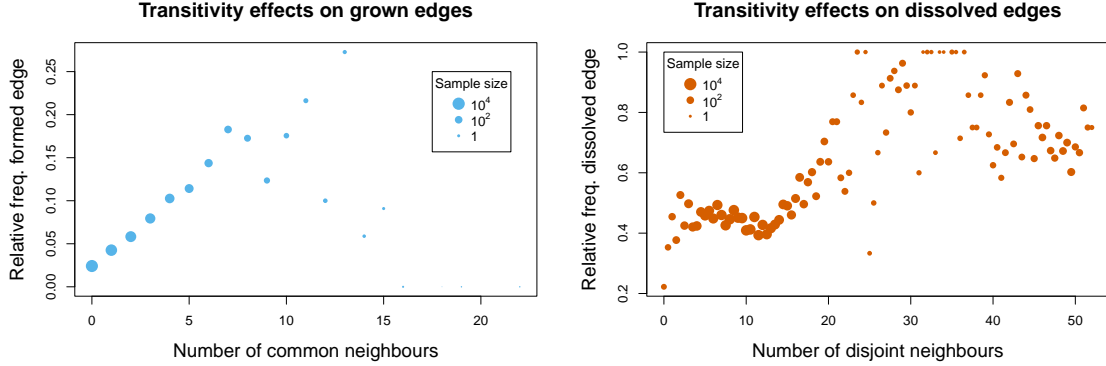


Figure S3: Left panel: the plot of relative edge frequency $|\mathcal{U}_\ell^1|/|\mathcal{U}_\ell|$ against ℓ , email interaction networks. Right panel: the plot of relative non-edge frequency $|\mathcal{V}_\ell^0|/|\mathcal{V}_\ell|$ against ℓ , email interaction networks. In both panels, point size is proportional to the log sample sizes $\log |\mathcal{U}_\ell|$ and $\log |\mathcal{V}_\ell|$ respectively.

(such as effects of weekends, holidays, and periodicity through the week). The difference between the first 13 weeks and the last 26 weeks is more clearly exhibited in the weekly data. Figure S5 reproduces Figure S3 for the daily network data. Though the transitivity is still present with the daily data, it is mixed with more irregular signals. In the right panel of Figure S5, we do not see a clear effect of number of disjoint neighbours on edge dissolution; the daily networks are much sparser than the weekly ones, implying a lack of effective sample size to see meaningful patterns in edge dissolution. By accumulating information on a weekly level, the data is more stationary and the empirical transitivity patterns are clearer.

E.2 Comparative STERGM analysis of email interactions

In order to compare the effects of the transitivity statistics $\{U_{i,j}^{t-1}\}$ and $\{V_{i,j}^{t-1}\}$ on the manufacturing email networks, we fit STERGM models using an implementation in the R package `tergm` from the `statnet` suite of software (Krivitsky et al., 2025). First we fit a sequence of models, one for each transition from \mathbf{X}_{t-1} to \mathbf{X}_t for each t within periods 1 and 2. Following Krivitsky and Handcock (2014) and the notation introduced in our Appendix A, for each t , we specify a formation model by

$$\mathbb{P}(\mathbf{X}_t^+ \mid \mathbf{X}_{t-1}) \propto \exp \left(\beta_0^+ \sum_{i,j: i \neq j} X_{i,j}^{t,+} + \beta_U^+ \sum_{i,j: i \neq j} U_{i,j}^{t-1} X_{i,j}^{t,+} + \beta_V^+ \sum_{i,j: i \neq j} V_{i,j}^{t-1} X_{i,j}^{t,+} \right)$$

and $\mathbf{X}_t^+ \in \mathcal{Y}^+(\mathbf{X}_{t-1})$, where $\mathcal{Y}^+(\mathbf{X}_{t-1})$ denotes the sample space of formation networks, i.e., all networks obtained by adding edges to \mathbf{X}_{t-1} , and $\mathbf{X}_t^+ = (X_{i,j}^{t,+})_{p \times p}$ with $X_{i,j}^{t,+}$ defined in

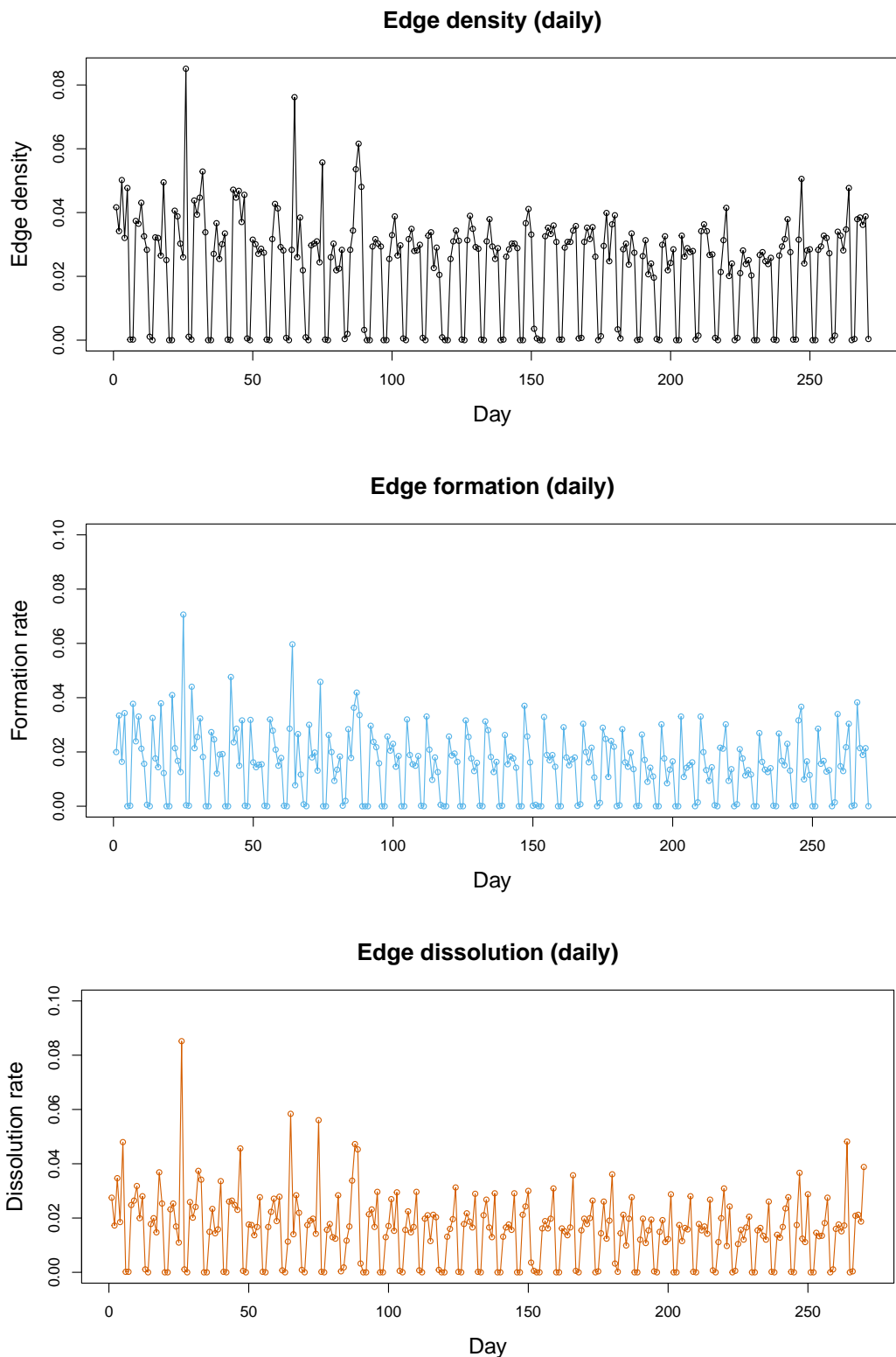


Figure S4: Evolution of edge density D_t (top panel), percentage of grown $D_{1,t}$ (blue, center panel) and dissolved $D_{0,t}$ (orange, bottom panel) edges, manufacturing email networks constructed on a daily level.

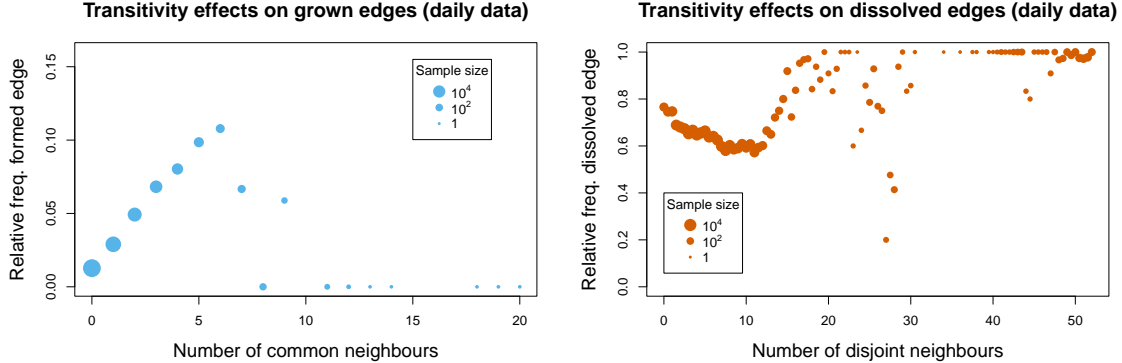


Figure S5: Left panel: the plot of relative edge frequency $|\mathcal{U}_\ell^1|/|\mathcal{U}_\ell|$ against ℓ , email interaction networks. Right panel: the plot of relative non-edge frequency $|\mathcal{V}_\ell^0|/|\mathcal{V}_\ell|$ against ℓ , email interaction networks. In both panels, point size is proportional to the log sample sizes $\log |\mathcal{U}_\ell|$ and $\log |\mathcal{V}_\ell|$ respectively. The plots are constructed based on daily data.

(A.5). We similarly specify a persistence model by

$$\mathbb{P}(\mathbf{X}_t^- \mid \mathbf{X}_{t-1}) \propto \exp \left(\beta_0^- \sum_{i,j: i \neq j} X_{i,j}^{t,-} + \beta_U^- \sum_{i,j: i \neq j} U_{i,j}^{t-1} X_{i,j}^{t,-} + \beta_V^- \sum_{i,j: i \neq j} V_{i,j}^{t-1} X_{i,j}^{t,-} \right)$$

and $\mathbf{X}_t^- \in \mathcal{Y}^-(\mathbf{X}_{t-1})$, where $\mathcal{Y}^-(\mathbf{X}_{t-1})$ denotes the sample space of dissolution networks, i.e., all networks obtained by removing edges from \mathbf{X}_{t-1} , and $\mathbf{X}_t^- = (X_{i,j}^{t,-})_{p \times p}$ with $X_{i,j}^{t,-}$ defined in (A.5). Note that the edges present in \mathbf{X}_t^- are those that persist (i.e., are not dissolved) from \mathbf{X}_{t-1} to \mathbf{X}_t , whereas our AR framework models edge dissolution. To fit this separable model, we call `tergm` with the formula $\sim \text{Form}(\sim \text{edges} + \text{edgecov}(U) + \text{edgecov}(V)) + \text{Persist}(\sim \text{edges} + \text{edgecov}(U) + \text{edgecov}(V))$. The resulting coefficient estimates are plotted in Figure S6. We expect the coefficients corresponding to `edgecov(U)` to influence edge formation and dissolution probabilities similarly to our AR transitivity model parameter a : positive values of β_U^+ and β_U^- imply that more common neighbours in the previous snapshot increases probability of formation, and increases probability of persistence (decreases probability of dissolution). Analogously, we expect the coefficients corresponding to `edgecov(V)` to influence edge formation and dissolution probabilities inversely to our AR transitivity model parameter b (see Section 4.3).

Consistent with the analysis with the AR network model, we find that there is a strong effect of number of common neighbours in the previous time step on edge formation. `tergm` reports that all 38 of these parameter estimates are significantly different from 0 at the Bonferroni-corrected level $0.05/(6 \times 38)$. The signs of the estimated coefficients agree with

TERGM transition model parameter estimates

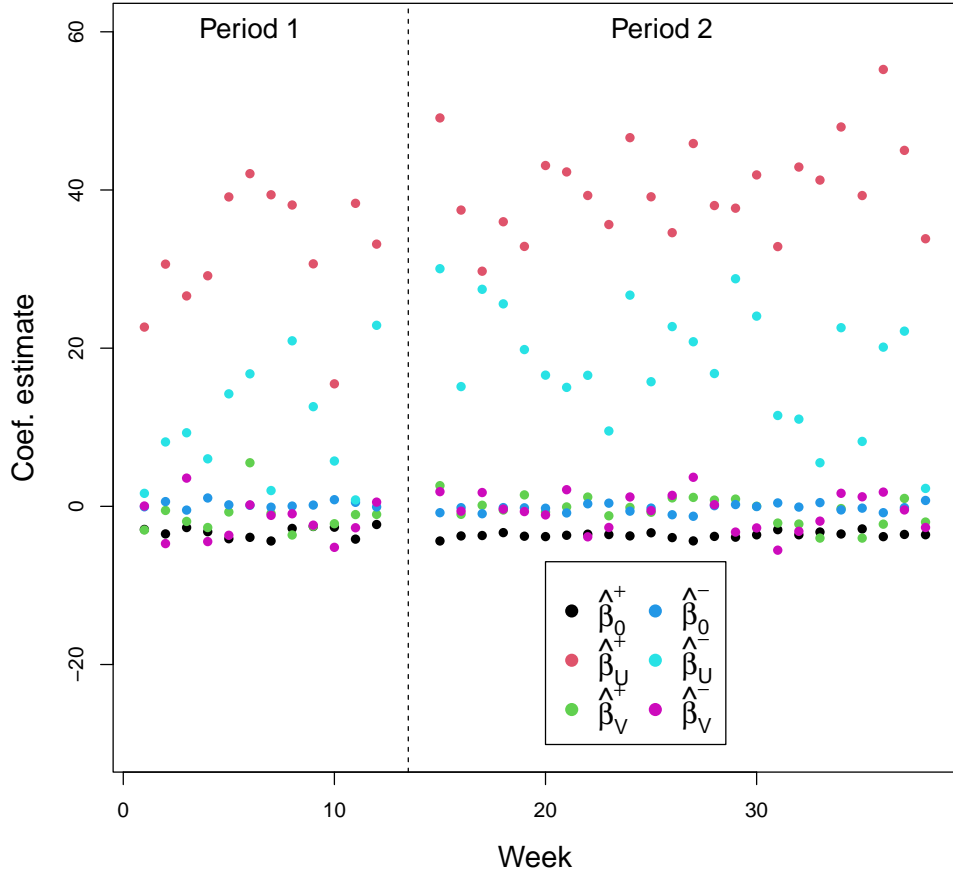


Figure S6: Sequence of TERGM parameter estimates for each network transition.

our analysis (see Section 6), showing that number of common neighbours has an increasing relationship with edge formation probability. Also similar to our analysis, `tergm` finds that the magnitude of these effects are higher on average in period 2 than period 1. `tergm` reports (Bonferroni) significant coefficients for 19 out of 38 effects of $\{U_{i,j}^{t-1}\}$ on edge persistence (dissolution); the signs of these estimated coefficients are all positive, which agrees with our analysis. For the estimated `edgecov(V)` coefficients, `tergm` reports (Bonferroni) significant coefficients for only 2 out of 38 effects of $\{V_{i,j}^{t-1}\}$ on edge formation, and 7 out of 38 effects of $\{V_{i,j}^{t-1}\}$ on edge persistence (dissolution). Relative to our analysis, which pools information across time, and between formation and dissolution, this sequential analysis with `tergm` finds a less consistent effect of $\{V_{i,j}^{t-1}\}$ (normalized number of distinct neighbours) on edge formation and dissolution in \mathbf{X}_t .

In order to inspect the node heterogeneity of the manufacturing email networks, we fit TERGM models to the sequences of snapshots from periods 1 and 2 with sociality effects, which fit one parameter per node to describe the degree heterogeneity in the formation and dissolution models. The precise formation and persistence models are given by

$$\begin{aligned}\mathbb{P}(\mathbf{X}_t^+ | \mathbf{X}_{t-1}) &\propto \exp \left(\alpha_0^+ \sum_{i,j: i \neq j} X_{i,j}^{t,+} + \sum_{i=1}^p \alpha_i^+ \sum_{j: j \neq i} X_{i,j}^{t,+} \right), \quad \mathbf{X}_t^+ \in \mathcal{Y}^+(\mathbf{X}_{t-1}), \\ \mathbb{P}(\mathbf{X}_t^- | \mathbf{X}_{t-1}) &\propto \exp \left(\alpha_0^- \sum_{i,j: i \neq j} X_{i,j}^{t,-} + \sum_{i=1}^p \alpha_i^- \sum_{j: j \neq i} X_{i,j}^{t,-} \right), \quad \mathbf{X}_t^- \in \mathcal{Y}^-(\mathbf{X}_{t-1}).\end{aligned}$$

We fit this separable model by calling `tergm` with the formula $\sim \text{Form}(\sim \text{edges} + \text{sociality}) + \text{Persist}(\sim \text{edges} + \text{sociality})$. We expect the coefficients corresponding to the formation model sociality term to influence edge formation probabilities similarly to our local parameters $\{\xi_i\}$. We expect the coefficients corresponding to the persistence model sociality term to influence edge dissolution probabilities inversely to our local parameters $\{\eta_i\}$ (see Section 4.3).

In Figure S7, we summarize the fitted sociality effects by comparing them to the corresponding local parameters fit by our AR network model in Section 6. Broadly, we see the expected increasing relationship between estimates of $\{\xi_i\}$ parameters and formation model sociality effects, and a decreasing relationship between estimates of $\{\eta_i\}$ parameters and persistence model sociality effects.

However, there are also subtle differences in interpretation of these parameters afforded by our new model formulation. The multiplicative structure of our model means that while each ξ_i and η_i are related to observed degree, their direct impact on the edge formation and dissolution is to modulate the strength of transitivity for each individual node. In Figure S7, we see a wide range of $\{\xi_i\}$ and $\{\eta_i\}$ estimates even for nodes with very similar estimates of their TERGM sociality parameters α_i^+ and α_i^- , implying that there is not a perfect correspondence between these two phenomena: nodes with similar socialities may still vary considerably in the strength of transitivity on their formed and dissolved connections.

E.3 Analysis of conference interactions

We also apply our dependent AR model with transitivity to an additional dynamic network dataset, in this case of face-to-face interactions among attendees of an academic conference.

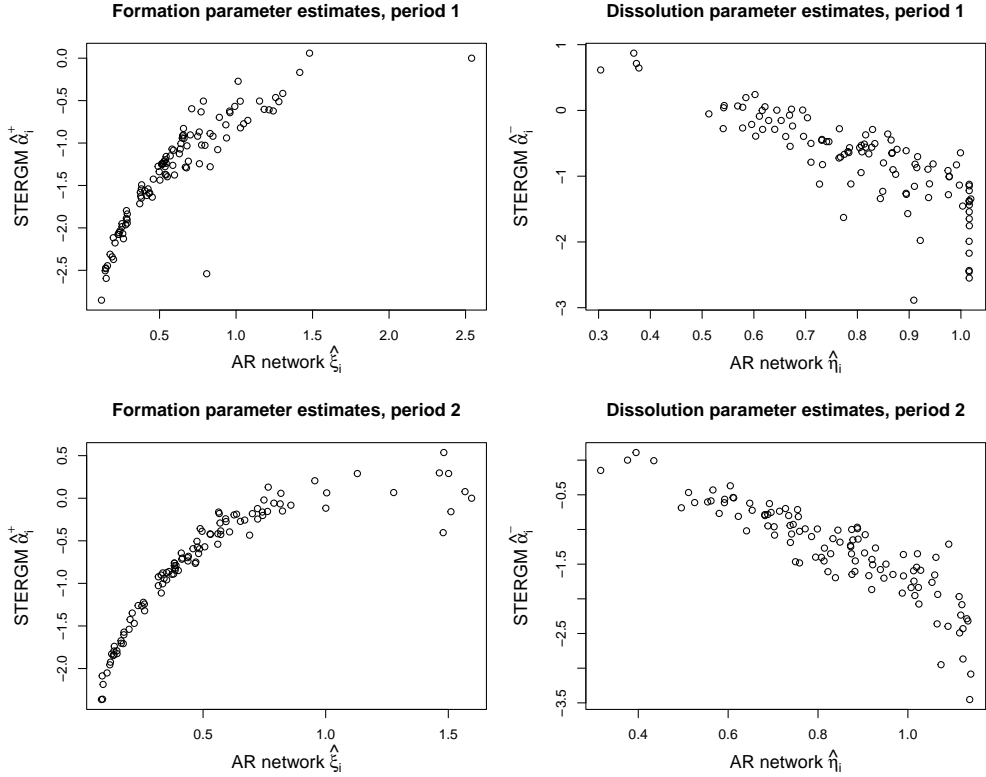


Figure S7: TERGM sociality parameter estimates plotted against AR network local parameter estimates.

The conference in question was the 2009 congress of the Société Française d’Hygiène Hospitalière (SFHH) (Cattuto et al., 2010; Genois and Barrat, 2018). The original data was collected automatically by RFID badges worn by the conference participants. We analyze a subset of the data corresponding to an active portion of the first day of the congress (June 4, 2009) from about 11:00AM to 6:00PM among the $p = 200$ most active participants out of the total 403. Each of the $n = 22$ network snapshots corresponds to a non-overlapping time window, with $X_{i,j}^t = 1$ if participants were in close proximity at any time during the prior 20 minutes.

Similar to Appendix E.1, we summarize some key features of this dataset. Figure S8 (left panel) shows that while there are some spikes in edge density, there is no clear increasing or decreasing pattern, so we choose to model this dataset with a single AR network model. Figures S8 and S9 show empirical evidence of temporal edge dependence, as well as transitivity effects: after accounting for edge density, edges persist at a higher rate than they grow, they more often grow for node pairs which had more common neighbours, and they

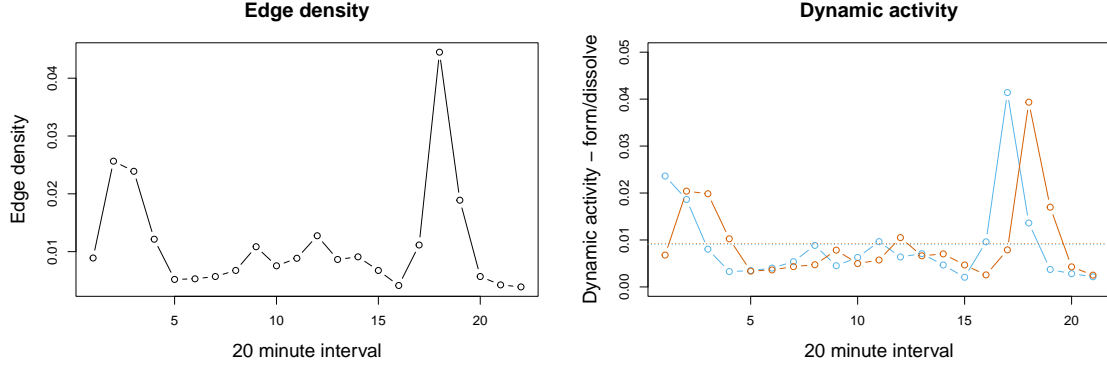


Figure S8: Evolution of edge density D_t (left panel), percentage of grown $D_{1,t}$ (blue) and dissolved $D_{0,t}$ (orange) edges (right panel), SFHH participant networks. The quantities D_t , $D_{0,t}$, and $D_{1,t}$ are defined as in Section E.1.

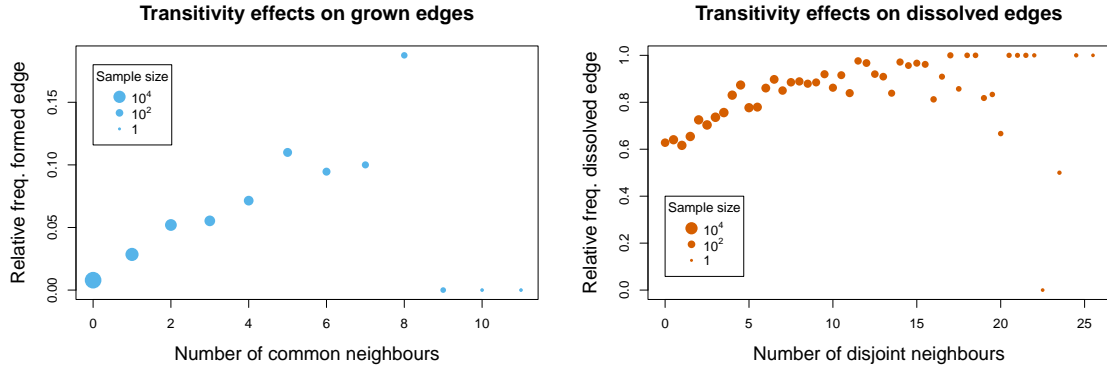


Figure S9: Left panel: the plot of relative edge frequency $|\mathcal{U}_\ell^1|/|\mathcal{U}_\ell|$ against ℓ , SFHH participant networks. Right panel: the plot of relative non-edge frequency $|\mathcal{V}_\ell^0|/|\mathcal{V}_\ell|$ against ℓ , SFHH participant networks. In both panels, point size is proportional to the log sample sizes $\log |\mathcal{U}_\ell|$ and $\log |\mathcal{V}_\ell|$ respectively. The quantities \mathcal{U}_ℓ , \mathcal{U}_ℓ^1 , \mathcal{V}_ℓ , and \mathcal{V}_ℓ^0 are defined as in Section E.1.

more often dissolve for node pairs which had more disjoint neighbours.

Fitting our AR network model with transitivity, we estimate $\hat{a} = 23.20$ and $\hat{b} = 19.08$, confirming these empirical dynamic effects of common and disjoint neighbours. We summarize the estimates of the local parameters $\{\xi_i\}_{i=1}^{200}$ and $\{\eta_i\}_{i=1}^{200}$ in Figure S10.

The estimates $\{\hat{\xi}_i\}_{i=1}^{200}$ have mean 0.20 and a longer right tail, while the estimates $\{\hat{\eta}_i\}_{i=1}^{200}$ have mean 1.06 and a longer left tail. Moreover, their scatter plot shows that there is a negative relationship between these estimates for a given node. All of these observations are consistent with overall degree heterogeneity of the network. The estimates $\{\hat{\xi}_i\}_{i=1}^{200}$ have a wide range from 0.07 to 0.81, while the estimates $\{\hat{\eta}_i\}_{i=1}^{200}$ are all between 0.81 and 1.17. This

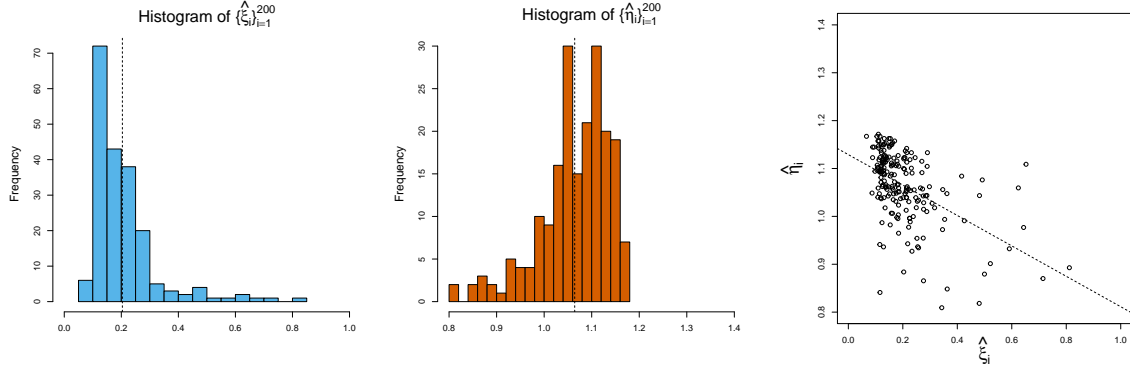


Figure S10: Histograms and scatter plot of estimates $\{\hat{\xi}_i\}_{i=1}^{200}$ and $\{\hat{\eta}_i\}_{i=1}^{200}$, SFHH participant networks.

Model	AIC	BIC
Transitivity AR model	48997	53397
Global AR model	48037	48059
Edgewise AR model	109284	544815
Edgewise mean model	71205	288970
Degree parameter mean model	54061	56250

Table S4: AIC and BIC performance for SFHH participant networks

implies that conference attendees are more heterogeneous in their propensity to form new connections than in their propensity to extend the length of existing ones.

Finally, we compare our model to the same competing models described in Section 6 in terms of AIC and BIC. These results are reported in Table S4. The global AR model, which only has 2 parameters, achieves the lowest AIC and BIC, followed closely by our AR network model with transitivity. Under either criterion, the two edgewise models require $O(p^2)$ parameters and thus perform poorly, as there are relatively many nodes ($p = 200$) compared to network samples ($n = 22$). Although the transitivity model has $O(p)$ parameters, it achieves the second lowest AIC and BIC, suggesting that degree heterogeneity parameters and the imposed transitivity form are an effective parameterization to summarize the structure in this dataset.

F Technical proofs

F.1 Proof of Proposition 1

Recall

$$\ell_{n,p}^{(l)}(\boldsymbol{\theta}) = \frac{1}{(n-m)|\mathcal{S}_l|} \sum_{t=m+1}^n \sum_{(i,j) \in \mathcal{S}_l} h_{i,j}^{t-1}(\boldsymbol{\theta})$$

with

$$h_{i,j}^{t-1}(\boldsymbol{\theta}) = \log\{1 - \gamma_{i,j}^{t-1}(\boldsymbol{\theta})\} + \gamma_{i,j}^{t-1}(\boldsymbol{\theta}_0) \log\left\{\frac{\gamma_{i,j}^{t-1}(\boldsymbol{\theta})}{1 - \gamma_{i,j}^{t-1}(\boldsymbol{\theta})}\right\}.$$

Then

$$\frac{\partial h_{i,j}^{t-1}(\boldsymbol{\theta})}{\partial \theta_{l_1}} = \frac{\gamma_{i,j}^{t-1}(\boldsymbol{\theta}_0) - \gamma_{i,j}^{t-1}(\boldsymbol{\theta})}{\gamma_{i,j}^{t-1}(\boldsymbol{\theta})\{1 - \gamma_{i,j}^{t-1}(\boldsymbol{\theta})\}} \frac{\partial \gamma_{i,j}^{t-1}(\boldsymbol{\theta})}{\partial \theta_{l_1}}, \quad (\text{F.1})$$

$$\begin{aligned} \frac{\partial^2 h_{i,j}^{t-1}(\boldsymbol{\theta})}{\partial \theta_{l_1} \partial \theta_{l_2}} &= - \left[\frac{1}{\gamma_{i,j}^{t-1}(\boldsymbol{\theta})\{1 - \gamma_{i,j}^{t-1}(\boldsymbol{\theta})\}} + \frac{\{\gamma_{i,j}^{t-1}(\boldsymbol{\theta}_0) - \gamma_{i,j}^{t-1}(\boldsymbol{\theta})\}\{1 - 2\gamma_{i,j}^{t-1}(\boldsymbol{\theta})\}}{\{\gamma_{i,j}^{t-1}(\boldsymbol{\theta})\}^2\{1 - \gamma_{i,j}^{t-1}(\boldsymbol{\theta})\}^2} \right] \\ &\quad \times \frac{\partial \gamma_{i,j}^{t-1}(\boldsymbol{\theta})}{\partial \theta_{l_1}} \frac{\partial \gamma_{i,j}^{t-1}(\boldsymbol{\theta})}{\partial \theta_{l_2}} \\ &\quad + \frac{\gamma_{i,j}^{t-1}(\boldsymbol{\theta}_0) - \gamma_{i,j}^{t-1}(\boldsymbol{\theta})}{\gamma_{i,j}^{t-1}(\boldsymbol{\theta})\{1 - \gamma_{i,j}^{t-1}(\boldsymbol{\theta})\}} \frac{\partial^2 \gamma_{i,j}^{t-1}(\boldsymbol{\theta})}{\partial \theta_{l_1} \partial \theta_{l_2}}, \end{aligned} \quad (\text{F.2})$$

$$\begin{aligned} \frac{\partial^3 h_{i,j}^{t-1}(\boldsymbol{\theta})}{\partial \theta_{l_1} \partial \theta_{l_2} \partial \theta_{l_3}} &= 2 \left[\frac{1 - 2\gamma_{i,j}^{t-1}(\boldsymbol{\theta})}{\{\gamma_{i,j}^{t-1}(\boldsymbol{\theta})\}^2\{1 - \gamma_{i,j}^{t-1}(\boldsymbol{\theta})\}^2} + \frac{\gamma_{i,j}^{t-1}(\boldsymbol{\theta}_0) - \gamma_{i,j}^{t-1}(\boldsymbol{\theta})}{\{\gamma_{i,j}^{t-1}(\boldsymbol{\theta})\}^2\{1 - \gamma_{i,j}^{t-1}(\boldsymbol{\theta})\}^2} \right. \\ &\quad \left. + \frac{\{\gamma_{i,j}^{t-1}(\boldsymbol{\theta}_0) - \gamma_{i,j}^{t-1}(\boldsymbol{\theta})\}\{1 - 2\gamma_{i,j}^{t-1}(\boldsymbol{\theta})\}^2}{\{\gamma_{i,j}^{t-1}(\boldsymbol{\theta})\}^3\{1 - \gamma_{i,j}^{t-1}(\boldsymbol{\theta})\}^3} \right] \frac{\partial \gamma_{i,j}^{t-1}(\boldsymbol{\theta})}{\partial \theta_{l_1}} \frac{\partial \gamma_{i,j}^{t-1}(\boldsymbol{\theta})}{\partial \theta_{l_2}} \frac{\partial \gamma_{i,j}^{t-1}(\boldsymbol{\theta})}{\partial \theta_{l_3}} \\ &\quad - \left[\frac{1}{\gamma_{i,j}^{t-1}(\boldsymbol{\theta})\{1 - \gamma_{i,j}^{t-1}(\boldsymbol{\theta})\}} + \frac{\{\gamma_{i,j}^{t-1}(\boldsymbol{\theta}_0) - \gamma_{i,j}^{t-1}(\boldsymbol{\theta})\}\{1 - 2\gamma_{i,j}^{t-1}(\boldsymbol{\theta})\}}{\{\gamma_{i,j}^{t-1}(\boldsymbol{\theta})\}^2\{1 - \gamma_{i,j}^{t-1}(\boldsymbol{\theta})\}^2} \right] \\ &\quad \times \left\{ \frac{\partial^2 \gamma_{i,j}^{t-1}(\boldsymbol{\theta})}{\partial \theta_{l_1} \partial \theta_{l_2}} \frac{\partial \gamma_{i,j}^{t-1}(\boldsymbol{\theta})}{\partial \theta_{l_3}} + \frac{\partial^2 \gamma_{i,j}^{t-1}(\boldsymbol{\theta})}{\partial \theta_{l_2} \partial \theta_{l_3}} \frac{\partial \gamma_{i,j}^{t-1}(\boldsymbol{\theta})}{\partial \theta_{l_1}} + \frac{\partial^2 \gamma_{i,j}^{t-1}(\boldsymbol{\theta})}{\partial \theta_{l_3} \partial \theta_{l_1}} \frac{\partial \gamma_{i,j}^{t-1}(\boldsymbol{\theta})}{\partial \theta_{l_2}} \right\} \\ &\quad + \frac{\gamma_{i,j}^{t-1}(\boldsymbol{\theta}_0) - \gamma_{i,j}^{t-1}(\boldsymbol{\theta})}{\gamma_{i,j}^{t-1}(\boldsymbol{\theta})\{1 - \gamma_{i,j}^{t-1}(\boldsymbol{\theta})\}} \frac{\partial^3 \gamma_{i,j}^{t-1}(\boldsymbol{\theta})}{\partial \theta_{l_1} \partial \theta_{l_2} \partial \theta_{l_3}}. \end{aligned} \quad (\text{F.3})$$

By the triangle inequality and Condition 1,

$$\left| \frac{\partial^3 h_{i,j}^{t-1}(\boldsymbol{\theta})}{\partial \theta_{l_1} \partial \theta_{l_2} \partial \theta_{l_3}} \right| \leq 2(2C_1^{-2} + C_1^{-3}) \left| \frac{\partial \gamma_{i,j}^{t-1}(\boldsymbol{\theta})}{\partial \boldsymbol{\theta}} \right|_\infty^3 + C_1^{-1} \left| \frac{\partial^3 \gamma_{i,j}^{t-1}(\boldsymbol{\theta})}{\partial \boldsymbol{\theta}^3} \right|_\infty$$

$$\begin{aligned}
& + 3(C_1^{-1} + C_1^{-2}) \left| \frac{\partial^2 \gamma_{i,j}^{t-1}(\boldsymbol{\theta})}{\partial \boldsymbol{\theta}^2} \right|_{\infty} \left| \frac{\partial \gamma_{i,j}^{t-1}(\boldsymbol{\theta})}{\partial \boldsymbol{\theta}} \right|_{\infty} \\
& \leq 2(2C_1^{-2} + C_1^{-3})C_2^3 + 3(C_1^{-1} + C_1^{-2})C_2^2 + C_1^{-1}C_2 =: C_*.
\end{aligned} \tag{F.4}$$

Write $\boldsymbol{\theta} = (\theta_1, \dots, \theta_q)^\top$ and $\boldsymbol{\theta}_0 = (\theta_{0,1}, \dots, \theta_{0,q})^\top$. By Taylor's theorem, (F.1) and (F.2),

$$\begin{aligned}
h_{i,j}^{t-1}(\boldsymbol{\theta}) - h_{i,j}^{t-1}(\boldsymbol{\theta}_0) &= \frac{\partial h_{i,j}^{t-1}(\boldsymbol{\theta}_0)}{\partial \boldsymbol{\theta}^\top}(\boldsymbol{\theta} - \boldsymbol{\theta}_0) + \frac{1}{2}(\boldsymbol{\theta} - \boldsymbol{\theta}_0)^\top \frac{\partial^2 h_{i,j}^{t-1}(\boldsymbol{\theta}_0)}{\partial \boldsymbol{\theta} \partial \boldsymbol{\theta}^\top}(\boldsymbol{\theta} - \boldsymbol{\theta}_0) + R_{i,j}^{t-1}(\boldsymbol{\theta}) \\
&= -\frac{1}{2\gamma_{i,j}^{t-1}(\boldsymbol{\theta}_0)\{1 - \gamma_{i,j}^{t-1}(\boldsymbol{\theta}_0)\}} \left| \frac{\partial \gamma_{i,j}^{t-1}(\boldsymbol{\theta}_0)}{\partial \boldsymbol{\theta}^\top}(\boldsymbol{\theta}_0 - \boldsymbol{\theta}) \right|^2 + R_{i,j}^{t-1}(\boldsymbol{\theta}),
\end{aligned}$$

where

$$\begin{aligned}
R_{i,j}^{t-1}(\boldsymbol{\theta}) &= \frac{1}{2} \sum_{l_1=1}^q (\theta_{l_1} - \theta_{0,l_1})^3 \int_0^1 (1-v)^2 \frac{\partial^3 h_{i,j}^{t-1}(\boldsymbol{\theta}_v)}{\partial \theta_{l_1}^3} dv \\
&\quad + \frac{3}{2} \sum_{l_1 \neq l_2} (\theta_{l_1} - \theta_{0,l_1})^2 (\theta_{l_2} - \theta_{0,l_2}) \int_0^1 (1-v)^2 \frac{\partial^3 h_{i,j}^{t-1}(\boldsymbol{\theta}_v)}{\partial \theta_{l_1}^2 \partial \theta_{l_2}} dv \\
&\quad + 3 \sum_{l_1 \neq l_2 \neq l_3} (\theta_{l_1} - \theta_{0,l_1})(\theta_{l_2} - \theta_{0,l_2})(\theta_{l_3} - \theta_{0,l_3}) \int_0^1 (1-v)^2 \frac{\partial^3 h_{i,j}^{t-1}(\boldsymbol{\theta}_v)}{\partial \theta_{l_1} \partial \theta_{l_2} \partial \theta_{l_3}} dv
\end{aligned}$$

with $\boldsymbol{\theta}_v = \boldsymbol{\theta}_0 + v(\boldsymbol{\theta} - \boldsymbol{\theta}_0)$. Recall $\mathcal{I}_{i,j} = \{l \subset [q] : \gamma_{i,j}^{t-1}(\boldsymbol{\theta}) \text{ involves } \theta_l \text{ for any } t \in [n] \setminus [m]\}$.

We have $\partial \gamma_{i,j}^{t-1}(\boldsymbol{\theta}) / \partial \theta_{l_1} \equiv 0$ if $l_1 \notin \mathcal{I}_{i,j}$, $\partial^2 \gamma_{i,j}^{t-1}(\boldsymbol{\theta}) / \partial \theta_{l_1} \partial \theta_{l_2} \equiv 0$ if $l_1 \notin \mathcal{I}_{i,j}$ or $l_2 \notin \mathcal{I}_{i,j}$, and $\partial^3 \gamma_{i,j}^{t-1}(\boldsymbol{\theta}) / \partial \theta_{l_1} \partial \theta_{l_2} \partial \theta_{l_3} \equiv 0$ if $l_1 \notin \mathcal{I}_{i,j}$ or $l_2 \notin \mathcal{I}_{i,j}$ or $l_3 \notin \mathcal{I}_{i,j}$. By (F.3), it holds that

$$\frac{\partial^3 h_{i,j}^{t-1}(\boldsymbol{\theta})}{\partial \theta_{l_1} \partial \theta_{l_2} \partial \theta_{l_3}} \equiv 0 \text{ if } l_1 \notin \mathcal{I}_{i,j} \text{ or } l_2 \notin \mathcal{I}_{i,j} \text{ or } l_3 \notin \mathcal{I}_{i,j}.$$

By Condition 2, it holds that $|R_{i,j}^{t-1}(\boldsymbol{\theta})| \leq C_* s^3 |\boldsymbol{\theta}_{\mathcal{I}_{i,j}} - \boldsymbol{\theta}_{0,\mathcal{I}_{i,j}}|_{\infty}^3$, which implies

$$\begin{aligned}
\ell_{n,p}^{(l)}(\boldsymbol{\theta}_0) - \ell_{n,p}^{(l)}(\boldsymbol{\theta}) &= \frac{1}{(n-m)|\mathcal{S}_l|} \sum_{t=m+1}^n \sum_{(i,j) \in \mathcal{S}_l} \{h_{i,j}^{t-1}(\boldsymbol{\theta}_0) - h_{i,j}^{t-1}(\boldsymbol{\theta})\} \\
&\geq \frac{1}{(n-m)|\mathcal{S}_l|} \sum_{t=m+1}^n \sum_{(i,j) \in \mathcal{S}_l} \frac{1}{2\gamma_{i,j}^{t-1}(\boldsymbol{\theta}_0)\{1 - \gamma_{i,j}^{t-1}(\boldsymbol{\theta}_0)\}} \left| \frac{\partial \gamma_{i,j}^{t-1}(\boldsymbol{\theta}_0)}{\partial \boldsymbol{\theta}^\top}(\boldsymbol{\theta}_0 - \boldsymbol{\theta}) \right|^2 \\
&\quad - \frac{C_* s^3}{|\mathcal{S}_l|} \sum_{(i,j) \in \mathcal{S}_l} |\boldsymbol{\theta}_{\mathcal{I}_{i,j}} - \boldsymbol{\theta}_{0,\mathcal{I}_{i,j}}|_{\infty}^3
\end{aligned} \tag{F.5}$$

$$\geq \frac{2}{(n-m)|\mathcal{S}_l|} \sum_{t=m+1}^n \sum_{(i,j) \in \mathcal{S}_l} \left| \frac{\partial \gamma_{i,j}^{t-1}(\boldsymbol{\theta}_0)}{\partial \boldsymbol{\theta}_{\mathcal{I}_{i,j}}^\top} (\boldsymbol{\theta}_{0,\mathcal{I}_{i,j}} - \boldsymbol{\theta}_{\mathcal{I}_{i,j}}) \right|^2 - \frac{C_* s^3}{|\mathcal{S}_l|} \sum_{(i,j) \in \mathcal{S}_l} \|\boldsymbol{\theta}_{\mathcal{I}_{i,j}} - \boldsymbol{\theta}_{0,\mathcal{I}_{i,j}}\|_\infty^3$$

for any $\boldsymbol{\theta} \in \Theta$. By Condition 3, it holds with probability approaching one that

$$\frac{1}{n-m} \sum_{t=m+1}^n \sum_{(i,j) \in \mathcal{S}_l} \left| \frac{\partial \gamma_{i,j}^{t-1}(\boldsymbol{\theta}_0)}{\partial \boldsymbol{\theta}_{\mathcal{I}_{i,j}}^\top} (\boldsymbol{\theta}_{0,\mathcal{I}_{i,j}} - \boldsymbol{\theta}_{\mathcal{I}_{i,j}}) \right|^2 \geq C_3 \sum_{(i,j) \in \mathcal{S}_l} \|\boldsymbol{\theta}_{0,\mathcal{I}_{i,j}} - \boldsymbol{\theta}_{\mathcal{I}_{i,j}}\|_2^2$$

for any $l \in [q]$, which implies

$$\ell_{n,p}^{(l)}(\boldsymbol{\theta}_0) - \ell_{n,p}^{(l)}(\boldsymbol{\theta}) \geq \frac{2C_3}{|\mathcal{S}_l|} \sum_{(i,j) \in \mathcal{S}_l} \|\boldsymbol{\theta}_{0,\mathcal{I}_{i,j}} - \boldsymbol{\theta}_{\mathcal{I}_{i,j}}\|_2^2 - \frac{C_* s^3}{|\mathcal{S}_l|} \sum_{(i,j) \in \mathcal{S}_l} \|\boldsymbol{\theta}_{\mathcal{I}_{i,j}} - \boldsymbol{\theta}_{0,\mathcal{I}_{i,j}}\|_\infty^3$$

for any $\boldsymbol{\theta} \in \Theta$ and $l \in [q]$ with probability approaching one. Since $d := \sup_{\boldsymbol{\theta} \in \Theta} \|\boldsymbol{\theta} - \boldsymbol{\theta}_0\|_\infty < 2C_3/(C_* s^3)$, there exists a universal constant $\tilde{C} > 0$ such that $d < \tilde{C} < 2C_3/(C_* s^3)$. Hence, it holds with probability approaching one that

$$\begin{aligned} \ell_{n,p}^{(l)}(\boldsymbol{\theta}_0) - \ell_{n,p}^{(l)}(\boldsymbol{\theta}) &\geq \frac{2C_3 - \tilde{C}C_* s^3}{|\mathcal{S}_l|} \sum_{(i,j) \in \mathcal{S}_l} \|\boldsymbol{\theta}_{0,\mathcal{I}_{i,j}} - \boldsymbol{\theta}_{\mathcal{I}_{i,j}}\|_2^2 \\ &\quad + \frac{\tilde{C}C_* s^3}{|\mathcal{S}_l|} \sum_{(i,j) \in \mathcal{S}_l} \|\boldsymbol{\theta}_{0,\mathcal{I}_{i,j}} - \boldsymbol{\theta}_{\mathcal{I}_{i,j}}\|_2^2 - \frac{C_* s^3}{|\mathcal{S}_l|} \sum_{(i,j) \in \mathcal{S}_l} \|\boldsymbol{\theta}_{\mathcal{I}_{i,j}} - \boldsymbol{\theta}_{0,\mathcal{I}_{i,j}}\|_\infty^3 \\ &\geq \frac{2C_3 - \tilde{C}C_* s^3}{|\mathcal{S}_l|} \sum_{(i,j) \in \mathcal{S}_l} \|\boldsymbol{\theta}_{0,\mathcal{I}_{i,j}} - \boldsymbol{\theta}_{\mathcal{I}_{i,j}}\|_2^2 \\ &\quad + \frac{\tilde{C}C_* s^3}{|\mathcal{S}_l|} \sum_{(i,j) \in \mathcal{S}_l} \|\boldsymbol{\theta}_{0,\mathcal{I}_{i,j}} - \boldsymbol{\theta}_{\mathcal{I}_{i,j}}\|_2^2 - \frac{C_* s^3 d}{|\mathcal{S}_l|} \sum_{(i,j) \in \mathcal{S}_l} \|\boldsymbol{\theta}_{\mathcal{I}_{i,j}} - \boldsymbol{\theta}_{0,\mathcal{I}_{i,j}}\|_\infty^2 \\ &\geq \frac{2C_3 - \tilde{C}C_* s^3}{|\mathcal{S}_l|} \sum_{(i,j) \in \mathcal{S}_l} \|\boldsymbol{\theta}_{0,\mathcal{I}_{i,j}} - \boldsymbol{\theta}_{\mathcal{I}_{i,j}}\|_2^2 \end{aligned}$$

for any $\boldsymbol{\theta} \in \Theta$ and $l \in [q]$. We then have Proposition 1 by selecting $\bar{C} = 2C_3 - \tilde{C}C_* s^3$. \square

F.2 Proof of Theorem 1

Recall $S_{\mathcal{H},\min} = \min_{l \in \mathcal{H}} |\mathcal{S}_l|$ for any $\mathcal{H} \subset [q]$, and

$$\begin{cases} c_{n,\mathcal{G}}^2 = \frac{q \log(n|\mathcal{S}_{l'}|)}{\sqrt{n|\mathcal{S}_{l'}|}} + \frac{q^{3/2} \log^{3/2}(n|\mathcal{S}_{l'}|)}{\sqrt{n|\mathcal{S}_{l'}|}}, \\ c_{n,\mathcal{G}^c}^2 = \frac{q \log(nS_{\mathcal{G}^c,\min})}{\sqrt{nS_{\mathcal{G}^c,\min}}} + \frac{q^{3/2} \log^{3/2}(nS_{\mathcal{G}^c,\min})}{\sqrt{nS_{\mathcal{G}^c,\min}}}, \end{cases}$$

where $l' \in \mathcal{G}$. To show Theorem 1, we first present the following lemma whose proof is given in Section F.5.1.

Lemma 2 *Assume Conditions 1 and 2 hold. Then*

$$\max_{l \in \mathcal{H}} \sup_{\boldsymbol{\theta} \in \Theta} |\hat{\ell}_{n,p}^{(l)}(\boldsymbol{\theta}) - \ell_{n,p}^{(l)}(\boldsymbol{\theta})| = O_p \left\{ \frac{q \log(nS_{\mathcal{H},\min})}{\sqrt{nS_{\mathcal{H},\min}}} \right\} + O_p \left\{ \frac{q^{3/2} \log^{3/2}(nS_{\mathcal{H},\min})}{\sqrt{nS_{\mathcal{H},\min}}} \right\}$$

for any $\mathcal{H} \subset [q]$.

Notice that $\hat{\boldsymbol{\theta}}_*^{(l)} = (\hat{\theta}_{*,1}^{(l)}, \dots, \hat{\theta}_{*,q}^{(l)})^\top = \arg \max_{\boldsymbol{\theta} \in \Theta} \hat{\ell}_{n,p}^{(l)}(\boldsymbol{\theta})$ for any $l \in [q]$. Then

$$\begin{aligned} \ell_{n,p}^{(l')}(\boldsymbol{\theta}_0) - \sup_{\boldsymbol{\theta} \in \Theta} |\hat{\ell}_{n,p}^{(l')}(\boldsymbol{\theta}) - \ell_{n,p}^{(l')}(\boldsymbol{\theta})| &\leq \hat{\ell}_{n,p}^{(l')}(\boldsymbol{\theta}_0) \\ &\leq \hat{\ell}_{n,p}^{(l')}(\hat{\boldsymbol{\theta}}_*^{(l')}) \leq \ell_{n,p}^{(l')}(\hat{\boldsymbol{\theta}}_*^{(l')}) + \sup_{\boldsymbol{\theta} \in \Theta} |\hat{\ell}_{n,p}^{(l')}(\boldsymbol{\theta}) - \ell_{n,p}^{(l')}(\boldsymbol{\theta})|, \end{aligned}$$

which implies

$$0 \leq \ell_{n,p}^{(l')}(\boldsymbol{\theta}_0) - \ell_{n,p}^{(l')}(\hat{\boldsymbol{\theta}}_*^{(l')}) \leq 2 \sup_{\boldsymbol{\theta} \in \Theta} |\hat{\ell}_{n,p}^{(l')}(\boldsymbol{\theta}) - \ell_{n,p}^{(l')}(\boldsymbol{\theta})|.$$

Recall $\tilde{\boldsymbol{\theta}}_{\mathcal{G}} = \hat{\boldsymbol{\theta}}_*^{(l')}$. Selecting $\mathcal{H} = \{l'\}$ in Lemma 2, we have $\sup_{\boldsymbol{\theta} \in \Theta} |\hat{\ell}_{n,p}^{(l')}(\boldsymbol{\theta}) - \ell_{n,p}^{(l')}(\boldsymbol{\theta})| = O_p(c_{n,\mathcal{G}}^2)$, which implies

$$\ell_{n,p}^{(l')}(\boldsymbol{\theta}_0) - \ell_{n,p}^{(l')}(\hat{\boldsymbol{\theta}}_*^{(l')}) = O_p(c_{n,\mathcal{G}}^2). \quad (\text{F.6})$$

For any diverging $\epsilon_{n,p} > 0$, if $|\tilde{\boldsymbol{\theta}}_{\mathcal{G}} - \boldsymbol{\theta}_{0,\mathcal{G}}|_2 \geq \epsilon_{n,p} c_{n,\mathcal{G}}$, Proposition 1 yields that

$$\ell_{n,p}^{(l')}(\boldsymbol{\theta}_0) - \ell_{n,p}^{(l')}(\hat{\boldsymbol{\theta}}_*^{(l')}) \geq \bar{C} \epsilon_{n,p}^2 c_{n,\mathcal{G}}^2$$

with probability approaching one, which contradicts with (F.6) and then implies $|\tilde{\boldsymbol{\theta}}_{\mathcal{G}} - \boldsymbol{\theta}_{0,\mathcal{G}}|_2 = O_p(\epsilon_{n,p} c_{n,\mathcal{G}})$. Notice that we can select arbitrary slowly diverging $\epsilon_{n,p}$. Following a standard result from probability theory, we have $|\tilde{\boldsymbol{\theta}}_{\mathcal{G}} - \boldsymbol{\theta}_{0,\mathcal{G}}|_2 = O_p(c_{n,\mathcal{G}})$.

For any $l \in \mathcal{G}^c$, we also have

$$0 \leq \ell_{n,p}^{(l)}(\boldsymbol{\theta}_0) - \ell_{n,p}^{(l)}(\hat{\boldsymbol{\theta}}_*^{(l)}) \leq 2 \sup_{\boldsymbol{\theta} \in \boldsymbol{\Theta}} |\hat{\ell}_{n,p}^{(l)}(\boldsymbol{\theta}) - \ell_{n,p}^{(l)}(\boldsymbol{\theta})|.$$

Recall $\tilde{\boldsymbol{\theta}}_{\mathcal{G}^c} = (\hat{\theta}_{*,l}^{(l)})_{l \in \mathcal{G}^c}$. Selecting $\mathcal{H} = \mathcal{G}^c$ in Lemma 2, we have $\max_{l \in \mathcal{G}^c} \sup_{\boldsymbol{\theta} \in \boldsymbol{\Theta}} |\hat{\ell}_{n,p}^{(l)}(\boldsymbol{\theta}) - \ell_{n,p}^{(l)}(\boldsymbol{\theta})| = O_p(c_{n,\mathcal{G}^c}^2)$, which implies

$$\max_{l \in \mathcal{G}^c} \{\ell_{n,p}^{(l)}(\boldsymbol{\theta}_0) - \ell_{n,p}^{(l)}(\hat{\boldsymbol{\theta}}_*^{(l)})\} = O_p(c_{n,\mathcal{G}^c}^2). \quad (\text{F.7})$$

For any diverging $\epsilon_{n,p} > 0$, if $|\tilde{\boldsymbol{\theta}}_{\mathcal{G}^c} - \boldsymbol{\theta}_{0,\mathcal{G}^c}|_\infty \geq \epsilon_{n,p} c_{n,\mathcal{G}^c}$, Proposition 1 yields that

$$\max_{l \in \mathcal{G}^c} \{\ell_{n,p}^{(l)}(\boldsymbol{\theta}_0) - \ell_{n,p}^{(l)}(\hat{\boldsymbol{\theta}}_*^{(l)})\} \geq \bar{C} \epsilon_{n,p}^2 c_{n,\mathcal{G}^c}^2$$

with probability approaching one, which contradicts with (F.7) and then implies $|\tilde{\boldsymbol{\theta}}_{\mathcal{G}^c} - \boldsymbol{\theta}_{0,\mathcal{G}^c}|_\infty = O_p(\epsilon_{n,p} c_{n,\mathcal{G}^c})$. Notice that we can select arbitrary slowly diverging $\epsilon_{n,p}$. Following a standard result from probability theory, we have $|\tilde{\boldsymbol{\theta}}_{\mathcal{G}^c} - \boldsymbol{\theta}_{0,\mathcal{G}^c}|_\infty = O_p(c_{n,\mathcal{G}^c})$. We complete the proof of Theorem 1. \square

F.3 Proof of Proposition 2

Given $\boldsymbol{\varphi}_l$ specified in Condition 4, define

$$f_t^{(l)}(\boldsymbol{\theta}) = \boldsymbol{\varphi}_l^\top \mathbf{g}_t^{(l)}(\boldsymbol{\theta})$$

for any $t \in [n] \setminus [m]$ and $\boldsymbol{\theta} \in \boldsymbol{\Theta}$. To show Proposition 2, we need the following lemmas whose proofs are given in Sections F.5.2–F.5.4.

Lemma 3 *Assume Condition 1 holds. Then*

$$\left| \frac{1}{n-m} \sum_{t=m+1}^n \{\hat{f}_t^{(l)}(\boldsymbol{\theta}_{0,l}, \tilde{\boldsymbol{\theta}}_{-l}) - \hat{f}_t^{(l)}(\boldsymbol{\theta}_0)\} \right| \leq \tau |\tilde{\boldsymbol{\theta}} - \boldsymbol{\theta}_0|_1 + C_* |\hat{\boldsymbol{\varphi}}_l|_1 |\tilde{\boldsymbol{\theta}} - \boldsymbol{\theta}_0|_1^2$$

for any $l \in [q]$, where C_* is a universal constant specified in (F.4).

Lemma 4 Assume Conditions 1 and 4 hold. Then

$$\begin{aligned} & \max_{l \in \mathcal{H}} \left| \frac{1}{n-m} \sum_{t=m+1}^n \hat{f}_t^{(l)}(\boldsymbol{\theta}_0) \right| \\ &= O_p \left\{ \frac{\sqrt{\log(1+|\mathcal{H}|) \log(n|\mathcal{H}|)}}{\sqrt{nS_{\mathcal{H},\min}}} \right\} + O_p \left\{ \frac{\sqrt{\log(1+|\mathcal{H}|) \log(n|\mathcal{H}|)}}{\sqrt{nS_{\mathcal{H},\min}}} \right\} \end{aligned}$$

for any $\mathcal{H} \subset [q]$.

Lemma 5 Assume Condition 1 holds. Then

$$\sup_{\theta_l \in B(\tilde{\theta}_l, \tilde{r})} \left| \frac{1}{n-m} \sum_{t=m+1}^n \frac{\hat{f}_t^{(l)}(\theta_l, \tilde{\boldsymbol{\theta}}_{-l})}{\partial \theta_l} - 1 \right| \leq \tau + C_* \tilde{r} |\hat{\boldsymbol{\varphi}}_l|_1$$

for any $l \in [q]$, where C_* is a universal constant specified in (F.4).

Recall $|\tilde{\boldsymbol{\theta}}_{\mathcal{G}} - \boldsymbol{\theta}_{0,\mathcal{G}}|_2 = O_p(c_{n,\mathcal{G}})$ and $|\tilde{\boldsymbol{\theta}}_{\mathcal{G}^c} - \boldsymbol{\theta}_{0,\mathcal{G}^c}|_\infty = O_p(c_{n,\mathcal{G}^c})$ with

$$\begin{cases} c_{n,\mathcal{G}}^2 = \frac{q \log(n|\mathcal{S}_{l'}|)}{\sqrt{n|\mathcal{S}_{l'}|}} + \frac{q^{3/2} \log^{3/2}(n|\mathcal{S}_{l'}|)}{\sqrt{n|\mathcal{S}_{l'}|}}, \\ c_{n,\mathcal{G}^c}^2 = \frac{q \log(nS_{\mathcal{G}^c,\min})}{\sqrt{nS_{\mathcal{G}^c,\min}}} + \frac{q^{3/2} \log^{3/2}(nS_{\mathcal{G}^c,\min})}{\sqrt{nS_{\mathcal{G}^c,\min}}}, \end{cases}$$

where $l' \in \mathcal{G}$. Then $|\tilde{\boldsymbol{\theta}} - \boldsymbol{\theta}_0|_1 = |\tilde{\boldsymbol{\theta}}_{\mathcal{G}} - \boldsymbol{\theta}_{0,\mathcal{G}}|_1 + |\tilde{\boldsymbol{\theta}}_{\mathcal{G}^c} - \boldsymbol{\theta}_{0,\mathcal{G}^c}|_1 = O_p(|\mathcal{G}|^{1/2} c_{n,\mathcal{G}}) + O_p(|\mathcal{G}^c| c_{n,\mathcal{G}^c}) = O_p(\Delta_n^{1/2})$. Based on Lemmas 3 and 4, due to $\tau \lesssim \Delta_n^{1/2}$ and $|\mathcal{G}| + |\mathcal{G}^c| = q$, we have

$$\begin{aligned} & \max_{l \in \mathcal{G}} \left| \frac{1}{n-m} \sum_{t=m+1}^n \hat{f}_t^{(l)}(\theta_{0,l}, \tilde{\boldsymbol{\theta}}_{-l}) \right| \\ &= O_p(\Delta_n) + O_p \left\{ \frac{\sqrt{\log(1+|\mathcal{G}|) \log(n|\mathcal{G}|)}}{\sqrt{n|\mathcal{S}_{l'}|}} \right\} + O_p \left\{ \frac{\sqrt{\log(1+|\mathcal{G}|) \log(n|\mathcal{G}|)}}{\sqrt{n|\mathcal{S}_{l'}|}} \right\} \\ &= O_p(\Delta_n) \end{aligned}$$

for some $l' \in \mathcal{G}$, and

$$\begin{aligned} & \max_{l \in \mathcal{G}^c} \left| \frac{1}{n-m} \sum_{t=m+1}^n \hat{f}_t^{(l)}(\theta_{0,l}, \tilde{\boldsymbol{\theta}}_{-l}) \right| \\ &= O_p(\Delta_n) + O_p \left\{ \frac{\sqrt{\log(1+|\mathcal{G}^c|) \log(n|\mathcal{G}^c|)}}{\sqrt{nS_{\mathcal{G}^c,\min}}} \right\} + O_p \left\{ \frac{\sqrt{\log(1+|\mathcal{G}^c|) \log(n|\mathcal{G}^c|)}}{\sqrt{nS_{\mathcal{G}^c,\min}}} \right\} \end{aligned}$$

$$= O_p(\Delta_n).$$

Due to $\check{\theta}_l = \arg \min_{\theta_l \in B(\tilde{\theta}_l, \tilde{r})} |(n-m)^{-1} \sum_{t=m+1}^n \hat{f}_t^{(l)}(\theta_l, \tilde{\theta}_{-l})|^2$ and $\theta_{0,l} \in B(\tilde{\theta}_l, \tilde{r})$ with probability approaching one, then

$$\left| \frac{1}{n-m} \sum_{t=m+1}^n \hat{f}_t^{(l)}(\check{\theta}_l, \tilde{\theta}_{-l}) \right| \leq \left| \frac{1}{n-m} \sum_{t=m+1}^n \hat{f}_t^{(l)}(\theta_{0,l}, \tilde{\theta}_{-l}) \right|$$

with probability approaching one, which implies

$$\max_{l \in [q]} \left| \frac{1}{n-m} \sum_{t=m+1}^n \{ \hat{f}_t^{(l)}(\check{\theta}_l, \tilde{\theta}_{-l}) - \hat{f}_t^{(l)}(\theta_{0,l}, \tilde{\theta}_{-l}) \} \right| = O_p(\Delta_n). \quad (\text{F.8})$$

Notice that

$$\frac{1}{n-m} \sum_{t=m+1}^n \{ \hat{f}_t^{(l)}(\check{\theta}_l, \tilde{\theta}_{-l}) - \hat{f}_t^{(l)}(\theta_{0,l}, \tilde{\theta}_{-l}) \} = \left\{ \frac{1}{n-m} \sum_{t=m+1}^n \frac{\partial \hat{f}_t^{(l)}(\bar{\theta}_l, \tilde{\theta}_{-l})}{\partial \theta_l} \right\} (\check{\theta}_l - \theta_{0,l})$$

for some $\bar{\theta}_l$ on the joint line between $\check{\theta}_l$ and $\theta_{0,l}$. By Lemma 5 and Condition 4, due to $\tau = o(1)$ and $\tilde{r} = o(1)$, we know

$$\min_{l \in [q]} \left\{ \frac{1}{n-m} \sum_{t=m+1}^n \frac{\partial \hat{f}_t^{(l)}(\bar{\theta}_l, \tilde{\theta}_{-l})}{\partial \theta_l} \right\} > \frac{1}{2}$$

with probability approaching one. Hence, by (F.8), we have $|\check{\theta} - \theta_0|_\infty = O_p(\Delta_n)$. We complete the proof of Proposition 2. \square

F.4 Proof of Theorem 2

Recall $\hat{f}_t^{(l)}(\theta) = \hat{\varphi}_l^\top \mathbf{g}_t^{(l)}(\theta)$. By the definition of $\hat{\varphi}_l$ given in (9), we have

$$\max_{l \in [q]} \left| \frac{1}{n-m} \sum_{t=m+1}^n \frac{\partial \hat{f}_t^{(l)}(\tilde{\theta})}{\partial \theta_{-l}} \right|_\infty \leq \tau.$$

It follows from the Taylor expansion that

$$\left| \frac{1}{n-m} \sum_{t=m+1}^n \left\{ \frac{\partial \hat{f}_t^{(l)}(\check{\theta})}{\partial \theta_{-l}} - \frac{\partial \hat{f}_t^{(l)}(\tilde{\theta})}{\partial \theta_{-l}} \right\} \right|_\infty \leq \left| \frac{1}{n-m} \sum_{t=m+1}^n \frac{\partial^2 \hat{f}_t^{(l)}(\dot{\theta})}{\partial \theta_{-l} \partial \theta^\top} \right|_\infty |\check{\theta} - \tilde{\theta}|_1,$$

where $\dot{\boldsymbol{\theta}}$ is on the joint line between $\check{\boldsymbol{\theta}}$ and $\tilde{\boldsymbol{\theta}}$. Notice that $\dot{\boldsymbol{\theta}} \in B(\tilde{\theta}_1, \tilde{r}) \times \cdots \times B(\tilde{\theta}_q, \tilde{r})$. Following the same arguments for deriving (F.28) in Section F.5.2 for the proof of Lemma 3, we know

$$\sup_{\boldsymbol{\theta} \in B(\tilde{\theta}_1, \tilde{r}) \times \cdots \times B(\tilde{\theta}_q, \tilde{r})} \max_{l \in [q]} \left| \frac{1}{n-m} \sum_{t=m+1}^n \frac{\partial^2 \hat{f}_t^{(l)}(\boldsymbol{\theta})}{\partial \boldsymbol{\theta}_{-l} \partial \boldsymbol{\theta}^\top} \right|_\infty \leq C_* \max_{l \in [q]} |\hat{\boldsymbol{\varphi}}_l|_1$$

for some universal constant C_* specified in (F.4), which implies

$$\max_{l \in [q]} \left| \frac{1}{n-m} \sum_{t=m+1}^n \left\{ \frac{\partial \hat{f}_t^{(l)}(\check{\boldsymbol{\theta}})}{\partial \boldsymbol{\theta}_{-l}} - \frac{\partial \hat{f}_t^{(l)}(\tilde{\boldsymbol{\theta}})}{\partial \boldsymbol{\theta}_{-l}} \right\} \right|_\infty \leq C_* |\check{\boldsymbol{\theta}} - \tilde{\boldsymbol{\theta}}|_1 \max_{l \in [q]} |\hat{\boldsymbol{\varphi}}_l|_1.$$

By Condition 4, we have $\max_{l \in [q]} |\hat{\boldsymbol{\varphi}}_l|_1 = O_p(1)$, which implies

$$\max_{l \in [q]} \left| \frac{1}{n-m} \sum_{t=m+1}^n \left\{ \frac{\partial \hat{f}_t^{(l)}(\check{\boldsymbol{\theta}})}{\partial \boldsymbol{\theta}_{-l}} - \frac{\partial \hat{f}_t^{(l)}(\tilde{\boldsymbol{\theta}})}{\partial \boldsymbol{\theta}_{-l}} \right\} \right|_\infty \leq |\check{\boldsymbol{\theta}} - \tilde{\boldsymbol{\theta}}|_1 \cdot O_p(1).$$

Hence, it holds that

$$\max_{l \in [q]} \left| \frac{1}{n-m} \sum_{t=m+1}^n \frac{\partial \hat{f}_t^{(l)}(\check{\boldsymbol{\theta}})}{\partial \boldsymbol{\theta}_{-l}} \right|_\infty \leq \tau + |\check{\boldsymbol{\theta}} - \tilde{\boldsymbol{\theta}}|_1 \cdot O_p(1). \quad (\text{F.9})$$

Repeating the arguments for deriving Lemma 3 in Section F.5.2, we can also show

$$\begin{aligned} \max_{l \in [q]} \left| \frac{1}{n-m} \sum_{t=m+1}^n \left\{ \hat{f}_t^{(l)}(\theta_{0,l}, \check{\boldsymbol{\theta}}_{-l}) - \hat{f}_t^{(l)}(\boldsymbol{\theta}_0) \right\} \right| \\ \leq \{ \tau + |\check{\boldsymbol{\theta}} - \tilde{\boldsymbol{\theta}}|_1 \cdot O_p(1) \} |\check{\boldsymbol{\theta}} - \boldsymbol{\theta}_0|_1 + |\check{\boldsymbol{\theta}} - \boldsymbol{\theta}_0|_1^2 \cdot O_p(1) \\ \leq \{ \tau + |\tilde{\boldsymbol{\theta}} - \boldsymbol{\theta}_0|_1 \cdot O_p(1) \} |\check{\boldsymbol{\theta}} - \boldsymbol{\theta}_0|_1 + |\check{\boldsymbol{\theta}} - \boldsymbol{\theta}_0|_1^2 \cdot O_p(1). \end{aligned} \quad (\text{F.10})$$

Together with Lemma 4, it holds that

$$\max_{l \in [q]} \left| \frac{1}{n-m} \sum_{t=m+1}^n \hat{f}_t^{(l)}(\theta_{0,l}, \check{\boldsymbol{\theta}}_{-l}) \right| \leq O_p(q\Delta_n).$$

Since $\hat{\theta}_l = \arg \min_{\theta_l \in B(\check{\theta}_l, \check{r})} |(n-m)^{-1} \sum_{t=m+1}^n \hat{f}_t^{(l)}(\theta_l, \check{\theta}_{-l})|^2$ and $\theta_{0,l} \in B(\check{\theta}_l, \check{r})$ with probability approaching one, then

$$\left| \frac{1}{n-m} \sum_{t=m+1}^n \hat{f}_t^{(l)}(\hat{\theta}_l, \check{\theta}_{-l}) \right| \leq \left| \frac{1}{n-m} \sum_{t=m+1}^n \hat{f}_t^{(l)}(\theta_{0,l}, \check{\theta}_{-l}) \right|$$

with probability approaching one, which implies

$$\max_{l \in [q]} \left| \frac{1}{n-m} \sum_{t=m+1}^n \{ \hat{f}_t^{(l)}(\hat{\theta}_l, \check{\theta}_{-l}) - \hat{f}_t^{(l)}(\theta_{0,l}, \check{\theta}_{-l}) \} \right| = O_p(q\Delta_n). \quad (\text{F.11})$$

Following the same arguments for deriving Lemma 5 in Section F.5.4 and noting (F.9), we can also have

$$\sup_{\theta_l \in B(\check{\theta}_l, \check{r})} \left| \frac{1}{n-m} \sum_{t=m+1}^n \frac{\hat{f}_t^{(l)}(\theta_l, \check{\theta}_{-l})}{\partial \theta_l} - 1 \right| \leq \tau + o_p(1) + C_* \check{r} |\hat{\varphi}_l|_1 \quad (\text{F.12})$$

for any $l \in [q]$. Due to $\tau = o(1)$, $\check{r} = o(1)$ and $\max_{l \in [q]} |\hat{\varphi}_l|_1 = O_p(1)$, we have

$$\max_{l \in [q]} \sup_{\theta_l \in B(\check{\theta}_l, \check{r})} \left| \frac{1}{n-m} \sum_{t=m+1}^n \frac{\hat{f}_t^{(l)}(\theta_l, \check{\theta}_{-l})}{\partial \theta_l} - 1 \right| = o_p(1). \quad (\text{F.13})$$

Due to

$$\frac{1}{n-m} \sum_{t=m+1}^n \{ \hat{f}_t^{(l)}(\hat{\theta}_l, \check{\theta}_{-l}) - \hat{f}_t^{(l)}(\theta_{0,l}, \check{\theta}_{-l}) \} = \left\{ \frac{1}{n-m} \sum_{t=m+1}^n \frac{\partial \hat{f}_t^{(l)}(\bar{\theta}_l, \check{\theta}_{-l})}{\partial \theta_l} \right\} (\hat{\theta}_l - \theta_{0,l}) \quad (\text{F.14})$$

for some $\bar{\theta}_l$ on the joint line between $\hat{\theta}_l$ and $\theta_{0,l}$, by (F.11) and (F.12), we have $|\hat{\theta} - \theta_0|_\infty = O_p(q\Delta_n)$, which implies $|\hat{\theta} - \check{\theta}|_\infty \leq |\hat{\theta} - \theta_0|_\infty + |\check{\theta} - \theta_0|_\infty = O_p(q\Delta_n)$. Hence, $|\hat{\theta} - \check{\theta}|_\infty \ll \check{r}$ with probability approaching one. Therefore,

$$0 = \left\{ \frac{1}{n-m} \sum_{t=m+1}^n \hat{f}_t^{(l)}(\hat{\theta}_l, \check{\theta}_{-l}) \right\} \left\{ \frac{1}{n-m} \sum_{t=m+1}^n \frac{\partial \hat{f}_t^{(l)}(\hat{\theta}_l, \check{\theta}_{-l})}{\partial \theta_l} \right\}$$

with probability approaching one. Together with (F.13), we have

$$\frac{1}{n-m} \sum_{t=m+1}^n \hat{f}_t^{(l)}(\hat{\theta}_l, \check{\theta}_{-l}) = 0$$

with probability approaching one.

By (F.14) and (F.10), due to $|\check{\boldsymbol{\theta}} - \boldsymbol{\theta}_0|_1 = O_p(q\Delta_n)$, $|\tilde{\boldsymbol{\theta}} - \boldsymbol{\theta}_0|_1 = O_p(\Delta_n^{1/2})$ and $\tau \lesssim \Delta_n^{1/2}$, then

$$\begin{aligned}\hat{\theta}_l - \theta_{0,l} &= - \left\{ \frac{1}{n-m} \sum_{t=m+1}^n \frac{\partial \hat{f}_t^{(l)}(\bar{\theta}_l, \check{\boldsymbol{\theta}}_{-l})}{\partial \theta_l} \right\}^{-1} \left\{ \frac{1}{n-m} \sum_{t=m+1}^n \hat{f}_t^{(l)}(\theta_{0,l}, \check{\boldsymbol{\theta}}_{-l}) \right\} \\ &= - \left\{ \frac{1}{n-m} \sum_{t=m+1}^n \frac{\partial \hat{f}_t^{(l)}(\bar{\theta}_l, \check{\boldsymbol{\theta}}_{-l})}{\partial \theta_l} \right\}^{-1} \left\{ \frac{1}{n-m} \sum_{t=m+1}^n \hat{f}_t^{(l)}(\boldsymbol{\theta}_0) \right\} \\ &\quad + O_p(q\Delta_n^{3/2}) + O_p(q^2\Delta_n^2)\end{aligned}$$

with probability approaching one. As shown in (F.30) in Section F.5.3 for the proof of Lemma 4,

$$\begin{aligned}\left| \frac{1}{n-m} \sum_{t=m+1}^n \{ \hat{f}_t^{(l)}(\boldsymbol{\theta}_0) - f_t^{(l)}(\boldsymbol{\theta}_0) \} \right| \\ = O_p \left\{ \frac{\omega_n \sqrt{(\log q) \log(qn)}}{\sqrt{n|\mathcal{S}_l|}} \right\} + O_p \left\{ \frac{\omega_n (\log q)^{1/2} \log(qn)}{\sqrt{n}|\mathcal{S}_l|} \right\} = o_p \left(\frac{1}{\sqrt{n}|\mathcal{S}_l|} \right),\end{aligned}$$

where the last step is based on Condition 4. Hence,

$$\begin{aligned}\hat{\theta}_l - \theta_{0,l} &= - \left\{ \frac{1}{n-m} \sum_{t=m+1}^n \frac{\partial \hat{f}_t^{(l)}(\bar{\theta}_l, \check{\boldsymbol{\theta}}_{-l})}{\partial \theta_l} \right\}^{-1} \left\{ \frac{1}{n-m} \sum_{t=m+1}^n f_t^{(l)}(\boldsymbol{\theta}_0) \right\} \\ &\quad + O_p(q\Delta_n^{3/2}) + O_p(q^2\Delta_n^2) + o_p \left(\frac{1}{\sqrt{n}|\mathcal{S}_l|} \right)\end{aligned}\tag{F.15}$$

with probability approaching one.

Write

$$\check{Q}_{l,t} = \frac{1}{|\mathcal{S}_l|^{1/2}} \sum_{(i,j) \in \mathcal{S}_l} \frac{X_{i,j}^t - \gamma_{i,j}^{t-1}(\boldsymbol{\theta}_0)}{\gamma_{i,j}^{t-1}(\boldsymbol{\theta}_0)\{1 - \gamma_{i,j}^{t-1}(\boldsymbol{\theta}_0)\}} \left\{ \boldsymbol{\varphi}_l^\top \frac{\partial \gamma_{i,j}^{t-1}(\boldsymbol{\theta}_0)}{\partial \boldsymbol{\theta}} \right\}.$$

Then

$$\frac{1}{n-m} \sum_{t=m+1}^n f_t^{(l)}(\boldsymbol{\theta}_0) = \frac{1}{(n-m)|\mathcal{S}_l|^{1/2}} \sum_{t=m+1}^n \check{Q}_{l,t}.\tag{F.16}$$

In the sequel, we will use the martingale central limit theorem to establish the asymptotic distribution of $(n-m)^{-1/2} \sum_{t=m+1}^n \check{Q}_{l,t}$. Denote by $\mathbb{P}_{\mathcal{F}_{t-1}}(\cdot)$ and $\mathbb{E}_{\mathcal{F}_{t-1}}(\cdot)$, respectively, the conditional probability measure and the conditional expectation given \mathcal{F}_{t-1} with the unknown

true parameter vector $\boldsymbol{\theta}_0$. By Conditions 1 and 4, it holds that

$$\max_{(i,j) \in \mathcal{S}_l} \left| \frac{X_{i,j}^t - \gamma_{i,j}^{t-1}(\boldsymbol{\theta}_0)}{\gamma_{i,j}^{t-1}(\boldsymbol{\theta}_0)\{1 - \gamma_{i,j}^{t-1}(\boldsymbol{\theta}_0)\}} \left\{ \boldsymbol{\varphi}_l^\top \frac{\partial \gamma_{i,j}^{t-1}(\boldsymbol{\theta}_0)}{\partial \boldsymbol{\theta}} \right\} \right| \leq C_1^{-1} C_2 C_4 =: C_{**}.$$

It follows from the Bernstein inequality that

$$\mathbb{P}_{\mathcal{F}_{t-1}}(|\mathring{Q}_{l,t}| \geq x) \leq 2 \exp \left(- \frac{3|\mathcal{S}_l|^{1/2}x^2}{6|\mathcal{S}_l|^{1/2}C_{**}^2 + 2xC_{**}} \right)$$

for any $x > 0$, which implies, for any $\delta > 0$,

$$\begin{aligned} & \sum_{t=m+1}^n \mathbb{E}_{\mathcal{F}_{t-1}} \left\{ \left(\frac{\mathring{Q}_{l,t}}{\sqrt{n-m}} \right)^2 I \left(\frac{|\mathring{Q}_{l,t}|}{\sqrt{n-m}} \geq \delta \right) \right\} \\ &= \frac{1}{n-m} \sum_{t=m+1}^n \mathbb{E}_{\mathcal{F}_{t-1}} \{ \mathring{Q}_{l,t}^2 I(|\mathring{Q}_{l,t}| \geq \delta \sqrt{n-m}) \} \rightarrow 0 \end{aligned}$$

in probability as $n \rightarrow \infty$. Meanwhile, by Condition 5, we also have

$$\begin{aligned} & \frac{1}{n-m} \sum_{t=m+1}^n \mathbb{E}_{\mathcal{F}_{t-1}} (\mathring{Q}_{l,t}^2) \\ &= \frac{1}{(n-m)|\mathcal{S}_l|} \sum_{t=m+1}^n \sum_{(i,j) \in \mathcal{S}_l} \frac{1}{\gamma_{i,j}^{t-1}(\boldsymbol{\theta}_0)\{1 - \gamma_{i,j}^{t-1}(\boldsymbol{\theta}_0)\}} \left\{ \boldsymbol{\varphi}_l^\top \frac{\partial \gamma_{i,j}^{t-1}(\boldsymbol{\theta}_0)}{\partial \boldsymbol{\theta}} \right\}^2 \rightarrow \kappa_l \end{aligned}$$

in probability as $n \rightarrow \infty$. By Conditions 1 and 4, we know κ_l is a almost surely bounded random variable. Corollary 3.1 of [Hall and Heyde \(1980\)](#) implies

$$\frac{1}{\sqrt{n-m}} \sum_{t=m+1}^n \mathring{Q}_{l,t} \rightarrow \sqrt{\kappa_l} \cdot Z$$

in distribution as $n \rightarrow \infty$, where Z is a standard normally distributed random variable independent of κ_l . By (F.15) and (F.16), due to

$$\frac{1}{n-m} \sum_{t=m+1}^n \frac{\partial \hat{f}_t^{(l)}(\bar{\theta}_l, \check{\boldsymbol{\theta}}_{-l})}{\partial \theta_l} \rightarrow 1$$

in probability which is obtained in (F.13), it holds that

$$\sqrt{n|\mathcal{S}_l|}(\hat{\theta}_l - \theta_{0,l}) \rightarrow \sqrt{\kappa_l} \cdot Z$$

in distribution as $n \rightarrow \infty$, provided that $\sqrt{n|\mathcal{S}_l|} \max\{q\Delta_n^{3/2}, q^2\Delta_n^2\} = o(1)$. We complete the proof of Theorem 2. \square

F.5 Proofs of auxiliary lemmas

F.5.1 Proof of Lemma 2

Without loss of generality, we assume $\Theta = [-C, C]^q$ for some constant $C > 0$. For given $\epsilon > 0$ which will be specified later, we partition $[-C, C]$ into $K = \lceil 2C/\epsilon \rceil$ sub-intervals B_1, \dots, B_K with equal length, where the length of each B_k does not exceed ϵ . Based on such defined B_1, \dots, B_K , we can partition Θ as follows:

$$\Theta = \bigcup_{k_1=1}^K \cdots \bigcup_{k_q=1}^K B_{k_1} \times \cdots \times B_{k_q},$$

which includes K^q hyper-rectangles $\mathcal{B}_1, \dots, \mathcal{B}_{K^q}$. For each given $u \in [K^q]$, there exists $(k_{1,u}, \dots, k_{q,u}) \in [K]^q$ such that $\mathcal{B}_u = B_{k_{1,u}} \times \cdots \times B_{k_{q,u}}$. Let $\boldsymbol{\theta}_u$ be the center of \mathcal{B}_u .

For each $\boldsymbol{\theta} \in \mathcal{B}_u$, since $\gamma_{i,j}^{t-1}(\boldsymbol{\theta})$ only depends on θ_l with $l \in \mathcal{I}_{i,j}$, it follows from the Taylor expansion that

$$\begin{aligned} \hat{\ell}_{n,p}^{(l)}(\boldsymbol{\theta}) - \hat{\ell}_{n,p}^{(l)}(\boldsymbol{\theta}_u) &= \left[\frac{1}{(n-m)|\mathcal{S}_l|} \sum_{t=m+1}^n \sum_{(i,j) \in \mathcal{S}_l} \frac{X_{i,j}^t - \gamma_{i,j}^{t-1}(\tilde{\boldsymbol{\theta}}_u)}{\gamma_{i,j}^{t-1}(\tilde{\boldsymbol{\theta}}_u)\{1 - \gamma_{i,j}^{t-1}(\tilde{\boldsymbol{\theta}}_u)\}} \frac{\partial \gamma_{i,j}^{t-1}(\tilde{\boldsymbol{\theta}}_u)}{\partial \boldsymbol{\theta}^\top} \right] (\boldsymbol{\theta} - \boldsymbol{\theta}_u) \\ &= \frac{1}{(n-m)|\mathcal{S}_l|} \sum_{t=m+1}^n \sum_{(i,j) \in \mathcal{S}_l} \frac{X_{i,j}^t - \gamma_{i,j}^{t-1}(\tilde{\boldsymbol{\theta}}_u)}{\gamma_{i,j}^{t-1}(\tilde{\boldsymbol{\theta}}_u)\{1 - \gamma_{i,j}^{t-1}(\tilde{\boldsymbol{\theta}}_u)\}} \frac{\partial \gamma_{i,j}^{t-1}(\tilde{\boldsymbol{\theta}}_u)}{\partial \boldsymbol{\theta}_{\mathcal{I}_{i,j}}} (\boldsymbol{\theta}_{\mathcal{I}_{i,j}} - \boldsymbol{\theta}_{u,\mathcal{I}_{i,j}}), \end{aligned}$$

where $\tilde{\boldsymbol{\theta}}_u \in \mathcal{B}_u$ is on the joint line between $\boldsymbol{\theta}$ and $\boldsymbol{\theta}_u$. Write $\boldsymbol{\theta} = (\theta_1, \dots, \theta_q)^\top$ and $\boldsymbol{\theta}_u = (\theta_{u,1}, \dots, \theta_{u,q})^\top$. By Conditions 1 and 2, it holds that

$$\begin{aligned} |\hat{\ell}_{n,p}^{(l)}(\boldsymbol{\theta}) - \hat{\ell}_{n,p}^{(l)}(\boldsymbol{\theta}_u)| &\leq \frac{1}{(n-m)|\mathcal{S}_l|} \sum_{t=m+1}^n \sum_{(i,j) \in \mathcal{S}_l} \sum_{l \in \mathcal{I}_{i,j}} \left| \frac{X_{i,j}^t - \gamma_{i,j}^{t-1}(\tilde{\boldsymbol{\theta}}_u)}{\gamma_{i,j}^{t-1}(\tilde{\boldsymbol{\theta}}_u)\{1 - \gamma_{i,j}^{t-1}(\tilde{\boldsymbol{\theta}}_u)\}} \right| \left| \frac{\partial \gamma_{i,j}^{t-1}(\tilde{\boldsymbol{\theta}}_u)}{\partial \theta_l} \right| |\theta_l - \theta_{u,l}| \\ &\leq \frac{C_1^{-1}C_2\epsilon}{(n-m)|\mathcal{S}_l|} \sum_{t=m+1}^n \sum_{(i,j) \in \mathcal{S}_l} \sum_{l \in \mathcal{I}_{i,j}} |X_{i,j}^t - \gamma_{i,j}^{t-1}(\tilde{\boldsymbol{\theta}}_u)| \leq sC_1^{-1}C_2\epsilon \end{aligned}$$

for any $\boldsymbol{\theta} \in \mathcal{B}_u$ and $l \in [q]$. Analogously, we also have

$$\sup_{\boldsymbol{\theta} \in \mathcal{B}_u} |\ell_{n,p}^{(l)}(\boldsymbol{\theta}) - \ell_{n,p}^{(l)}(\boldsymbol{\theta}_u)| \leq sC_1^{-1}C_2\epsilon.$$

Therefore, by the triangle inequality, it holds that

$$\begin{aligned} \max_{l \in \mathcal{H}} \sup_{\boldsymbol{\theta} \in \Theta} |\hat{\ell}_{n,p}^{(l)}(\boldsymbol{\theta}) - \ell_{n,p}^{(l)}(\boldsymbol{\theta})| &= \max_{l \in \mathcal{H}} \max_{u \in [K^q]} \sup_{\boldsymbol{\theta} \in \mathcal{B}_u} |\hat{\ell}_{n,p}^{(l)}(\boldsymbol{\theta}) - \ell_{n,p}^{(l)}(\boldsymbol{\theta})| \\ &\leq \max_{l \in \mathcal{H}} \max_{u \in [K^q]} |\hat{\ell}_{n,p}^{(l)}(\boldsymbol{\theta}_u) - \ell_{n,p}^{(l)}(\boldsymbol{\theta}_u)| + \max_{l \in \mathcal{H}} \max_{u \in [K^q]} \sup_{\boldsymbol{\theta} \in \mathcal{B}_u} |\hat{\ell}_{n,p}^{(l)}(\boldsymbol{\theta}) - \hat{\ell}_{n,p}^{(l)}(\boldsymbol{\theta}_u)| \\ &\quad + \max_{l \in \mathcal{H}} \max_{u \in [K^q]} \sup_{\boldsymbol{\theta} \in \mathcal{B}_u} |\ell_{n,p}^{(l)}(\boldsymbol{\theta}) - \ell_{n,p}^{(l)}(\boldsymbol{\theta}_u)| \\ &\leq \max_{l \in \mathcal{H}} \max_{u \in [K^q]} |\hat{\ell}_{n,p}^{(l)}(\boldsymbol{\theta}_u) - \ell_{n,p}^{(l)}(\boldsymbol{\theta}_u)| + 2sC_1^{-1}C_2\epsilon. \end{aligned} \tag{F.17}$$

For each $l \in [q]$, $u \in [K^q]$ and $t \in [n] \setminus [m]$, define

$$Q_{u,t}^{(l)} = \frac{1}{|\mathcal{S}_l|^{1/2}} \sum_{(i,j) \in \mathcal{S}_l} \left[\{X_{i,j}^t - \gamma_{i,j}^{t-1}(\boldsymbol{\theta}_0)\} \log \left\{ \frac{\gamma_{i,j}^{t-1}(\boldsymbol{\theta}_u)}{1 - \gamma_{i,j}^{t-1}(\boldsymbol{\theta}_u)} \right\} \right].$$

Then

$$\hat{\ell}_{n,p}^{(l)}(\boldsymbol{\theta}_u) - \ell_{n,p}^{(l)}(\boldsymbol{\theta}_u) = \frac{1}{(n-m)|\mathcal{S}_l|^{1/2}} \sum_{t=m+1}^n Q_{u,t}^{(l)}. \tag{F.18}$$

Notice that

$$|X_{i,j}^t - \gamma_{i,j}^{t-1}(\boldsymbol{\theta}_0)| \left| \log \left\{ \frac{\gamma_{i,j}^{t-1}(\boldsymbol{\theta}_u)}{1 - \gamma_{i,j}^{t-1}(\boldsymbol{\theta}_u)} \right\} \right| \leq \max_{i \neq j} \left| \log \left\{ \frac{\gamma_{i,j}^{t-1}(\boldsymbol{\theta}_u)}{1 - \gamma_{i,j}^{t-1}(\boldsymbol{\theta}_u)} \right\} \right|.$$

Due to

$$\log \left[\gamma_{i,j}^{t-1}(\boldsymbol{\theta}_u) \{1 - \gamma_{i,j}^{t-1}(\boldsymbol{\theta}_u)\} \right] < \log \left\{ \frac{\gamma_{i,j}^{t-1}(\boldsymbol{\theta}_u)}{1 - \gamma_{i,j}^{t-1}(\boldsymbol{\theta}_u)} \right\} < -\log \left[\gamma_{i,j}^{t-1}(\boldsymbol{\theta}_u) \{1 - \gamma_{i,j}^{t-1}(\boldsymbol{\theta}_u)\} \right],$$

by Condition 1, we have

$$\begin{aligned} \max_{u \in [K^q]} \max_{t \in [n] \setminus [m]} |X_{i,j}^t - \gamma_{i,j}^{t-1}(\boldsymbol{\theta}_0)| \left| \log \left\{ \frac{\gamma_{i,j}^{t-1}(\boldsymbol{\theta}_u)}{1 - \gamma_{i,j}^{t-1}(\boldsymbol{\theta}_u)} \right\} \right| \\ \leq \max_{u \in [K^q]} \max_{t \in [n] \setminus [m]} \max_{i \neq j} \left| \log \left[\gamma_{i,j}^{t-1}(\boldsymbol{\theta}_u) \{1 - \gamma_{i,j}^{t-1}(\boldsymbol{\theta}_u)\} \right] \right| \leq \log C_1^{-1}. \end{aligned} \tag{F.19}$$

Denote by $\mathbb{P}_{\mathcal{F}_{t-1}}(\cdot)$ the conditional probability measure given \mathcal{F}_{t-1} with the unknown true parameter vector θ_0 . It follows from the Bernstein inequality that

$$\begin{aligned} & \max_{u \in [K^q]} \max_{t \in [n] \setminus [m]} \mathbb{P}_{\mathcal{F}_{t-1}}\{|Q_{u,t}^{(l)}| \geq x\} \\ & \leq 2 \exp \left\{ - \frac{3|\mathcal{S}_l|^{1/2}x^2}{6|\mathcal{S}_l|^{1/2}(\log C_1^{-1})^2 + 2x \log C_1^{-1}} \right\} \end{aligned} \quad (\text{F.20})$$

for any $x > 0$. Furthermore, due to $\mathbb{P}\{|Q_{u,t}^{(l)}| \geq x\} = \mathbb{E}[\mathbb{P}_{\mathcal{F}_{t-1}}\{|Q_{u,t}^{(l)}| \geq x\}]$, we also have

$$\max_{u \in [K^q]} \max_{t \in [n] \setminus [m]} \mathbb{P}\{|Q_{u,t}^{(l)}| \geq x\} \leq 2 \exp \left\{ - \frac{3|\mathcal{S}_l|^{1/2}x^2}{6|\mathcal{S}_l|^{1/2}(\log C_1^{-1})^2 + 2x \log C_1^{-1}} \right\} \quad (\text{F.21})$$

for any $x > 0$. Let

$$\tilde{Q}_{u,t}^{(l)} = Q_{u,t}^{(l)} I\{|Q_{u,t}^{(l)}| \leq M\} - \mathbb{E}_{\mathcal{F}_{t-1}}[Q_{u,t}^{(l)} I\{|Q_{u,t}^{(l)}| \leq M\}]$$

for some diverging $M > 0$ specified later. Notice that $\{\tilde{Q}_{u,t}^{(l)}\}_{t \in [n] \setminus [m]}$ is a martingale difference sequence with $\max_{t \in [n] \setminus [m]} |\tilde{Q}_{u,t}^{(l)}| \leq 2M$. By the Azuma's inequality (Azuma, 1967; see also Theorem 3.1 of Lesigne and Volny (2001)), we have

$$\max_{l \in [q]} \max_{u \in [K^q]} \mathbb{P} \left\{ \left| \frac{1}{n-m} \sum_{t=m+1}^n \tilde{Q}_{u,t}^{(l)} \right| \geq x \right\} \leq 2 \exp \left\{ - \frac{(n-m)x^2}{8M^2} \right\} \quad (\text{F.22})$$

for any $x > 0$. By (F.21),

$$\begin{aligned} & \max_{u \in [K^q]} \mathbb{P} \left[\left| \frac{1}{n-m} \sum_{t=m+1}^n Q_{u,t}^{(l)} I\{|Q_{u,t}^{(l)}| > M\} \right| > 0 \right] \leq \max_{u \in [K^q]} \mathbb{P} \left\{ \max_{t \in [n] \setminus [m]} |Q_{u,t}^{(l)}| > M \right\} \\ & \leq 2n \exp \left\{ - \frac{3|\mathcal{S}_l|^{1/2}M^2}{6|\mathcal{S}_l|^{1/2}(\log C_1^{-1})^2 + 2M \log C_1^{-1}} \right\}. \end{aligned}$$

Together with (F.22), by the Bonferroni inequality, we have

$$\begin{aligned} & \mathbb{P} \left(\max_{l \in \mathcal{H}} \max_{u \in [K^q]} \left| \frac{1}{n-m} \sum_{t=m+1}^n [\tilde{Q}_{u,t}^{(l)} + Q_{u,t}^{(l)} I\{|Q_{u,t}^{(l)}| > M\}] \right| > x \right) \\ & \leq 2|\mathcal{H}|K^q \exp \left\{ - \frac{(n-m)x^2}{8M^2} \right\} \\ & \quad + 2|\mathcal{H}|K^q n \max_{l \in \mathcal{H}} \exp \left\{ - \frac{3|\mathcal{S}_l|^{1/2}M^2}{6|\mathcal{S}_l|^{1/2}(\log C_1^{-1})^2 + 2M \log C_1^{-1}} \right\} \end{aligned}$$

for any $x > 0$. Recall $S_{\mathcal{H},\min} = \min_{l \in \mathcal{H}} |\mathcal{S}_l|$ and $|\mathcal{H}| \leq q$. Selecting

$$M = C \max \left(\sqrt{q \log K}, \frac{q \log K}{\sqrt{S_{\mathcal{H},\min}}}, \sqrt{\log n}, \frac{\log n}{\sqrt{S_{\mathcal{H},\min}}} \right) \quad (\text{F.23})$$

for some sufficiently large constant $C > 0$, it holds that

$$\begin{aligned} \max_{l \in \mathcal{H}} \max_{u \in [K^q]} \left| \frac{1}{n-m} \sum_{t=m+1}^n [\tilde{Q}_{u,t}^{(l)} + Q_{u,t}^{(l)} I\{|Q_{u,t}^{(l)}| > M\}] \right| &= O_p \left(M \sqrt{\frac{q \log K}{n}} \right) \\ &= O_p \left(\frac{q \log K}{\sqrt{n}} \right) + O_p \left\{ \frac{(q \log K)^{3/2}}{\sqrt{n S_{\mathcal{H},\min}}} \right\} \\ &\quad + O_p \left\{ \frac{\sqrt{q(\log K)(\log n)}}{\sqrt{n}} \right\} + O_p \left\{ \frac{(q \log K)^{1/2}(\log n)}{\sqrt{n S_{\mathcal{H},\min}}} \right\}. \end{aligned} \quad (\text{F.24})$$

On the other hand, by (F.20), it holds that

$$\begin{aligned} \mathbb{E}_{\mathcal{F}_{t-1}} [|Q_{u,t}^{(l)}| I\{|Q_{u,t}^{(l)}| > M\}] &= M \mathbb{P}_{\mathcal{F}_{t-1}} \{ |Q_{u,t}^{(l)}| > M \} + \int_M^\infty \mathbb{P}_{\mathcal{F}_{t-1}} (|Q_{u,t}| > x) dx \\ &\leq 2M \exp \left\{ - \frac{3|\mathcal{S}_l|^{1/2} M^2}{6|\mathcal{S}_l|^{1/2} (\log C_1^{-1})^2 + 2M \log C_1^{-1}} \right\} \\ &\quad + 2 \int_M^\infty \exp \left\{ - \frac{x^2}{4(\log C_1^{-1})^2} \right\} dx + 2 \int_M^\infty \exp \left(- \frac{3|\mathcal{S}_l|^{1/2} x}{4 \log C_1^{-1}} \right) dx \\ &\leq 2M \exp \left\{ - \frac{3|\mathcal{S}_l|^{1/2} M^2}{6|\mathcal{S}_l|^{1/2} (\log C_1^{-1})^2 + 2M \log C_1^{-1}} \right\} \\ &\quad + 4(\log C_1^{-1})^2 M^{-1} \exp \left\{ - \frac{M^2}{4(\log C_1^{-1})^2} \right\} + \frac{8 \log C_1^{-1}}{3|\mathcal{S}_l|^{1/2}} \exp \left(- \frac{3|\mathcal{S}_l|^{1/2} M}{4 \log C_1^{-1}} \right), \end{aligned}$$

which implies

$$\begin{aligned} \max_{u \in [K^q]} \left| \frac{1}{n-m} \sum_{t=m+1}^n \mathbb{E}_{\mathcal{F}_{t-1}} [Q_{u,t}^{(l)} I\{|Q_{u,t}^{(l)}| > M\}] \right| &\leq 2M \exp \left\{ - \frac{3|\mathcal{S}_l|^{1/2} M^2}{6|\mathcal{S}_l|^{1/2} (\log C_1^{-1})^2 + 2M \log C_1^{-1}} \right\} \\ &\quad + 4(\log C_1^{-1})^2 \exp \left\{ - \frac{M^2}{4(\log C_1^{-1})^2} \right\} + \frac{8 \log C_1^{-1}}{3|\mathcal{S}_l|^{1/2}} \exp \left(- \frac{3|\mathcal{S}_l|^{1/2} M}{4 \log C_1^{-1}} \right). \end{aligned} \quad (\text{F.25})$$

Due to $S_{\mathcal{H},\min} = \min_{l \in \mathcal{H}} |\mathcal{S}_l| \rightarrow \infty$ and $M \rightarrow \infty$ satisfying (F.23), by (F.25), we have

$$\begin{aligned} & \max_{l \in \mathcal{H}} \max_{u \in [K^q]} \left| \frac{1}{n-m} \sum_{t=m+1}^n \mathbb{E}_{\mathcal{F}_{t-1}} [Q_{u,t}^{(l)} I\{|Q_{u,t}^{(l)}| > M\}] \right| \\ & \lesssim \exp(-\tilde{C}_1 M^2) + \exp(-\tilde{C}_2 M S_{\mathcal{H},\min}^{1/2}) = o(n^{-1/2}), \end{aligned}$$

where $\tilde{C}_1 > 0$ and $\tilde{C}_2 > 0$ are two universal constants. Due to $Q_{u,t}^{(l)} = \tilde{Q}_{u,t}^{(l)} + Q_{u,t}^{(l)} I\{|Q_{u,t}^{(l)}| > M\} - \mathbb{E}_{\mathcal{F}_{t-1}, \theta_0} [Q_{u,t}^{(l)} I\{|Q_{u,t}^{(l)}| > M\}]$, together with (F.24), it holds that

$$\begin{aligned} \max_{l \in \mathcal{H}} \max_{u \in [K^q]} \left| \frac{1}{n-m} \sum_{t=m+1}^n Q_{u,t}^{(l)} \right| &= O_p \left(\frac{q \log K}{\sqrt{n}} \right) + O_p \left\{ \frac{(q \log K)^{3/2}}{\sqrt{n S_{\mathcal{H},\min}}} \right\} \\ &+ O_p \left\{ \frac{\sqrt{q(\log K)(\log n)}}{\sqrt{n}} \right\} + O_p \left\{ \frac{(q \log K)^{1/2}(\log n)}{\sqrt{n S_{\mathcal{H},\min}}} \right\}. \end{aligned} \quad (\text{F.26})$$

By (F.18), we have

$$\begin{aligned} \max_{l \in \mathcal{H}} \max_{u \in [K^q]} |\hat{\ell}_{n,p}^{(l)}(\boldsymbol{\theta}_u) - \ell_{n,p}^{(l)}(\boldsymbol{\theta}_u)| &= O_p \left(\frac{q \log K}{\sqrt{n S_{\mathcal{H},\min}}} \right) + O_p \left\{ \frac{(q \log K)^{3/2}}{\sqrt{n S_{\mathcal{H},\min}}} \right\} \\ &+ O_p \left\{ \frac{\sqrt{q(\log K)(\log n)}}{\sqrt{n S_{\mathcal{H},\min}}} \right\} + O_p \left\{ \frac{(q \log K)^{1/2}(\log n)}{\sqrt{n S_{\mathcal{H},\min}}} \right\}. \end{aligned}$$

Recall $K \asymp \epsilon^{-1}$. Together with (F.17), it holds that

$$\begin{aligned} \max_{l \in \mathcal{H}} \sup_{\boldsymbol{\theta} \in \Theta} |\hat{\ell}_{n,p}^{(l)}(\boldsymbol{\theta}) - \ell_{n,p}^{(l)}(\boldsymbol{\theta})| &\leq 2sC_1^{-1}C_2\epsilon + O_p \left(\frac{q \log K}{\sqrt{n S_{\mathcal{H},\min}}} \right) + O_p \left\{ \frac{(q \log K)^{3/2}}{\sqrt{n S_{\mathcal{H},\min}}} \right\} \\ &+ O_p \left\{ \frac{\sqrt{q(\log K)(\log n)}}{\sqrt{n S_{\mathcal{H},\min}}} \right\} + O_p \left\{ \frac{(q \log K)^{1/2}(\log n)}{\sqrt{n S_{\mathcal{H},\min}}} \right\}. \end{aligned}$$

Due to $s \leq q$, with selecting $\epsilon \asymp n^{-1/2} S_{\mathcal{H},\min}^{-1/2}$, we have

$$\max_{l \in \mathcal{H}} \sup_{\boldsymbol{\theta} \in \Theta} |\hat{\ell}_{n,p}^{(l)}(\boldsymbol{\theta}) - \ell_{n,p}^{(l)}(\boldsymbol{\theta})| = O_p \left\{ \frac{q \log(n S_{\mathcal{H},\min})}{\sqrt{n S_{\mathcal{H},\min}}} \right\} + O_p \left\{ \frac{q^{3/2} \log^{3/2}(n S_{\mathcal{H},\min})}{\sqrt{n S_{\mathcal{H},\min}}} \right\}.$$

We complete the proof of Lemma 2. \square

F.5.2 Proof of Lemma 3

By the Taylor expansion, we have

$$\begin{aligned}
& \frac{1}{n-m} \sum_{t=m+1}^n \{ \hat{f}_t^{(l)}(\theta_{0,l}, \tilde{\boldsymbol{\theta}}_{-l}) - \hat{f}_t^{(l)}(\boldsymbol{\theta}_0) \} \\
&= \frac{1}{n-m} \sum_{t=m+1}^n \frac{\partial \hat{f}_t^{(l)}(\theta_{0,l}, \bar{\boldsymbol{\theta}}_{-l})}{\partial \boldsymbol{\theta}_{-l}^\top} (\tilde{\boldsymbol{\theta}}_{-l} - \boldsymbol{\theta}_{0,-l}) \\
&= \underbrace{\frac{1}{n-m} \sum_{t=m+1}^n \frac{\partial \hat{f}_t^{(l)}(\theta_{0,l}, \tilde{\boldsymbol{\theta}}_{-l})}{\partial \boldsymbol{\theta}_{-l}^\top} (\tilde{\boldsymbol{\theta}}_{-l} - \boldsymbol{\theta}_{0,-l})}_{R_{1,l}} \\
&+ \underbrace{\frac{1}{n-m} \sum_{t=m+1}^n \left\{ \frac{\partial \hat{f}_t^{(l)}(\theta_{0,l}, \bar{\boldsymbol{\theta}}_{-l})}{\partial \boldsymbol{\theta}_{-l}^\top} - \frac{\partial \hat{f}_t^{(l)}(\theta_{0,l}, \tilde{\boldsymbol{\theta}}_{-l})}{\partial \boldsymbol{\theta}_{-l}^\top} \right\} (\tilde{\boldsymbol{\theta}}_{-l} - \boldsymbol{\theta}_{0,-l})}_{R_{2,l}},
\end{aligned}$$

where $\bar{\boldsymbol{\theta}}_{-l}$ is on the joint line between $\boldsymbol{\theta}_{0,-l}$ and $\tilde{\boldsymbol{\theta}}_{-l}$.

For $R_{1,l}$, by the Taylor expansion, it holds that

$$\begin{aligned}
R_{1,l} &= \frac{1}{n-m} \sum_{t=m+1}^n \frac{\partial \hat{f}_t^{(l)}(\tilde{\boldsymbol{\theta}})}{\partial \boldsymbol{\theta}_{-l}^\top} (\tilde{\boldsymbol{\theta}}_{-l} - \boldsymbol{\theta}_{0,-l}) \\
&+ (\theta_{0,l} - \tilde{\theta}_l) \left\{ \frac{1}{n-m} \sum_{t=m+1}^n \frac{\partial^2 \hat{f}_t^{(l)}(\bar{\theta}_l, \tilde{\boldsymbol{\theta}}_{-l})}{\partial \theta_l \partial \boldsymbol{\theta}_{-l}^\top} \right\} (\tilde{\boldsymbol{\theta}}_{-l} - \boldsymbol{\theta}_{0,-l}),
\end{aligned}$$

where $\bar{\theta}_l$ is on the joint line between $\theta_{0,l}$ and $\tilde{\theta}_l$. Recall $\hat{f}_t^{(l)}(\boldsymbol{\theta}) = \hat{\boldsymbol{\varphi}}_l^\top \mathbf{g}_t^{(l)}(\boldsymbol{\theta})$. By the definition of $\hat{\boldsymbol{\varphi}}_l$ given in (9), we have

$$\left| \frac{1}{n-m} \sum_{t=m+1}^n \frac{\partial \hat{f}_t^{(l)}(\tilde{\boldsymbol{\theta}})}{\partial \boldsymbol{\theta}_{-l}} \right|_\infty \leq \tau,$$

which implies

$$\begin{aligned}
\left| \frac{1}{n-m} \sum_{t=m+1}^n \frac{\partial \hat{f}_t^{(l)}(\tilde{\boldsymbol{\theta}})}{\partial \boldsymbol{\theta}_{-l}^\top} (\tilde{\boldsymbol{\theta}}_{-l} - \boldsymbol{\theta}_{0,-l}) \right| &\leq \left| \frac{1}{n-m} \sum_{t=m+1}^n \frac{\partial \hat{f}_t^{(l)}(\tilde{\boldsymbol{\theta}})}{\partial \boldsymbol{\theta}_{-l}} \right|_\infty |\tilde{\boldsymbol{\theta}}_{-l} - \boldsymbol{\theta}_{0,-l}|_1 \\
&\leq \tau |\tilde{\boldsymbol{\theta}}_{-l} - \boldsymbol{\theta}_{0,-l}|_1.
\end{aligned} \tag{F.27}$$

For any $k \in [q]$, due to

$$\frac{\partial^2 \hat{f}_t^{(l)}(\bar{\theta}_l, \tilde{\boldsymbol{\theta}}_{-l})}{\partial \theta_l \partial \theta_k} = \hat{\boldsymbol{\varphi}}_l^\top \frac{\partial^2 \mathbf{g}_t^{(l)}(\bar{\theta}_l, \tilde{\boldsymbol{\theta}}_{-l})}{\partial \theta_l \partial \theta_k},$$

we then have

$$\begin{aligned} \left| \frac{\partial^2 \hat{f}_t^{(l)}(\bar{\theta}_l, \tilde{\boldsymbol{\theta}}_{-l})}{\partial \theta_l \partial \theta_k} \right| &\leq |\hat{\boldsymbol{\varphi}}_l|_1 \left| \frac{\partial^2 \mathbf{g}_t^{(l)}(\bar{\theta}_l, \tilde{\boldsymbol{\theta}}_{-l})}{\partial \theta_l \partial \theta_k} \right|_\infty \\ &\leq \frac{|\hat{\boldsymbol{\varphi}}_l|_1}{|\mathcal{S}_l|} \sum_{(i,j) \in \mathcal{S}_l} \left| \frac{\partial^2}{\partial \theta_l \partial \theta_k} \left[\frac{X_{i,j}^t - \gamma_{i,j}^{t-1}(\boldsymbol{\theta})}{\gamma_{i,j}^{t-1}(\boldsymbol{\theta}) \{1 - \gamma_{i,j}^{t-1}(\boldsymbol{\theta})\}} \frac{\partial \gamma_{i,j}^{t-1}(\boldsymbol{\theta})}{\partial \boldsymbol{\theta}} \right] \right|_\infty \end{aligned}$$

Notice that

$$\begin{aligned} &\frac{\partial^2}{\partial \theta_{l_1} \partial \theta_{l_2}} \left[\frac{X_{i,j}^t - \gamma_{i,j}^{t-1}(\boldsymbol{\theta})}{\gamma_{i,j}^{t-1}(\boldsymbol{\theta}) \{1 - \gamma_{i,j}^{t-1}(\boldsymbol{\theta})\}} \frac{\partial \gamma_{i,j}^{t-1}(\boldsymbol{\theta})}{\partial \theta_{l_3}} \right] \\ &= 2 \left[\frac{1 - 2\gamma_{i,j}^{t-1}(\boldsymbol{\theta})}{\{\gamma_{i,j}^{t-1}(\boldsymbol{\theta})\}^2 \{1 - \gamma_{i,j}^{t-1}(\boldsymbol{\theta})\}^2} + \frac{X_{i,j}^t - \gamma_{i,j}^{t-1}(\boldsymbol{\theta})}{\{\gamma_{i,j}^{t-1}(\boldsymbol{\theta})\}^2 \{1 - \gamma_{i,j}^{t-1}(\boldsymbol{\theta})\}^2} \right. \\ &\quad \left. + \frac{\{X_{i,j}^t - \gamma_{i,j}^{t-1}(\boldsymbol{\theta})\} \{1 - 2\gamma_{i,j}^{t-1}(\boldsymbol{\theta})\}^2}{\{\gamma_{i,j}^{t-1}(\boldsymbol{\theta})\}^3 \{1 - \gamma_{i,j}^{t-1}(\boldsymbol{\theta})\}^3} \right] \frac{\partial \gamma_{i,j}^{t-1}(\boldsymbol{\theta})}{\partial \theta_{l_1}} \frac{\partial \gamma_{i,j}^{t-1}(\boldsymbol{\theta})}{\partial \theta_{l_2}} \frac{\partial \gamma_{i,j}^{t-1}(\boldsymbol{\theta})}{\partial \theta_{l_3}} \\ &\quad - \left[\frac{1}{\gamma_{i,j}^{t-1}(\boldsymbol{\theta}) \{1 - \gamma_{i,j}^{t-1}(\boldsymbol{\theta})\}} + \frac{\{X_{i,j}^t - \gamma_{i,j}^{t-1}(\boldsymbol{\theta})\} \{1 - 2\gamma_{i,j}^{t-1}(\boldsymbol{\theta})\}}{\{\gamma_{i,j}^{t-1}(\boldsymbol{\theta})\}^2 \{1 - \gamma_{i,j}^{t-1}(\boldsymbol{\theta})\}^2} \right] \\ &\quad \times \left\{ \frac{\partial^2 \gamma_{i,j}^{t-1}(\boldsymbol{\theta})}{\partial \theta_{l_1} \partial \theta_{l_2}} \frac{\partial \gamma_{i,j}^{t-1}(\boldsymbol{\theta})}{\partial \theta_{l_3}} + \frac{\partial^2 \gamma_{i,j}^{t-1}(\boldsymbol{\theta})}{\partial \theta_{l_2} \partial \theta_{l_3}} \frac{\partial \gamma_{i,j}^{t-1}(\boldsymbol{\theta})}{\partial \theta_{l_1}} + \frac{\partial^2 \gamma_{i,j}^{t-1}(\boldsymbol{\theta})}{\partial \theta_{l_3} \partial \theta_{l_1}} \frac{\partial \gamma_{i,j}^{t-1}(\boldsymbol{\theta})}{\partial \theta_{l_2}} \right\} \\ &\quad + \frac{X_{i,j}^t - \gamma_{i,j}^{t-1}(\boldsymbol{\theta})}{\gamma_{i,j}^{t-1}(\boldsymbol{\theta}) \{1 - \gamma_{i,j}^{t-1}(\boldsymbol{\theta})\}} \frac{\partial^3 \gamma_{i,j}^{t-1}(\boldsymbol{\theta})}{\partial \theta_{l_1} \partial \theta_{l_2} \partial \theta_{l_3}}. \end{aligned}$$

By the triangle inequality and Condition 1, we know

$$\max_{k \in [q]} \left| \frac{\partial^2 \hat{f}_t^{(l)}(\bar{\theta}_l, \tilde{\boldsymbol{\theta}}_{-l})}{\partial \theta_l \partial \theta_k} \right| \leq C_* |\hat{\boldsymbol{\varphi}}_l|_1 \tag{F.28}$$

for some universal constant C_* specified in (F.4), which implies

$$\begin{aligned} &\left| (\theta_{0,l} - \tilde{\theta}_l) \left\{ \frac{1}{n-m} \sum_{t=m+1}^n \frac{\partial^2 \hat{f}_t^{(l)}(\bar{\theta}_l, \tilde{\boldsymbol{\theta}}_{-l})}{\partial \theta_l \partial \boldsymbol{\theta}_{-l}^\top} \right\} (\tilde{\boldsymbol{\theta}}_{-l} - \boldsymbol{\theta}_{0,-l}) \right| \\ &\leq |\theta_{0,l} - \tilde{\theta}_l| \left| \frac{1}{n-m} \sum_{t=m+1}^n \frac{\partial^2 \hat{f}_t^{(l)}(\bar{\theta}_l, \tilde{\boldsymbol{\theta}}_{-l})}{\partial \theta_l \partial \boldsymbol{\theta}_{-l}^\top} \right|_\infty |\tilde{\boldsymbol{\theta}}_{-l} - \boldsymbol{\theta}_{0,-l}|_1 \end{aligned}$$

$$\leq C_* |\hat{\boldsymbol{\varphi}}_l|_1 |\theta_{0,l} - \tilde{\theta}_l| |\tilde{\boldsymbol{\theta}}_{-l} - \boldsymbol{\theta}_{0,-l}|_1.$$

Together with (F.27), it holds that $|R_{1,l}| \leq \tau |\tilde{\boldsymbol{\theta}}_{-l} - \boldsymbol{\theta}_{0,-l}|_1 + C_* |\hat{\boldsymbol{\varphi}}_l|_1 |\theta_{0,l} - \tilde{\theta}_l| |\tilde{\boldsymbol{\theta}}_{-l} - \boldsymbol{\theta}_{0,-l}|_1$.

For $R_{2,l}$, by the Taylor expansion, we have

$$R_{2,l} = (\bar{\boldsymbol{\theta}}_{-l} - \tilde{\boldsymbol{\theta}}_{-l})^\top \left\{ \frac{1}{n-m} \sum_{t=m+1}^n \frac{\partial^2 \hat{f}_t^{(l)}(\theta_{0,l}, \dot{\boldsymbol{\theta}}_{-l})}{\partial \boldsymbol{\theta}_{-l} \partial \boldsymbol{\theta}_{-l}^\top} \right\} (\tilde{\boldsymbol{\theta}}_{-l} - \boldsymbol{\theta}_{0,-l})$$

for some $\dot{\boldsymbol{\theta}}_{-l}$ on the joint line between $\bar{\boldsymbol{\theta}}_{-l}$ and $\tilde{\boldsymbol{\theta}}_{-l}$, which implies

$$|R_{2,l}| \leq |\bar{\boldsymbol{\theta}}_{-l} - \tilde{\boldsymbol{\theta}}_{-l}|_1 |\tilde{\boldsymbol{\theta}}_{-l} - \boldsymbol{\theta}_{0,-l}|_1 \left| \frac{1}{n-m} \sum_{t=m+1}^n \frac{\partial^2 \hat{f}_t^{(l)}(\theta_{0,l}, \dot{\boldsymbol{\theta}}_{-l})}{\partial \boldsymbol{\theta}_{-l} \partial \boldsymbol{\theta}_{-l}^\top} \right|_\infty.$$

Since $\bar{\boldsymbol{\theta}}_{-l}$ is on the joint line between $\boldsymbol{\theta}_{0,-l}$ and $\tilde{\boldsymbol{\theta}}_{-l}$, then $|\bar{\boldsymbol{\theta}}_{-l} - \tilde{\boldsymbol{\theta}}_{-l}|_1 \leq |\tilde{\boldsymbol{\theta}}_{-l} - \boldsymbol{\theta}_{0,-l}|_1$. Parallel to (F.28), we can also show

$$\left| \frac{1}{n-m} \sum_{t=m+1}^n \frac{\partial^2 \hat{f}_t^{(l)}(\theta_{0,l}, \dot{\boldsymbol{\theta}}_{-l})}{\partial \boldsymbol{\theta}_{-l} \partial \boldsymbol{\theta}_{-l}^\top} \right|_\infty \leq C_* |\hat{\boldsymbol{\varphi}}_l|_1.$$

Hence, $|R_{2,l}| \leq C_* |\hat{\boldsymbol{\varphi}}_l|_1 |\tilde{\boldsymbol{\theta}}_{-l} - \boldsymbol{\theta}_{0,-l}|_1^2$. Then

$$\begin{aligned} & \left| \frac{1}{n-m} \sum_{t=m+1}^n \{ \hat{f}_t^{(l)}(\theta_{0,l}, \tilde{\boldsymbol{\theta}}_{-l}) - \hat{f}_t^{(l)}(\boldsymbol{\theta}_0) \} \right| \leq |R_{1,l}| + |R_{2,l}| \\ & \leq \tau |\tilde{\boldsymbol{\theta}}_{-l} - \boldsymbol{\theta}_{0,-l}|_1 + C_* |\hat{\boldsymbol{\varphi}}_l|_1 |\theta_{0,l} - \tilde{\theta}_l| |\tilde{\boldsymbol{\theta}}_{-l} - \boldsymbol{\theta}_{0,-l}|_1 + C_* |\hat{\boldsymbol{\varphi}}_l|_1 |\tilde{\boldsymbol{\theta}}_{-l} - \boldsymbol{\theta}_{0,-l}|_1^2 \\ & = \tau |\tilde{\boldsymbol{\theta}}_{-l} - \boldsymbol{\theta}_{0,-l}|_1 + C_* |\hat{\boldsymbol{\varphi}}_l|_1 |\tilde{\boldsymbol{\theta}}_{-l} - \boldsymbol{\theta}_0|_1 |\tilde{\boldsymbol{\theta}}_{-l} - \boldsymbol{\theta}_{0,-l}|_1 \\ & \leq \tau |\tilde{\boldsymbol{\theta}}_{-l} - \boldsymbol{\theta}_0|_1 + C_* |\hat{\boldsymbol{\varphi}}_l|_1 |\tilde{\boldsymbol{\theta}}_{-l} - \boldsymbol{\theta}_0|_1^2. \end{aligned}$$

We complete the proof of Lemma 3. □

F.5.3 Proof of Lemma 4

Due to $\hat{f}_t^{(l)}(\boldsymbol{\theta}) = \hat{\boldsymbol{\varphi}}_l^\top \mathbf{g}_t^{(l)}(\boldsymbol{\theta})$ and $f_t^{(l)}(\boldsymbol{\theta}) = \boldsymbol{\varphi}_l^\top \mathbf{g}_t^{(l)}(\boldsymbol{\theta})$, then

$$\left| \frac{1}{n-m} \sum_{t=m+1}^n \{ \hat{f}_t^{(l)}(\boldsymbol{\theta}_0) - f_t^{(l)}(\boldsymbol{\theta}_0) \} \right| \leq |\hat{\boldsymbol{\varphi}}_l - \boldsymbol{\varphi}_l|_1 \left| \frac{1}{n-m} \sum_{t=m+1}^n \mathbf{g}_t^{(l)}(\boldsymbol{\theta}_0) \right|_\infty.$$

Write $(G_1^{(l)}, \dots, G_q^{(l)})^\top = (n-m)^{-1} \sum_{t=m+1}^n \mathbf{g}_t^{(l)}(\boldsymbol{\theta}_0)$. Due to

$$\mathbf{g}_t^{(l)}(\boldsymbol{\theta}_0) = \frac{1}{|\mathcal{S}_l|} \sum_{(i,j) \in \mathcal{S}_l} \frac{X_{i,j}^t - \gamma_{i,j}^{t-1}(\boldsymbol{\theta}_0)}{\gamma_{i,j}^{t-1}(\boldsymbol{\theta}_0)\{1 - \gamma_{i,j}^{t-1}(\boldsymbol{\theta}_0)\}} \frac{\partial \gamma_{i,j}^{t-1}(\boldsymbol{\theta}_0)}{\partial \boldsymbol{\theta}},$$

we then have

$$\begin{aligned} G_k^{(l)} &= \frac{1}{(n-m)|\mathcal{S}_l|} \sum_{t=m+1}^n \sum_{(i,j) \in \mathcal{S}_l} \frac{X_{i,j}^t - \gamma_{i,j}^{t-1}(\boldsymbol{\theta}_0)}{\gamma_{i,j}^{t-1}(\boldsymbol{\theta}_0)\{1 - \gamma_{i,j}^{t-1}(\boldsymbol{\theta}_0)\}} \frac{\partial \gamma_{i,j}^{t-1}(\boldsymbol{\theta}_0)}{\partial \theta_k} \\ &:= \frac{1}{(n-m)|\mathcal{S}_l|^{1/2}} \sum_{t=m+1}^n \check{Q}_{k,t}^{(l)} \end{aligned}$$

for any $k \in [q]$. Using the same arguments for deriving (F.26), we can also show

$$\max_{l \in \mathcal{H}} \max_{k \in [q]} |G_k^{(l)}| = O_p \left\{ \frac{\sqrt{(\log q) \log(qn)}}{\sqrt{nS_{\mathcal{H},\min}}} \right\} + O_p \left\{ \frac{(\log q)^{1/2} \log(qn)}{\sqrt{nS_{\mathcal{H},\min}}} \right\}, \quad (\text{F.29})$$

where $S_{\mathcal{H},\min} = \min_{l \in \mathcal{H}} |\mathcal{S}_l|$. Together with Condition 4, it holds that

$$\begin{aligned} \max_{l \in \mathcal{H}} \left| \frac{1}{n-m} \sum_{t=m+1}^n \{ \hat{f}_t^{(l)}(\boldsymbol{\theta}_0) - f_t^{(l)}(\boldsymbol{\theta}_0) \} \right| \\ = O_p \left\{ \frac{\omega_n \sqrt{(\log q) \log(qn)}}{\sqrt{nS_{\mathcal{H},\min}}} \right\} + O_p \left\{ \frac{\omega_n (\log q)^{1/2} \log(qn)}{\sqrt{nS_{\mathcal{H},\min}}} \right\}. \end{aligned} \quad (\text{F.30})$$

Notice that

$$\frac{1}{n-m} \sum_{t=m+1}^n f_t^{(l)}(\boldsymbol{\theta}_0) = \frac{1}{(n-m)|\mathcal{S}_l|} \sum_{t=m+1}^n \sum_{(i,j) \in \mathcal{S}_l} \frac{X_{i,j}^t - \gamma_{i,j}^{t-1}(\boldsymbol{\theta}_0)}{\gamma_{i,j}^{t-1}(\boldsymbol{\theta}_0)\{1 - \gamma_{i,j}^{t-1}(\boldsymbol{\theta}_0)\}} \left\{ \boldsymbol{\varphi}_l^\top \frac{\partial \gamma_{i,j}^{t-1}(\boldsymbol{\theta}_0)}{\partial \boldsymbol{\theta}} \right\}.$$

By Conditions 1 and 4, we know

$$\max_{l \in [q]} \max_{t \in [n] \setminus [m]} \max_{(i,j) \in \mathcal{S}_l} \left| \boldsymbol{\varphi}_l^\top \frac{\partial \gamma_{i,j}^{t-1}(\boldsymbol{\theta}_0)}{\partial \boldsymbol{\theta}} \right| \leq C_2 C_4.$$

Using the same arguments for deriving (F.29), we can also show

$$\max_{l \in \mathcal{H}} \left| \frac{1}{n-m} \sum_{t=m+1}^n f_t^{(l)}(\boldsymbol{\theta}_0) \right|$$

$$= O_p \left\{ \frac{\sqrt{\log(1 + |\mathcal{H}|) \log(n|\mathcal{H}|)}}{\sqrt{nS_{\mathcal{H},\min}}} \right\} + O_p \left\{ \frac{\sqrt{\log(1 + |\mathcal{H}|) \log(n|\mathcal{H}|)}}{\sqrt{nS_{\mathcal{H},\min}}} \right\}.$$

Together with (F.30), due to $\omega_n(\log q)^{1/2} \log(qn) = o(1)$, we have Lemma 4. \square

F.5.4 Proof of Lemma 5

For any $\theta_l \in B(\tilde{\theta}_l, \tilde{r})$, by the Taylor expansion, we have

$$\frac{1}{n-m} \sum_{t=m+1}^n \left\{ \frac{\partial \hat{f}_t^{(l)}(\theta_l, \tilde{\theta}_{-l})}{\partial \theta_l} - \frac{\partial \hat{f}_t^{(l)}(\tilde{\theta})}{\partial \theta_l} \right\} = \left\{ \frac{1}{n-m} \sum_{t=m+1}^n \frac{\partial^2 \hat{f}_t^{(l)}(\bar{\theta}_l, \tilde{\theta}_{-l})}{\partial \theta_l^2} \right\} (\theta_l - \tilde{\theta}_l)$$

for some $\bar{\theta}_l$ on the joint line between θ_l and $\tilde{\theta}_l$, which implies

$$\left| \frac{1}{n-m} \sum_{t=m+1}^n \left\{ \frac{\partial \hat{f}_t^{(l)}(\theta_l, \tilde{\theta}_{-l})}{\partial \theta_l} - \frac{\partial \hat{f}_t^{(l)}(\tilde{\theta})}{\partial \theta_l} \right\} \right| = \left| \frac{1}{n-m} \sum_{t=m+1}^n \frac{\partial^2 \hat{f}_t^{(l)}(\bar{\theta}_l, \tilde{\theta}_{-l})}{\partial \theta_l^2} \right| |\theta_l - \tilde{\theta}_l|.$$

Due to $\theta_l \in B(\tilde{\theta}_l, \tilde{r})$, by (F.28), it holds that

$$\sup_{\theta_l \in B(\tilde{\theta}_l, \tilde{r})} \left| \frac{1}{n-m} \sum_{t=m+1}^n \left\{ \frac{\partial \hat{f}_t^{(l)}(\theta_l, \tilde{\theta}_{-l})}{\partial \theta_l} - \frac{\partial \hat{f}_t^{(l)}(\tilde{\theta})}{\partial \theta_l} \right\} \right| \leq C_* \tilde{r} |\hat{\varphi}_l|_1.$$

Since

$$\frac{1}{n-m} \sum_{t=m+1}^n \frac{\partial \hat{f}_t^{(l)}(\tilde{\theta})}{\partial \theta_l} = \frac{\hat{\varphi}_l^\top}{n-m} \sum_{t=m+1}^n \frac{\partial \mathbf{g}_t^{(l)}(\tilde{\theta})}{\partial \theta_l},$$

by (9), we know

$$\left| \frac{1}{n-m} \sum_{t=m+1}^n \frac{\partial \hat{f}_t^{(l)}(\tilde{\theta})}{\partial \theta_l} - 1 \right| \leq \tau,$$

which implies

$$\sup_{\theta_l \in B(\tilde{\theta}_l, \tilde{r})} \left| \frac{1}{n-m} \sum_{t=m+1}^n \frac{\partial \hat{f}_t^{(l)}(\theta_l, \tilde{\theta}_{-l})}{\partial \theta_l} - 1 \right| \leq \tau + C_* \tilde{r} |\hat{\varphi}_l|_1.$$

We complete the proof of Lemma 5. \square

References

Azuma, K. (1967). Weighted sums of certain dependent random variables. *The Tohoku Mathematical Journal. Second Series*, **19**, 357–367.

Brémaud, P. (1998). *Markov Chains: Gibbs Fields, Monte Carlo Simulation, and Queues*. Springer.

Cattuto, C., Van den Broeck, W., Barrat, A., Colizza, V., Pinton, J.-F. and Vespignani, A. (2010). Dynamics of person-to-person interactions from distributed RFID sensor networks. *PloS ONE*, **5**, e11596.

Génois, M. and Barrat, A. (2018). Can co-location be used as a proxy for face-to-face contacts? *EPJ Data Science*, **7**, 1–18.

Hall, P. and Heyde, C. C. (1980). *Martingale Limit Theory and Its Application*. Academic Press.

Hanneke, S., Fu, W. and Xing, E. (2010). Discrete temporal models of social networks. *Electronic Journal of Statistics*, **4**, 585–605.

Krivitsky, P.N. and Handcock, M. (2014). A separable model for dynamic networks. *Journal of the Royal Statistical Society: Series B*, **76**, 29–48.

Krivitsky, P.N., Handcock, M., Hunter, D. R., Butts, C. T., Bojanowski, M., Klumb, C., Goodreau, S. M. and Morris, M. (2025). Statnet: Tools for the statistical modeling of network data. URL: <https://statnet.org>.

Lesigne, E. and Volný, D. (2001). Large deviations for martingales. *Stochastic Processes and their Applications*, **96**, 143–159.